

Towards Examining the Effectiveness of Boxing Headguards with Thermoplastic
Polyurethane in Mitigating Acceleration and Risk of Head Injury Using a Dynamic Head
Model

Tyson Rybak

0576192

Supervisors: Dr. Carlos Zerpa and Dr. Meilan Liu

Committee Member: Dr. Paolo Sanzo

Lakehead University

Thunder Bay, Ontario, Canada

January 2021

ABSTRACT

The sport of boxing historically symbolises a high-risk injury sport due the number of concussions occurring on athletes. Indeed, boxing has shown to have the highest rate of concussions of any individual male sport. Research studies, however, indicate that boxing headgears are generally effective in minimizing concussion risk for training and competitions. Unfortunately, concussions continue to occur even when wearing a protective headguard. As a result, athletes do not always use boxing headguards during training, matches and competitions at the professional level. Based on these concerns, this study examined the capacity of three different types of boxing headguard models to mitigate the risk of concussions by using static and dynamic headguard testing techniques. The researcher included the use of thermoplastic polyurethane (TPU) material inserts in one of the headguard models to observe changes in headguard performance to mitigate concussion risk. The researcher performed static quasi-compression tests to observe changes to the material properties of the headguards, specifically testing percent reduction in the energy absorption, force and deformation of the headguard material. The researcher also performed dynamic tests by mounting the headguard on a surrogate headform and imparting linear and shear impacts to the headform model at different velocities across different headgear locations. The researcher used the dynamic measures of linear and angular accelerations to compute the risk of head injury across the headgear locations. A set of analyses were conducted to examine the capacity of the headguards with and without the TPU material to limit these acceleration measures, and subsequently mitigate the risk of concussion. The results of this study revealed that the TPU material, when implemented into the headguard, had significant effects in mitigating linear accelerations and risk of head injury. This study also found significant interactions between headguard types and impact locations on measures of angular accelerations and risk of head injury, which included measures of Angular Gadd Severity

Index and GAMBIT (Generalized Acceleration Model for Brain Injury Threshold) – an index that combines linear and rotational accelerations. This study is the first to implement TPU material into a boxing headguard and provides strong evidence to mitigate concussion risk in the sport of boxing based on measures of linear and rotational accelerations. In addition, it offers another avenue for manufacturers to improve the capacity of current boxing headgear technologies to better support athletes' safety while practicing in the sport.

Acknowledgements

There are a number of people who have had a major contribution both directly and indirectly in the completion of this project. First, I would like to thank my supervisors Dr. Carlos Zerpa and Dr. Meilan Liu for their continuous guidance, patience, feedback, and countless hours worked to help me along this process. I would also like to thank my committee member Dr. Paolo Sanzo for his valuable feedback and continuous support along the duration of this project.

Second, I would like to thank my family and friends for their love and support along this process. To my mother Lisa, father Randy, my siblings, and all of my family and friends, thank you for helping in all ways possible to motivate and assist me.

Lastly, I would like to thank the Kinesiology faculty at Lakehead University and all of my fellow master's students for continued support and assistance over the duration of my master's degree. Words cannot properly express my gratitude for the strong support system you all have given me.

Table of Contents

ABSTRACT.....	2
Acknowledgements.....	4
List of Figures.....	8
List of Tables.....	10
List of Abbreviations.....	11
List of Equations.....	12
Introduction.....	13
Literature Review.....	19
Concussions.....	19
Diffuse axonal injury.....	20
Pathophysiology of concussions.....	20
Concussion symptoms.....	21
Impact forces causing concussions.....	22
Influence of acceleration in concussion.....	23
Influence of impact location.....	24
Risk of Injury Measures.....	25
Wayne State Tolerance Curve.....	25
Head Injury Criterion.....	26
Gadd Severity Index.....	27
GAMBIT.....	28
Rates of Head Trauma in the Sport of Boxing.....	29
Types of Boxing Injury.....	31
Dynamic Head Responses to a Boxing Punch.....	32
Boxing Safety Recommendations.....	35
Headguard.....	35
Headguard rules.....	35
Headguard specifications.....	36
Thermoplastic polyurethane.....	38
Impact Testing.....	39
Standards for impact testing of boxing headguards.....	39
Previous impact test research on boxing headgear.....	40
Research Problem.....	44
Research Purpose.....	45
Research Questions.....	46
Methods.....	48
Instrumentation.....	48
Chatillon® TCD1100 Force Tester.....	48
Pneumatic horizontal impactor.....	48

Headform.....	50
Mechanical neckform.....	50
Accelerometers, power supply, and software interfaces.....	51
Headguard models.....	53
Thermoplastic polyurethane.....	54
Procedure.....	57
Static testing.....	57
Dynamic testing.....	60
Impact locations.....	60
Impact velocity.....	63
Neck strength.....	64
Linear acceleration.....	65
Angular acceleration.....	65
Risk of injury.....	66
Independent and dependent variables.....	68
Analysis.....	68
Results.....	70
Static Testing.....	70
Front static tests.....	70
Side static tests.....	73
Dynamic Testing.....	76
Linear impact acceleration.....	76
Angular acceleration.....	79
Comparing headguard types for each impact location.....	80
Comparing the impact locations for each headguard.....	82
Head Injury Risk.....	84
Gadd severity index (GSI).....	85
Angular Gadd Severity Index (AGSI).....	87
Comparing headguard types for each impact location.....	88
Comparing the impact locations for each headguard.....	90
GAMBIT.....	92
Comparing headguard types for each impact location.....	93
Comparing the impact locations for each headguard.....	95
Discussion.....	98
Static Testing.....	100
Front energy absorption.....	100
Side energy absorption.....	100
Dynamic Testing.....	102
Linear acceleration.....	102
GSI.....	103
Angular acceleration.....	105
AGSI.....	108
GAMBIT.....	110
Conclusion.....	116
Strengths.....	117

Limitations	118
Future Directions	119
References	121

List of Figures

Figure 1: Wayne State Tolerance Curve.....	26
Figure 2: The Hybrid III head, neck and torso model with boxing headguard.....	33
Figure 3: The frangible faceform model with the boxing headguard removed.....	33
Figure 4: A schematic of the Chatillon® TCD1100 Force Tester.....	48
Figure 5: A schematic of the pneumatic horizontal impactor.....	49
Figure 6: Mechanical headform and neckform assembly.....	50
Figure 7: Mechanical neckform assembly.....	51
Figure 8: Delsy's Trigno™ Wireless Gyroscope Sensor.....	53
Figure 9: Century® Drive headguard model.....	53
Figure 10: Adidas® headguard model.....	54
Figure 11: TPU inserts.....	55
Figure 12: TPU inserts placed into Century® Drive headguard.....	55
Figure 13: Side section of the TPU- Century® Drive headguard.....	56
Figure 14: Chatillon® TCD1100 Force Tester with modified block formation.....	57
Figure 15: Free-body diagram and components of displacement.....	58
Figure 16: Front static compression test of the Adidas® headguard.....	59
Figure 17: Front Impact Location.....	61
Figure 18: Front Boss Impact Location.....	62
Figure 19: Side Impact Location.....	62
Figure 20: Neck strength adjustment setup.....	65
Figure 21: Total percent of energy absorption for the Adidas®, Century® Drive, and TPU- Century® Drive headguards at the front location during static testing.....	71
Figure 22: Percent compression energy absorption of the Adidas®, Century® Drive, and TPU-Century® Drive headguards at the front location during static testing.....	72
Figure 23: Percent shear energy absorption of the Adidas®, Century® Drive, and TPU- Century® Drive headguards at the front location during static testing.....	73
Figure 24: Total percent energy absorption of the Adidas®, Century® Drive, and TPU- Century® Drive headguards at the side location during static testing.....	74
Figure 25: Percent compression energy absorption of the Adidas®, Century® Drive, and TPU-Century® Drive headguards at the side location during static testing.....	75
Figure 26: Percent shear energy absorption of the Adidas®, Century® Drive, and TPU- Century® Drive headguards at the side location during static testing.....	76
Figure 27: Estimated marginal means of PRLA across headguard types.....	78
Figure 28: Estimated marginal means of PRLA across impact locations.....	79
Figure 29: Interaction effect of headguard type and impact location on the estimated marginal means of angular acceleration.....	80
Figure 30: Estimated marginal means of angular acceleration across headguard types for front impacts.....	81
Figure 31: Estimated marginal means of angular acceleration across impact locations for Adidas® headguard impacts.....	82
Figure 32: Estimated marginal means of angular acceleration across impact locations for Century® Drive headguard impacts.....	83
Figure 33: Estimated marginal means of angular acceleration across impact locations for TPU-Century® Drive headguard impacts.....	84
Figure 34: Estimated marginal means of Gadd Severity Index across headguard conditions.....	86
Figure 35: Estimated marginal means of Gadd Severity Index across impact locations.....	87
Figure 36: Interaction effect of headguard type and impact location on the estimated marginal means of Gadd Severity Index.....	88

Figure 37: Estimated marginal means of AGSI across headguard types for front impacts.	89
Figure 38: Estimated marginal means of AGSI for Adidas® headguard across impact locations.	90
Figure 39: Estimated marginal means of AGSI for Century® Drive headguard across impact locations.	91
Figure 40: Estimated marginal means of AGSI for TPU-Century® Drive headguard across impact locations.	92
Figure 41: Interaction effect of headguard type and impact location on the estimated marginal means of GAMBIT.	93
Figure 42: Estimated marginal means of GAMBIT across headguard types for front impacts.	94
Figure 43: Estimated marginal means of GAMBIT across headguard types for side impacts.	95
Figure 44: Estimated marginal means of GAMBIT for Adidas® headguard across impact locations.	96
Figure 45: Estimated marginal means of GAMBIT for Century® Drive across impact locations.	97

List of Tables

Table 1: Impact location specifications for a medium-sized headform.....	61
Table 2: Compressed air tank pressure of the horizontal impactor and corresponding impact velocity.....	63
Table 3: Results for significant main effect tests for linear impact measure testing	105
Table 4: Interaction tests for headguard type and location on measures of angular acceleration, AGSI, and GAMBIT	113

List of Abbreviations

AGSI	Angular Gadd Severity Index
AIBA	International Boxing Association
CTE	Chronic traumatic encephalopathy
DAI	Diffuse axonal injury
EPP	Expanded propylene
GAMBIT	Generalized Acceleration Model for Brain Injury Threshold
GSI	Gadd Severity Index
ICC	Intraclass correlation
ICP	Integrated circuit piezoelectric sensor
KO	Knockout
LOC	Loss of consciousness
MMA	Mixed martial arts
mTBI	Mild traumatic brain injury
NCAA	National Collegiate Athletic Association
NOCSAE	National Operating Committee on Standards for Athletic Equipment
PRLA	Peak resultant linear acceleration
PVA	Polyvinyl alcohol sponge
RLA	Resultant linear acceleration
TKO	Technical knockout
TPU	Thermoplastic polyurethane
TBI	Traumatic brain injury
WSTC	Wayne State Tolerance Curve

List of Equations

Equation 1: Head Injury Criterion	26
Equation 2: Gadd Severity Index	27
Equation 3: Original GAMBIT	28
Equation 4: Gravity units conversion	52
Equation 5: Horizontal force.....	59
Equation 6: Compressive force	59
Equation 7: Shear force.....	59
Equation 8: Percent total energy absorption	60
Equation 9: Percent compressive energy absorption	60
Equation 10: Percent shear energy absorption.....	60
Equation 11: Pressure-velocity formula.....	63
Equation 12: Resultant linear acceleration	65
Equation 13: Resultant angular displacement.....	65
Equation 14: Resultant angular acceleration.....	Error! Bookmark not defined.
Equation 15: Linear to angular GSI adjustment	67
Equation 16: Angular Gadd Severity Index.....	67
Equation 17: Modified GAMBIT	67

Introduction

Boxing is a combat sport often criticized in society because it poses a high-level risk of injury to athletes. Mild traumatic brain injuries (mTBI), or concussions, and long term traumatic neurologic impairments, for example, represent the major concerns of risk of injury for the medical community. The basic intent of boxing is often to harm or incapacitate the opponent and as such, an emphasis is placed on scoring head blows (Canadian Medical Association, 2001).

In boxing, mTBI are often associated with long term, irreversible, and progressive effects, previously described as *Punch Drunk Syndrome*; and now referred to as *Chronic Traumatic Encephalopathy* (Ling et al., 2015). In addition, the formation of subdural hematoma due to the collection of blood external to the brain as a result of the head impacts represents the leading cause of sports related traumatic brain injuries in boxers (Ling et al., 2015).

The definition of concussion, or mTBI, varies among medical professionals because a concussion can result from many types of traumatic brain injuries. The American Academy for Neurology defines concussion as a “clinical syndrome of biomechanically induced alteration of brain function typically affecting memory and orientation, which may involve a loss of consciousness” (Giza et al., 2013, p. 2250).

The causes of concussion can include direct trauma, rapid acceleration-deceleration of the head, or a blast injury (Mullally, 2017). Primary injuries of the brain in combat sports such as boxing occur from an external head impact to the head or face. Secondary injuries, on the other hand, result in a molecular, chemical, and inflammatory cascade, occurring minutes to days after the brain impact (Galgano et al., 2017). Concussed brain cells are vulnerable while still in the recovery process after the head impact and can face irreversible damage by the occurrence of swelling if a second concussion is sustained, which is referred to as *Second*

Impact Syndrome (Signoretti et al., 2011). The magnitude of the acceleration of the head also plays a significant role in the risk of brain injuries and the severity of the damage (Rowson et al., 2016). Concussions more often occur when an impact generates an acceleration of the skull, but the brain lags behind due to inertia leading to the strain on the neural tissue and the development of various symptoms (Rowson et al., 2016). As concussion mechanisms are variable, there are a wide range of signs and symptoms that can present differently from case to case.

A concussion can generate several symptoms in athletes including confusion, disorientation, unsteadiness, dizziness, headache, and visual disturbances (Giza & Hovda, 2001). Concussion symptoms are often undetectable anatomically, meaning that they do not typically present as outward physical signs that can be seen visually. The symptoms, however, are typically expected to resolve over time due to temporary neuronal dysfunction as opposed to cell death (Giza & Hovda, 2001). A concussion can also result in a loss of consciousness (LOC), however; LOC occurs in less than 10% of patients who suffer a concussion (Mullally, 2017).

As previously stated, concussion injuries are very prevalent in boxing during training and competition, with the most common impacts occurring at the head and facial locations (Adkitte et al., 2016; Purcell, 2011). Rates of knockout (KO) and technical knockout (TKO) are high in boxing, primarily in male competitions. It has been shown that over half of male boxing bouts (51.6%) at the professional level end in a KO or TKO, more than double the rate of females (24.4%; Bledsoe et al., 2005). Consequently, the rates of concussion in boxing are the highest of any individual male sport, with 0.8 incidences of concussions occurring per 10 rounds of professional competition, and 7.9 incidences occurring per every 1000 competition minutes in amateur competition (Tommasone & Mcleod, 2006).

Recovery and return-to-play (RTP) protocols are important in sports due to the concern of *Second Impact Syndrome* and the severity of the concussion (Keenan & Mahaffey, 2017). Gradual introduction to daily activities, such as walking and other controlled physical activities, are emphasized in concussion recovery as opposed to rest (Keenan & Mahaffey, 2017). When determining a timeline for RTP, assessment of reaction time, balance, and oculomotor screening are useful tools (Keenan & Mahaffey, 2017). It is important to mention, however, that competition RTP protocols for athletes after suffering a concussion are not standardized and in the case of boxers often involve an arbitrary 30 to 90-day suspension from competition, with neurologic clearance not always being required (Sethi, 2016).

While RTP protocols offer an avenue to help injured athletes go back to competitions, the use of protective headguards provides another path to prevent the occurrence of concussions. In the sport of boxing, Canada has different headguard rules by gender and competition levels. In the official rules, Boxing Canada states that headguard use is mandatory for elite male open boxers, with the exception of National Championship bouts (Boxing Canada, 2017). In provincial championships, Boxing Canada gives boxers the option of choosing if they want to use headguards as long as both participants agree on the use of headguard protection (Boxing Canada, 2017). The International Boxing Organization (AIBA), however, prohibits the use of headguards in AIBA open boxing men's elite competition (AIBA, 2019). The AIBA has noted that this ban is motivated by their own internal, unpublished studies that show decreased head injury incidences following headguard removal (Dickinson & Rempel, 2016).

Several studies have been performed to test the effectiveness of boxing headguards under impacts, showing headguards to be generally useful for reducing concussion risk. Using a linear impactor with a semi rigid fist fitted with a glove, McIntosh and Patton

(2015a) tested several AIBA approved headguards for their head impact dynamics and injury risk under a range of impact velocities. Through the use of a Hybrid III head and neck system, McIntosh and Patton (2015a) noted significant differences were seen between headguard and non-headguard impacts, showing mean peak resultant angular head acceleration to be nearly halved by the headguard. The headguards also reduced mean peak resultant linear accelerations (RLA), showing that AIBA headguard models to be useful in reducing concussion risk.

Despite these research findings, there are several gaps in the existing literature regarding the effectiveness of boxing headguards in mitigating the risk of concussion. Furthermore, little research has been conducted to explore the behaviour of boxing headguard material in minimizing dynamics shear force impacts to the head. Shear forces are caused by rotational accelerations and cause a “jarring” effect to the head, producing more deformation to the brain than rotational acceleration would produce in other tissues of the body (Meaney & Smith, 2011). In addition, some research has been done to compare the effectiveness of headguards at mitigating impact at different impact velocities, however; the velocity impact ranges were small to represent the velocity of boxer’s punch. Finally, thermoplastic polyurethane (TPU), a material high in tensile and flexural strength, has been recently introduced into helmet design (Lin, *et al.*, 2017); however; research on its effectiveness is lacking.

This study examined the material properties of commercial boxing headgear and innovated TPU liner inserts in mitigating linear and angular impact kinematics. The study also explored the capacity of these headguards in mitigating the risk of concussion in the sport of boxing. More specifically, this study included three research purposes. The first purpose of this study was to analyze the material properties of TPU and boxing headguards statically to test the stiffness of the material across different boxing headgear locations. The

second purpose of this study was to examine the effect of headguard type and impact location on measures of peak linear acceleration and peak angular acceleration during simulated dynamic impacts. The third purpose of the study was to examine the effect of headguard type and impact location on head injury risk using measures of linear and rotational impact accelerations separately and in combination during simulated dynamic head collisions.

The study implemented a static testing technique by compressing the headguard material to measure the force and deformation for each headguard respectively. The study also implemented a dynamic testing technique by impacting a surrogate headform. From the results of the static and dynamic tests, the capacity of the headguards to limit concussion risk was analyzed based on measures of energy absorption, linear acceleration, rotational acceleration and computations of risk of concussion based on linear and rotational impacts to the head.

This study found that the TPU-commercial headguard combination was the most effective headguard in absorbing both shear and compression energy in static testing at both front and side locations. This finding is indicative of an increased capability of the helmet materials to mitigate concentrated loads placed on the head by absorbing more energy across the surface of the headguard (Di Landro et al., 2002). This study also found that the TPU-headguard combination was significantly more effective in mitigating linear acceleration, and Gadd Severity Index (GSI) of the headform at front, front boss, and side locations. Finally, this study found a significant interaction effect between headguard type and impact location on angular acceleration, Angular Gadd Severity Index (AGSI), and Generalized Acceleration Model for Brain Injury Threshold (GAMBIT). When analyzing GSI and GAMBIT in comparison to threshold measures, the TPU-headguard combination showed a consistent capability to reduce impacts below the thresholds, where other headguards surpassed them several times (NOCSAE, 2017; Newman et al., 1999).

This study is the first to incorporate TPU material into a boxing headguard and it shows very promising results in mitigating concussion risk. These results seem to provide an avenue for improvement in boxing headguard safety. Upon more research and possible addition of TPU to headguard production, this type of research may help provide a stronger case in support of headguard use in boxing competitions at the amateur and professional levels to decrease the occurrence of concussions.

Literature Review

Concussions

Concussions have been recognized clinically for over 1000 years and studied extensively in the 20th century (Mullally, 2017). The definition of what constitutes a concussion, however, is rather inconsistent between researchers and medical sources. Mullally (2017) stated that concussions can be caused by direct trauma, rapid acceleration-deceleration of the head (whiplash), or in a blast injury commonly seen by military personnel (Mullally, 2017). Concussion diagnosis is based on the completion of a clinical assessment (Mullally, 2017). Several definitions of concussion state that a concussed patient may report feeling dazed or “seeing stars” along with momentary confusion (Mullally, 2017). Based on this premise, Giza and Hovda (2001) described concussions as “any transient neurologic dysfunction resulting from a biomechanical force” (p.1).

A traumatic brain injury (TBI) ranges from a mild disruption in consciousness, to a state of comatose, or death (Galgano et al., 2017). The occurrence of TBIs results from primary or secondary impact injuries to the brain, which cause neurological deficits of varying severities. These neurological deficits can be either temporary or permanent (Galgano et al., 2017). More specifically, primary injuries relate to a crucial external brain impact; whereas secondary injuries affect a molecular, chemical, and inflammatory cascade and can occur minutes to days after a primary impact (Galgano et al., 2017). This cascade is responsible for the depolarization of neurons and the release of excitatory neurotransmitters that lead to an increase in intracellular calcium (Galgano et al., 2017). This increase in calcium causes the neuronal cells to degrade and consequently, an inflammatory response, which further damages the neuronal cells, breaching the blood brain barrier and resulting in cerebral edema (Galgano et al., 2017). A common type of TBI is a diffuse axonal injury (DAI).

Diffuse axonal injury. A DAI is a type of brain injury occurring most often in higher energy trauma, primarily seen in traffic accidents (Vieira et al., 2016). A DAI is associated with microscopic damage to the axons of the brain and neural tracts, corpus callosum, and brainstem (Vieira et al., 2016). Diffuse axonal injury result from rotational impact forces, which differentiate from cortical contusions and other haemorrhages resulting from acceleration/deceleration of the head (Sahler & Greenwald, 2012). Diffuse axonal injuries are clinically defined by the presence of coma lasting six or more hours after the TBI (Vieira et al., 2016). These injuries are often associated with posttraumatic coma, persistent neurovegetative states, and varying levels of disability following TBIs (Vieira et al., 2016). Diffuse axonal injuries are the most important factor in determining morbidity and mortality in a person suffering a TBI (Vieira et al., 2016).

Diffuse axonal injuries can result in many neurological impairments including cognitive, physical, and behavioural changes and compromise a person's social and physical abilities (Vieira et al., 2016). These impairments can occur long beyond the acute phase of treatment until the brain regains normal function as neural connections are re-established (Vieira et al., 2016). Neurological impairments can be better understood by describing the pathophysiology of concussions.

Pathophysiology of concussions. When describing the pathophysiology of concussion and the symptoms produced due to a biomechanical impact force, Signoretti et al. (2011) stated that a concussion results form a complex cascade of metabolic events triggering a disturbance to a delicate homeostatic balance of neurons in the brain. This complex cascade of metabolic events results in post-concussive symptoms caused primarily from neurotoxicity; that is, when the energetic metabolism of brain neurons is disturbed by mitochondrial dysfunction (Signoretti et al., 2011). Concussed cells become vulnerable and irreversibly damaged by the occurrence of swelling especially if a second concussion is

sustained while cells are still in the state of recovery (Signoretti et al., 2011). This complication is referred to as *Second Impact Syndrome* (Signoretti et al., 2011). Research has suggested that N-acetylaspartate, a brain compound that represents neuronal metabolic wellness, can be a marker of post-traumatic biochemical damage (Signoretti et al., 2011). N-acetylaspartate is easily detectable through proton magnetic resonance spectroscopy and can be useful in monitoring the recovery of the functional disturbances of the brain (Signoretti et al., 2011). Changes in homeostatic balance of neurons in the brain due to a mTBI leads to a variety of symptoms affecting the performance of a person and his/her functioning in activities of daily living.

Concussion symptoms. Symptoms of concussions may include confusion, disorientation, unsteadiness, dizziness, headache, and visual disturbances (Giza & Hovda, 2001). The loss of consciousness (LOC) is a strong indicator of a concussion but is not required to make a concussion diagnosis (Giza & Hovda, 2001). The LOC is seen in less than 10% of patients who suffer a concussion (Mullally, 2017). A LOC is caused by “rotational forces at the junction of the midbrain in the thalamus, resulting in a transient disruption of the reticular activating system” (Mullally, 2017, p. 886). Concussion symptoms are typically undetectable anatomically and often resolve over time, indicating that they are due to temporary neuronal dysfunction rather than cell death (Giza & Hovda, 2001).

The severity of concussion injuries can be assessed by symptoms such as prolonged LOC on individuals after a head impact. In some cases, however, it may indicate the presence of a severe TBI rather than a concussion (Mullally, 2017). The duration of posttraumatic amnesia is also an indicator of concussion severity (Mullally, 2017). Posttraumatic amnesia includes anterograde (inability to assimilate new memory) and retrograde (memory of events preceding the injury), which in some concussion cases is difficult to assess (Mullally, 2017).

The severity of these symptoms, however, depends on the magnitude of the linear and rotational forces induced in the brain during a head collision.

Impact forces causing concussions. Concussions are produced by the combination of linear and rotational forces causing acceleration-deceleration of the brain during a head impact (Meaney et al., 1995). Linear forces cause the brain to elongate and deform, putting a stretch on various structures of the brain, including the neurons, glial cells, and blood vessels altering membrane permeability (Mckee & Daneshvar, 2015). These types of brain injuries also produce a rapid release of neurotransmitters, an influx of calcium, and an efflux of potassium (Mckee & Daneshvar, 2015). Due to these chemical changes, the cellular sodium-potassium pump must be accelerated to maintain membrane homeostasis, which requires a large increase in glucose metabolism and is referred to as the neurometabolic cascade of concussion (Giza & Hovda, 2001). These chemical changes cause post-concussive hypermetabolism resulting in a decrease in cerebral blood flow and creating a disparity between glucose supply and demand (Giza & Hovda, 2001). This outcome can lead to a variety of symptoms affecting the physical and cognitive performance of the concussed person.

Rotational forces, on the other hand, cause shear brain injury. This type of brain injury disrupts the white matter and its connections in the brain, disturbing the axons of neurons biomechanically and biochemically (Rush, 2011). The disturbances of white matter can result in cell death, as well as functional impairments including slowed cognitive speed, decreased motor coordination, and a disturbance in higher-level executive functioning (Rush, 2011). Indeed, the brain tissue deforms more readily with shear forces as compared to other biologic tissues due to the physical properties of the brain (Meaney & Smith, 2011). This result can be attributed to shear strains causing distortion and the rupture of axons, blood vessels, and major fibre tracts (Peerless & Rewcastle, 1967). Subsequently, several studies

have suggested that shear deformation resulting from rotational acceleration is the predominant injury mechanism in concussion (Adams et al., 1982; Gennarelli et al., 1982; Meaney & Smith, 2011; Unterharnscheidt & Higgins, 1969).

Influence of acceleration in concussion. As previously stated, impact forces induced to the head and brain represent a motion that generates an acceleration of the skull where the brain lags behind due to inertia (Rowson et al., 2016). With concussions, there is a common notion that the brain has a large amount of movement, creating a sloshing effect in the skull (Rowson et al., 2016). In reality, a minimal and small amount of brain motion and deformation can produce a concussion, with more severe impacts causing more brain movement and intracranial pressure resulting in more severe injuries (Rowson et al., 2016). The brain can move a maximum of 7 mm relative to the skull (Rowson et al., 2016) and head accelerations can occur in multiple directions of movement (Browne, et al, 2011). Subsequently, the resultant acceleration is the vector sum of all accelerations (Donegan, 2012) used to quantify the magnitude of the impact and the severity of the concussion.

In the case of rotational acceleration, the impact occurs more in an oblique direction. This type of acceleration is more associated to strain response and seems to produce more damage to the deep internal structures of the brain. As stated by Meaney and Smith (2011), the patterns of strain of the brain due to a head impact are dependent on where the force is applied, such as stress being placed on the coronal (lateral), horizontal (axial), and sagittal planes. Shear forces are often produced by rotational motions and present more harm to brain tissue, making it more responsible for mTBI than linear accelerations (Meaney & Smith, 2011). The LOC occurs more during a rotational impact of the brain than a primarily linear impact, as the shear forces readily produce more deformation to the brain than any other body tissue (Meaney & Smith, 2011). Concussions are primarily caused by inertial loading or

acceleration of the brain that are often the result of a combination of linear and rotational accelerations (Meaney & Smith, 2011). Linear acceleration is a good predictor of peak pressure occurring within the brain, however, the strains created by pressure gradients are more significant with rotational accelerations than linear accelerations (Meaney & Smith, 2011). With this said, the severity of rotational acceleration injuries differs with relation to the site of the brain injury and the amount of tissue injured (Meaney & Smith, 2011).

Influence of impact location. Brain tissue deformation is influenced by the rotational accelerations, intracranial partitioning membranes, and material properties of the tissue (Meaney & Smith, 2011). Patterns of deformation are significantly different in a mechanism of injury involving rotational acceleration compared to an acceleration applied in the coronal (linear), horizontal, or sagittal planes (Meaney & Smith, 2011). The direction of acceleration has a strong effect on the corresponding impairment, with lateral (coronal) plane accelerations producing the most damage to the internal structures of the brain (Gennarelli et al., 1982; Meaney & Smith, 2011). This impairment can be explained through research that has shown that coronal plane head motions were the only type of motion that produces axonal damage in the brainstem (Gennarelli et al., 1987). Neurological impairment is the result of forces applied in the coronal plane, however; similar impairments can be produced with rotational accelerations along the horizontal and sagittal planes (Meaney & Smith, 2011). The ventricular system of the brain provides a damping effect to the strains that occur in the brain during rotational accelerations (Meaney & Smith, 2011). Additionally, the membranes that partition the cerebral hemispheres and cerebellum from the cerebrum also influence these patterns of deformation (Meaney & Smith, 2011).

Kerr et al. (2014) explored the effect of impact location on concussion using the injury data for high school football players. The study used National High School Sports-Related Injury Surveillance Study data (2008/2009–2012/2013) to analyze the details and

circumstances of concussions. The study found that concussions occurred primarily from impacts at the front of the head (44.7%) and side of the head (22.3%). There was no significant relationship between the impact location and concussion characteristics such as the symptoms and recovery time. Loss of consciousness was more prominent with impacts to the top of the head (8%) than other areas of the head (3.5%).

A similar study by Liao, Lynall, and Mihalik (2016) analyzed the data for 33 Division I National Collegiate Athletic Association (NCAA) football players to examine the relationship between impact location and concussions. Twenty-four concussions were matched with impacts of similar kinematic and injury criterion values, such as linear and rotational acceleration, that occurred during the same type of event (game, practice, or scrimmage). The same matching criteria were also used to match players in the closest kinematic or same player group. The data revealed that on the day of the injury, players in the concussed group sustained a lower percentage of impacts to the front of the head than the non-concussed group (34.5% versus 43.5%, respectively). Comparatively, players in the concussed group had a greater frequency of impacts to the sides and top of the head than the non-concussed group (side = 19.6% versus 16.6%; and top = 18.9 versus 14%, respectively). These findings suggested that it may be more difficult to mitigate concussion sustained with side and top of the head impact locations than frontal impacts. These types of concussions are also very prominent in the sport of boxing resulting in acute neurological injuries in the athlete. Although impact location can be a useful measure for determining concussion risk, other measures should be taken to account for the severity of an impact and how it corresponds to the risk of injury.

Risk of Injury Measures

Wayne State Tolerance Curve. A number of injury tolerance measures have been developed to link the relationship between linear acceleration and head injury risk. The

Wayne State Tolerance curve (WSTC) was initially developed as a head injury acceleration tolerance measure used for automobile crashes (Greenwald, Gwin, Chu, & Crisco, 2008). This curve determines injury threshold using a linear acceleration versus impact time duration curve (Greenwald et al., 2008). Head injury risk is determined using the onset of a skull fracture as the injury criterion as opposed to a brain injury (Greenwald et al., 2008). The WSTC is shown in Figure 1. Several injury risk measures have been developed as an extension of the WSTC using acceleration-time profiles (Greenwald et al., 2008).

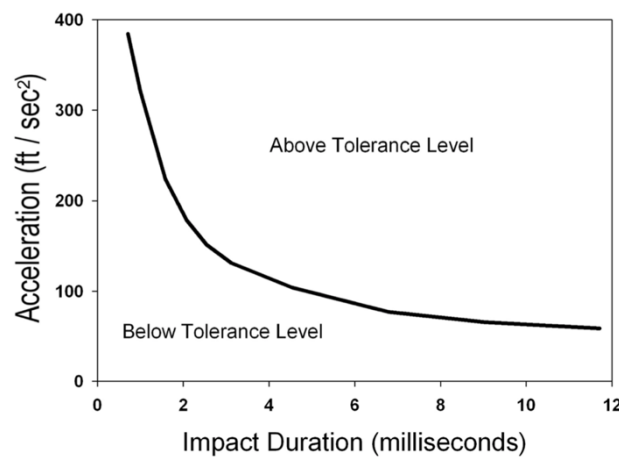


Figure 1: Wayne State Tolerance Curve. Adapted from “Head impact severity measures for evaluating mild traumatic brain injury risk exposure”, R. Greenwald, J. Gwin, J. Chu, and J. Crisco, 2008, *Neurosurgery*, 62(4), p. 789-798. Copyright 2008 by Neurosurgery.

Head Injury Criterion. Head injury criterion (HIC) is a valid measure for predicting skull fractures and cerebral contusions occurring from linear accelerations of the head (Kimpara & Iwamoto, 2012). The formula for HIC is shown in Equation 1. A cut-off of 36 ms is applied to the HIC to utilize the time interval that produced the maximum HIC, removing the influence of long durations and low acceleration impacts (Ouckama, 2013).

$$HIC = \left\{ (t_2 - t_1) \left[\frac{1}{t_2 - t_1} \int_{t_1}^{t_2} a(t) dt \right]^{2.5} \right\}_{max} \quad (1)$$

where:

a = linear acceleration

$t_2 - t_1$ = time interval where peak acceleration occurs; $t_2 - t_1 \leq 36$ ms

A threshold of injury of $HIC = 1000$, equates to an 18% chance of a life-threatening injury, or a 50% chance of a severe head injury (Hutchinson, Kaiser, & Lankarani, 1998).

Gadd Severity Index. Gadd Severity Index (GSI) is a measure of instantaneous acceleration of a headform when impacted (Jeffries, 2017). The equation for GSI is shown in Equation 2.

$$GSI = \int_0^T [a(t)]^{2.5} dt \quad (2)$$

where:

a = instantaneous resultant linear acceleration of the headform

T = impulse duration

Severity Index is a method of testing helmet effectiveness that integrates acceleration over time and provides an accurate head injury risk assessment that can be replicated under different impact conditions (NOCSAE, 2017). The GSI assessment is supported by the logic that the acceleration/time curve could provide a risk index (Jeffries, 2017; Ouckama, 2013). Furthermore, this means that the risk for certain impulse values could be the same if the impact had short duration and high acceleration characteristics, or long duration and low acceleration characteristics (Jeffries, 2017; Ouckama, 2013). A 2.5 weighting factor is applied to acceleration values to compensate for the fact that lower duration impacts have a decreased risk of head injury when exposed to higher acceleration (Jeffries, 2017; Ouckama, 2013). The National Operating Committee on Standards for Athletic Equipment (NOCSAE, 2017) sets the pass/fail threshold to a 1200 GSI score, meaning that values above this threshold do not meet performance criteria for football helmets. Measures regarding HIC and GSI can be useful for determining a helmet's protection capacity; however, measures such as energy dissipation and energy loading/unloading may be more useful for measuring injury

risk with a given head impact (Jeffries, 2017, Carlson, 2016). These measurement techniques also apply to the sport of boxing, which poses a high risk of concussion on athletes.

GAMBIT. The Head Injury Criterion (HIC) and Gadd Severity Index (GSI) do not account for measures of rotational acceleration or the combination of both linear and rotational accelerations. To address this limitation, Newman et al. (1999) developed a Generalized Acceleration Model for Brain Injury Threshold (GAMBIT), which is an injury risk measure designed to incorporate both translational and rotational acceleration. The GAMBIT model was originally proposed by Newman (1986) as a time dependent non-linear weighted sum of linear and rotational acceleration of the head. The formula for GAMBIT is shown in Equation 3 (Newman, 1986).

$$G_{max}(t) = \left[\left(\frac{a_{res}(t)}{250} \right)^2 + \left(\frac{\alpha_{res}(t)}{25000} \right)^2 \right]^{0.5} \quad (3)$$

where:

$a_{res}(t)$ = instantaneous translational acceleration

$\alpha_{res}(t)$ = instantaneous rotational acceleration

The GAMBIT model was later simplified to include time duration as a separate independent variable (Newman et al., 1999). The current model of GAMBIT incorporates average translational and rotational accelerations as well as time durations as separate independent variables (Newman et al., 1999). To create a formula for GAMBIT, Newman et al., (1999) ran a correlation exercise using a finite element model (FEM) of the human brain for a series of hypothetical time dependent translational and rotational acceleration combinations. From this analysis, the researchers considered the average accelerations and fixed time durations from different spatial orientations. The GAMBIT formula then represents the magnitude of internal energy increments in the brain, which indicate the risk of head injury when this energy exceeds some limiting value (Newman et al., 1999). In their study, Newman et al.

(1999) replicated 24 cases of helmeted head impacts in football, 9 of which resulted in concussions in real-life impacts, using a Hybrid III head model. With these replications, rigid body translational and rotational accelerations were measured and correlations between head injury and head kinematics were assessed (Newman et al., 1999). A logistic regression model showed GAMBIT to be a strong predictor of concussion risk ($p < .05$) in these cases, inferring it to be a useful measurement tool in dynamic concussion testing (Newman et al., 1999).

Although there is not a threshold recognized by NOCSAE for GAMBIT, the authors (1999) correlate GAMBIT scores to Abbreviated Injury Scale (AIS) scores, which are graded on a 1-6 scale (from minor to unsurvivable). Carroll et al. (2010) note that the 1998 version of AIS scoring quantifies a score of AIS=1 as a minor head injury, and a score of AIS=3 as a serious head injury. As noted by Newman et al. (1999), a GAMBIT score of $g=1$ corresponds to a 50-50 (%) chance of AIS=3 (serious). Furthermore, a GAMBIT score of $g=0.4$ translates to 50-50 (%) chance of AIS=1 (minor; Newman et al., 1999). These techniques can be very useful to assess the rates of head trauma in the sport of boxing when designing headguard protective equipment to mitigate concussion risk.

Rates of Head Trauma in the Sport of Boxing

The sport of boxing poses a high risk of concussions for amateur and professional athletes. A study examining 16 years of professional boxing fight outcomes and injury reports in the state of Victoria, Australia found that the most commonly injured body region was the head, neck, and face, combining to make up 89.8% of the total injuries (Zazryn et al., 2003). The study analyzed 107 injuries occurring in 427 fight participations between August 1985 and August 2001 (Zazryn et al., 2003). The researchers found that concussions represented the second most common type of injury (15.9%), but eye injuries were the most prominent, making up 45.8% of the total injuries (Zazryn et al., 2003).

Previous literature has shown some discrepancies in the rate of concussions in boxing. In professional boxing, for example, the literature has shown that between 15.9% and 69.7% of all injuries are acute neurological injuries (McCown, 1959; Jordan & Campbell, 1988; Zazryn et al., 2003; Zazryn et al., 2009). In amateur boxing, the rates of concussion are reported to be between 6.5% and 51.6% (Estwanik, Boitano, & Ari, 1984; Jordan, Voy, & Stone, 1990; Larsson et al., 1954; Porter & O'Brien, 1996; Welch, Sitler, & Kroeten, 1986; Zazryn et al., 2009).

Tommasone and Mcleod (2006) compared the concussion rates in boxing to other contact sports through a MEDLINE search of previously published studies. Of the individual male sports studied, boxing had the highest rates of concussion, with 0.8 incidences of concussion occurring per every 10 rounds of professional competition. In amateur competition, boxing was shown to have 7.9 incidences of concussion per 1000 man-minutes of competition, which under typical AIBA competition would correspond to approximately 333 rounds (AIBA, 2019). Ultimately, concussions occur much more typically at the professional level (Tommasone & McLeod, 2006). Tommasone and Mcleod (2006) noted that due to this concern, boxing would likely benefit from slower return to play progressions compared to lower-risk sports.

Bledsoe, Li, and Levy (2005) estimated the prevalence of boxing concussions by analyzing medical records and outcome data for 524 Nevada boxing matches occurring between September 2001 and March 2003. To do this, a pair-matched, case-control design was used to explore the rates of KO and TKO. The cases included in this study were boxers who received an injury during competition. The overall incidence of injury in these matches was 17.1 incidences per 100 boxer-matches, or 3.4 per 100 rounds. The study found that male bouts resulted in a KO or TKO at over twice the rate of female bouts (51.4% versus 24.4%,

respectively). High rates of head-trauma induced bout stoppages may be a strong indicator that concussion rates are high in boxing, specifically in male competitions.

Types of Boxing Injury

The aforementioned study by Bledsoe et al. (2005) explored the types of injury in the same set of matches to determine the most common types of injury. Of the incidences of injury (17.1 per 100 matches or 3.4 per 100 rounds), facial lacerations accounted for 51% of injuries, followed by hand injuries (17%), eye injuries (14%), and nose injuries (5%).

Knockouts and TKOs were not regarded as injury. With this said, the authors (2005) note that these bout results should not be ignored, stating “neurologic dysfunction significant enough to cause the clinical “knocked out” picture is no doubt evidence of damage, and it can be argued that a knockout may represent severe injury” (Bledsoe et al., 2005, p. 997).

Furthermore, male boxers were significantly more likely to experience an injury than female boxers (3.6 versus 1.2 per 100 boxer-rounds). Boxers who lost their bout were nearly twice as likely to suffer an injury than the winners of bouts.

A retrospective study by Adkitt et al. (2016) was conducted on 54 National boxers in India to determine the prevalence of injuries occurring in boxing training and competition. The 54 boxers reported 820 injuries over a two-year period, comprising an average of 15.18 injuries per boxer over the two years. Subsequently, the injury rate per boxer was 9.64 incidences per 1000 hours of training. Of these injuries, injuries of the head (42.93%) were the most frequent, followed by injuries of the upper limbs (33.90). Soft tissue injuries and concussions were also common sources of injury. Of the 54 boxers, 33 (61%) reported at least one concussion sustained. The results of this study indicated that injuries were very high in boxing training and competition, with injuries of the head and face being the most common.

Purcell & Leblanc (2011) analyzed the rates of injury in boxing to examine the safety of the sport. The study noted that thousands of males and females under 19 years of age participated in boxing in North America, with over 18 thousand being registered in USA Boxing in 2008 (Purcell & Leblanc, 2011). Rates of concussions in amateur boxing range from 6.5% to 51.6% of all injuries (Zazryn et al., 2009). In this study of amateur boxing, over half of the injuries sustained in boxing competition were concussions (51.6%), with an incidence rate of 11.4 concussions per 1000 boxing exposures (Zazryn et al., 2009). Other research has observed a concussion rate of 0.58 concussions per 100 athlete exposures in amateur boxing, compared to 0.28 in male youth hockey, and 0.38 in high school rugby (Toth, McNeil, & Feasby, 2005). A final study showed that in amateur boxing competition, 13% of matches ended resulting from a concussion (Matser et al., 2000). Due to the concerns associated with the high rates of concussion in boxing, the American Medical Association (2007), Canadian Medical Association (2001) and World Medical Association (2017) all noted that boxing competition should be banned. Researchers, however, decided to study the mechanisms of injury causing concussions using dynamic head response models to better understand how the concussions occurred and how to possibly prevent the occurrence of concussions in the sport of boxing.

Dynamic Head Responses to a Boxing Punch

Walilko et al. (2005) used a Hybrid III head, neck, and torso model to measure the biomechanical impact of a punch to the head. The Hybrid III was a biofidelic model designed to simulate human biomechanical responses to impact. The model was designed to replicate the 50th percentile of males (O'Sullivan & Fife, 2016), equipped with a headform, neckform, and frangible faceform (see Figure 2).



Figure 2: The Hybrid III head, neck and torso model with boxing headguard. Adapted from “Biomechanics of the head for Olympic boxer punches to the face”, T. Walilko, D. Viano, and C. Bir, 2005, *British Journal of Sports Medicine*, 39 (10), p. 710-719. Copyright 2005 by British Journal of Sports Medicine.

This model was equipped with a frangible faceform designed to simulate the dynamic responses of the human face when subjected to an impact. The faceform is displayed in Figure 3.



Figure 3: The frangible faceform model with the boxing headguard removed. Adapted from “Biomechanics of the head for Olympic boxer punches to the face”, T. Walilko, D. Viano, and C. Bir, 2005, *British Journal of Sports Medicine*, 39 (10), p. 710-719. Copyright 2005 by British Journal of Sports Medicine.

Using the Hybrid III model, the study had seven Olympic level boxers of five different weight categories deliver 18 straight punches to the face of the model. The headform was fitted with an Olympic-style headguard for each of the trials, as shown in

Figure 2; however, due to the punches being delivered to the face, the headguard was not actively engaged. Accelerometers were attached to both the hands of the boxers, as well as the headform to test the acceleration of the hand prior to impact and acceleration of the head following the impact. From the punches, data were collected for peak translational and rotational head acceleration, neck responses, and jaw pressure distribution. Average peak rotational acceleration was 6343 rad/s^2 , significantly higher than the 4500 rad/s^2 , a threshold observed by Ommaya et al. (2002). Head injury risks were calculated according to the protocol by Pellman et al. (2003). From these calculated risks (Pellman et al., 2003), rotational acceleration had the largest effect on head injury risks, having a 68% risk rating. Translational acceleration resulted in a 20% concussion risk, while HIC and change in velocity had 13% and 3% risks, respectively. Punch force increased linearly as the boxer's weight increased. The findings of this study revealed that boxers at the Olympic level pose a high risk of concussions to opponents with a single punch. Additionally, rotational acceleration of the head is a significant factor for concussion risk.

Head dynamic responses and brain tissue deformations resulting from boxing punches were analyzed by Cournoyer and Hoshizaki (2019). Using an anthropometric headform and a finite element model, physical representations of boxing punches presenting with and without LOC were performed. The purpose, as such, was to compare magnitudes of head acceleration and brain tissue deformation for punches resulting in a LOC and punches not resulting in a LOC. Peak linear acceleration, peak rotational acceleration, and strain measures in five regions of the brain were measured from the punch representations. The LOC most often resulted from hook punches (lateral impact to the head involving a rotational motion) to the side of the mandible, which caused high levels of rotational acceleration and increased the magnitude of trauma in all areas of the brain. The differences between punches resulting in a LOC as opposed to those not resulting in a LOC were found in differences in maximum

principal strain for different brain regions. It was also noted that a LOC was caused by higher levels of brain trauma and should be subject to longer recovery times. The results of these types of studies showed that the traumatic effects of boxing led researchers and medical professionals to caution against participation in the sport.

Boxing Safety Recommendations

A previously noted, Purcell & Leblanc (2011) included statements made by the American Medical Association (2007), Canadian Medical Association (2001), and World Medical Association (2017) that all stated that boxing should be banned. As time passed, these organizations have not changed their stance. The World Medical Association (2017) stated that boxing is qualitatively different from other sports due to the injuries caused and that it should be banned. Until a full ban is achieved, the World Medical Association stated that several changes should be made, including that all boxers be licensed, no children should be permitted to compete, and that protective equipment such as headguards should be considered. Similar to the World Medical Association, the American Medical Association included increasing glove size and decreasing scoring emphasis for head blows in its recommendations. The Canadian Medical Association (2001) provided a similar statement, recommending the use of protective headguards and the prohibition of head blows.

Headguard

Headguard rules. Boxing competition is typically sanctioned under a sport governing body which is an organization within a state or country, but can be sanctioned by an international organization, such as the AIBA. These organizations often have their own rules related to competition, including differing regulations for protective equipment such as the use of gloves and headguards (often referred to as headgear or boxing helmets).

Boxing Canada, the national sport governing body for Canada as recognized by the Canadian Olympic Committee, has different headguard rules by gender and competition level. As stated in the official rules, Boxing Canada deems headguards mandatory for elite male open boxers, with the exception of bouts at the National Championships (Boxing Canada, 2017). Additionally, in their provincial championships, Boxing Canada requires headguards to be used until the final, where the boxers are given the option, with headguards prevailing in the case of a disagreement between fighters (Boxing Canada, 2017). For all other Boxing Canada competitions, boxers must use headguards manufactured by the AIBA Official Boxing Equipment License (Boxing Canada, 2017). In the master's Division, boxers are required to use USA Boxing approved Master's headguards (Boxing Canada, 2017).

The AIBA requires headguards to be used at all levels of competition, except in elite male competition, where it is prohibited (AIBA, 2019). United States of America (USA) Boxing requires headguards to be used in all competitive divisions, with the only exception to this rule being in the finals of the national championships, where elite level male boxers may be prohibited from wearing it in accordance with AIBA rules (USA Boxing, 2017).

Headguard specifications. Rules for boxing headguards can vary between boxing organizations. The AIBA, whose rules are used by many major boxing organizations including Boxing Canada, sets out several standards for competition headguards. The following section lists these guidelines as listed in the AIBA Handbook (2019, p. 77-78). Several headguard specifications are set out in the AIBA (2019), including a minimum weight of 450 grams (16 ounces), and a Velcro closing system for fitting. Furthermore, the headguards are required to have a minimum of 2-3 cm of padding, and to be made of high-quality leather, such as cowhide or Grade A leather. As per USA Boxing (2017), USA Boxing requires headguards to be approved by AIBA or USA Boxing. The rule book does not state any specifications to their headguards, only that they must have cheek protectors and an

open face (USA Boxing, 2017). Boxing Canada requires that headguards used in their competitions must be those approved by the AIBA or by USA Boxing (Boxing Canada, 2017).

Testing the material properties of boxing headguards can be useful for determining their energy absorption ability. The ability of protective headwear to mitigate the effects posed to the head and brain relates to energy dissipation. Energy dissipation is the conversion of mechanical energy into another form of energy, such as heat (McLean et al., 1997; Zerpa et al., 2016). A material absorbing energy has a loading and an unloading phase. The most ideal response to energy absorption would be for the foam of a helmet to be loaded with all of the energy of an impact and all of this energy then being dissipated out during the unloading phase (Zerpa et al., 2016). Subsequently, all of the energy would be absorbed and directed away from the head and brain (Zerpa et al., 2016). A higher dissipation value translates to a lower rebound velocity, reducing the risk of a contrecoup injury, where the brain collides with the skull as a result of the impact (Barth et al., 2001; Zerpa et al., 2016).

Subsequently, testing which materials are the most effective in dissipating energy can be useful for determining the most effective headguard design. Razaghi et al. (2018) examined three different types of headguard materials including expanded propylene (EPP), expanded polystyrene foam (EPS), and polyvinyl alcohol sponge (PVA) to analyze the most effective material for reducing the amount of injury resulting from a right hook to the face. Using a finite element model of the skull, headgear, and punch, von Mises stress (distributions of effective/fringe stress) of the zygomatic bone was analyzed under the three different materials. It was reported that the EPS material was more effective than the other two materials for reducing the von Mises stress, and subsequently the amount of injury, to the face of the model. Despite these results, a much wider range of material properties can be tested to assess concussion risk. Similarly, a number of different headguard materials not

analyzed in the aforementioned study can have an effect on these material properties to mitigate not only linear acceleration impact but also rotational accelerations and consequently, the risk of concussion.

Thermoplastic polyurethane. The use of thermoplastic polyurethane (TPU) material has been shown in several protective sports headwear models. Thermoplastic polyurethane is a polymer containing a hard segment composed of urethane groups and a soft segment composed of polyol (Lin et al., 2017). The TPU compound has the elasticity of rubber and the mechanical properties of plastic materials. When used with other materials, TPU has demonstrated high tensile and flexural strength making it effective for impact absorption (Lin et al., 2017). Several helmet models incorporated TPU material into their design, including several NOCSAE-approved helmets (Cournoyer, Post, Rousseau, & Hoshizaki, 2016).

Previous research has also shown TPU material to be effective for reducing lower peak accelerations at lower velocities (Barker et al., 2018). Furthermore, quasi-static testing has shown three-dimensional printed TPU to be useful for energy absorption and impact protection when compressed given its tailorable and flexible structure (Bates et al., 2019). Finally, high velocity impact testing performed in a study by Rizzo et al. (2020) has shown that energy absorption and damage mitigation of hybrid structures is optimized when a TPU layer is introduced into the lamination sequence. Results of this study found that a reduction of at least 54% of absorbed energy, damage extension, and maximum indentation were seen in the hybrid structures when a 1 mm thick TPU layer was applied on the impact surface (Rizzo et al., 2020).

Zerpa et al. (2020) examined the effectiveness of TPU material to reduce concussion likelihood when incorporated into cycling helmets. To do this, a set of 4.8 m/s impacts to the front, side, and rear locations of a NOCSAE headform were conducted with a cycling helmet tested with and without TPU material. The study found reductions in peak resultant linear

acceleration scores ranging between 8.37% and 25.48% when TPU was used. The study also found reductions in GSI scores ranging between 20.97% and 27.62% across impact locations with use of TPU. This provides evidence of the effectiveness of TPU to minimize concussion risk caused by linear accelerations with use in cycling helmets.

Impact Testing

Standards for impact testing of boxing headguards. To date, the standards of testing for boxing headguards are very minimal. As noted by McIntosh and Patton (2015a), the AIBA does not specify impact performance tests for head guards nor do they mandate any standard. The only standards noted by AIBA are in the construction and dimensions of their headguards (AIBA, 2019).

The NOCSAE sets out standards for various types of athletic equipment, including standards for pneumatic ram testing of protective headgear. Several studies have complied with NOCSAE standards in their methods, including studies performed by Jeffries et al. (2017a) and Zerpa et al. (2016) but these NOCSAE standards techniques have not been used extensively for boxing equipment testing.

Several standards for tests on the performance of headgear and face guards through the use of linear pneumatic ram testing have been identified (NOCSAE, 2018). Pneumatic ram, or linear impact testing, has been designed to deliver an impact to a helmeted and instrumented headform on a Hybrid III neck (NOCSAE, 2018). This system is designed to measure both linear and rotational acceleration through subjecting the headgear to both centric and non-centric impacts, ultimately providing evidence regarding the performance capacity of the headgear (NOCSAE, 2018). Rotational acceleration is defined by NOCSAE (2018, p. 1) as “a measure of impact severity with respect to the peak acceleration experienced by the headform measured in radians per second squared (rad/s^2).” Furthermore, NOCSAE (2018) reported that this testing method was a reliable and repeatable measure for

evaluating protective headgear. The method was based on pass or fail criteria for Severity Index (SI), rotational acceleration, and within specified tolerances for other measures (NOCSAE, 2018).

In describing the test method for pneumatic ram testing, NOCSAE (2018) identified that the headgear was positioned on a headform mounted onto a 50th percentile Hybrid III neck model that was mounted to a linear bearing table. This assembly was designed to replicate and achieve post impact kinematics. To test this, an impactor was propelled at the headgear at a velocity within 2% of a specified level over a distance of no more than 2 in. (NOCSAE, 2018). With each impact, the resultant peak linear acceleration, SI, and resultant peak rotational acceleration was captured (NOCSAE, 2018).

For impact locations, NOCSAE (2018) identified several impact locations relative to the size of the NOCSAE standard headform. For a medium sized headform, side impacts on the coronal plane were set to $\alpha = 7^\circ$ and $\beta = -90^\circ$. The NOCSAE (2018) also suggested that side impacts should be +60 mm on the Z-axis relative to the basic plane. For front impacts in the midsagittal plane, NOCSAE (2018) defined that impacts should be positioned at $\alpha = 15^\circ$, $\beta = 0^\circ$, and +78 mm on the Z-axis relative to the basic plane.

The NOCSAE defined headgear impact testing standards for certain sports such as ice hockey, football, baseball, and lacrosse; however, no testing standards specific for boxing headgear testing have been identified. As a result, little research conforming to the NOCSAE standards have been performed to evaluate boxing headguard performance.

Previous impact test research on boxing headgear. Using a linear impactor, McIntosh and Patton (2015a) tested several AIBA approved boxing headguards to examine the effects of the headguards on head impact dynamics and injury risk. Impacts ranging between 4.1 and 8.3 m/s were imparted by the impactor comprised of a 4 kg semi rigid fist fitted with a glove. These impacts were delivered to the head of a Hybrid III head and neck

system equipped with and without a headguard. Significant differences in head impact responses were seen between the headguard models in lateral and forehead tests with peak contact forces ranging between 1.9 and 5.9 kilonewtons (kN). With an impact speed of 8.3 m/s, mean peak resultant acceleration was 130 g for bare headform impacts to the forehead. Comparatively, the use of the headguard reduced mean peak resultant acceleration to 85 g. Additionally, for impacts at a speed of 6.85 m/s to the bare headform, mean peak resultant angular head acceleration ranged between 5200 - 5600 rad/s^2 , which was almost halved by the use of the headguard. For 45° forehead and 60° jaw impacts, linear and angular accelerations were also reduced with the use of the headguard. The findings of this study confirmed that the use of AIBA headguard was useful in reducing the forces that may result in concussion in boxing.

Dau et al. (2006) also examined the ability of boxing headguard to mitigate peak rotational head acceleration, peak linear head acceleration, peak punch force, and HIC by using a Hybrid III headform model. This study had 27 amateur boxers impact the head of the model with a dominant hand hook punch. Similar to the previous study, accelerometers were positioned on both the hands of the boxers and on the head of the dummy. This study compared the results for boxers of different heights, masses, ages, and sexes and trials were recorded with and without the use of a headguard. The use of a headguard was particularly effective for mitigating many of the aforementioned head injury measures. Significant decreases were seen in peak rotational acceleration (9164.10 to 5534.78 rad/s^2), peak resultant acceleration (78.04 to 51.79 g), punch force (4260.51 to 2815.59 N), and HIC (79.23 to 47.34) when the headguard was worn by the model. It is important to note that despite the significant decreases seen in peak rotational acceleration, the measures found both with and without the use of the headguard were still well above the aforementioned threshold

of 4500 rad/s². The findings of this study showed that although the use of a headguard may not eliminate concussion in boxing, it is still beneficial for reducing the risk.

McIntosh and Patton (2015b) tested the impact energy attenuation ability of boxing headguards in a number of drop tests. The study tested seven different commonly used training and competition headguards, including two approved by the AIBA. Tests were performed by completing repeated drops from different heights against a flat rigid anvil fixed with or without a boxing glove. Impacts were imparted on an International Organization for Standardization® (ISO®) rigid headform. Peak linear acceleration of the headform was measured on the centre forehead and lateral headguard impact areas.

The effectiveness of the headguard varied by testing condition but the thicker-designed headguards showed the best performance for 0.4 m (drop height) rigid anvil tests. In these tests, the average peak linear headform acceleration was 48 g, significantly less than the lowest model, which produced 456 g peak acceleration. As well, deterioration of the headguard with repeated drops was found to be reduced when impacted against a glove. There was a 72 - 93% reduction in the overall acceleration with the combination of the use of gloves and headguard as opposed to only the headguard for 0.6 and 0.8 m drop tests. Overall, it was reported that each style and brand of headguard performed differently, showing that testing is beneficial for determining the effectiveness of different headguards for competition. Of these brands, the Adidas® taekwondo model was the worst performing headguard for frontal and lateral drop test, while the Top Ten® AIBA model was superior to the Adidas® AIBA model used in the study.

O'Sullivan and Fife (2016) also tested the ability of headguards in mitigating the RLA of the head when impacted by using the Hybrid III model. The study tested two AIBA approved boxing headguards and two World Taekwondo Federation (WTF) approved karate headguards to compare the headguards used in each of their respective sports. Impacts were

imparted on the head of the Hybrid III dummy at a terminal striking velocity of 5.0 m/s using a standardized martial arts head striker. A total of five impacts were imparted to the left side of the headguard. The Adidas® taekwondo headguard was the most useful for limiting resultant acceleration (60.5 ± 4.3 g), followed by the Adidas® boxing headguard (75.4 ± 9.9 g). The findings of this study suggested that there are not significant differences between boxing and taekwondo headguard for mitigating RLA and also suggested that different models may produce different results with the headguard manufactured by Adidas® providing the most protection.

To explore linear and rotational impact effects of the boxing glove and headguard padding, Bartsch et al. (2012) performed pendulum impacts to a Hybrid III model with hook punch impacts at low and high energy levels. From these impacts, five padding conditions were analyzed including unpadded (control), mixed martial arts (MMA) glove–unpadded head, boxing glove–unpadded head, unpadded pendulum–boxing headgear, and boxing glove–boxing headgear. These impacts were used to test the theoretical brain, skull, and neck injury risk based on 17 injury risk parameters. It was reported that each of the padding conditions reduced linear impact dosage based on the 17 injury risks, but the boxing glove–headgear condition was the most effective in reducing linear impact dosage. The results of this study found that head and neck injury risk accumulated the fastest with less padding on the hands and head.

Studies published to date have shown strong evidence supporting the use of headguards in the sport of boxing. Much of this research can be used to infer that headguards perform well to mitigate linear and angular impacts. The literature, however, fails to show a strong connection between the performance differences in headguards relating to material differences. Specifically, very little research to date has shown the influence of TPU and other materials to mitigate head injury risk under different impact conditions.

Research Problem

Despite advances in boxing headguard production, the current literature shows that concussions are still highly prevalent in boxing competition, which highlights the need for the use of innovative technologies and precautionary measures to be taken to mitigate the risk of concussions. The literature also shows that despite the use of TPU material in some helmet research studies for different sports (e.g., hockey and cycling) to minimize the magnitude of head impacts, no research has been conducted to demonstrate the usefulness of this TPU technology in boxing headgear as an avenue to mitigate the risk of concussions. Based on these constraints, there is a need to examine the material properties of boxing headguards with and without TPU to measure the structural integrity and energy absorption of the boxing headgear at different locations. Furthermore, there is a need to understand the impact attenuation ability of TPU with the headguard under impact conditions similar to those that one would experience in boxing competition. This need includes testing the commercial headguards, and TPU-commercial headguard combinations with impacts of different velocities and impacts directed at different head locations. This approach may be useful for providing evidence of the TPU material effectiveness in mitigating the risk of concussion for future headguard production in the sport of boxing.

Research Purpose

Based on the gaps in the existing literature, this study examined the material properties of commercial boxing headgear and innovated TPU liner inserts in mitigating linear and angular impact kinematics. The study also explored other avenues to assess the risk of concussion in the sport of boxing using measures of linear and rotational impacts to the head in combination or separately. Specifically, the first purpose of this study was to analyze the material properties of TPU and boxing headguards statically to test the energy absorption capacity of the material across different boxing headgear locations. The second purpose of this study was to examine the effect of headguard type and impact location on measures of peak resultant linear acceleration and peak resultant angular acceleration during simulated dynamic impacts. The third purpose of the study was to examine the effect of headguard type and impact location on head injury risk using measures of linear and rotational impact accelerations separately and in combination during simulated dynamic head collisions.

Research Questions

The first purpose of the study was addressed by the following question:

- 1) Which boxing headguard (Century® Drive, Adidas®, and TPU-Century® Drive) absorbed the most energy when loaded with a compressive and shear force across locations (front and side) during static testing?

The second purpose of the study was addressed by the following questions:

- 2) Which boxing headguard (Century® Drive, Adidas®, and TPU-Century® Drive) would perform better in decreasing linear impact acceleration across different impact locations (front, front boss, and side) during dynamic testing?
- 3) Which boxing headguard (Century® Drive, Adidas®, and TPU-Century® Drive) would be more effective in mitigating angular acceleration at each impact location (front, side, front boss, and side) during dynamic testing?

The third purpose of this study was addressed by the following questions:

- 4) Which boxing headguard (Century® Drive, Adidas®, and TPU-Century® Drive) would perform better at decreasing the risk of head injury due to the effect of linear impact acceleration across different headgear locations (front, front boss, and side) during dynamic testing?
- 5) Which boxing headguard (Century® Drive, Adidas®, and TPU-Century® Drive) would perform better at decreasing the risk of head injury due to the effect of angular impact acceleration across different locations (front, front boss, and side) during dynamic testing?
- 6) Which boxing headguard (Century® Drive, Adidas®, and TPU-Century® Drive) would perform better at decreasing the risk of head injury due to the shared effect of

linear and angular impact accelerations across different headgear locations (front, front boss, and side) during dynamic testing?

Method

Instrumentation

Chatillon® TCD1100 Force Tester, and American Mechanical Technology Incorporated (AMTI®) Force Plate. The Chatillon® force tester and AMTI® force plate were used to measure the energy absorption properties of the boxing headguards (Century® Drive, Adidas®, and TPU-Century® Drive). The energy absorption of the boxing headguards was computed by compressing the sample against the TLC© series load cell. The tester compressed the headguards by a given distance. It then uncompressed the materials to the undeformed state. The force plate recorded the forces. Plots of compressive force versus material compression, and shear force versus shear displacement were obtained for both the compressing and uncompressing stages. The enclosed area between the plots was evaluated to indicate the energy absorbed. The Chatillon® TCD1100 machine is illustrated in Figure 4.

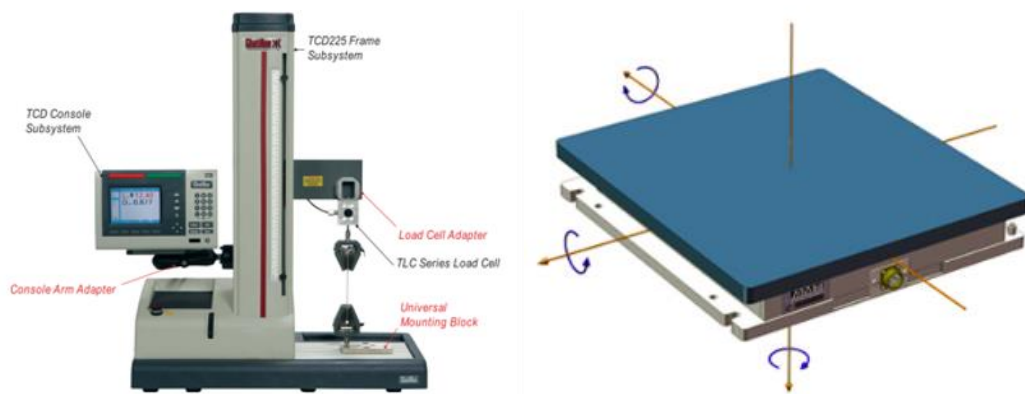
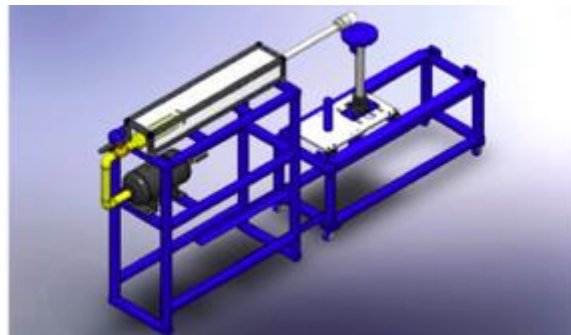


Figure 4: A schematic of the Chatillon® TCD1100 Force Tester (left) and the American Mechanical Technology Incorporated (AMTI®) Force Plate (right). Adapted from “Chatillon® TCD Series Console, For Use with TCD110, TCD225 and TCD1100 Series Digital Force Testers, User’s Guide”, Ametek Inc., 2008, p. 1-2; and “Choosing a Force Plate”, Advanced Mechanical Technology Inc., n.d.

Pneumatic horizontal impactor. The pneumatic horizontal impactor used in this study included a large welded steel structure composed of a main frame, linear bearing table, and an impacting rod. The subcomponents of the main frame contained a compressed air

tank, air cylinder, and air release valve. An MGA-100-A digital pressure gauge© was used to fill the air tank with compressed air corresponding to an impact velocity as shown in Table 2. When air was released, the air cylinder propelled the impact rod towards the headform of the model up to a velocity of 7 m/s (Jeffries et al., 2017a). The impactor rod weighed 13.1 kg and it was composed of a cylindrical nylon pad attached to a metal disc. The linear bearing steel table designed to secure and position the headform, contained a shuttle plate that moved along a 0.49 m track before being stopped by rubber blocks. This movement allowed for the simulation of backward movement that might take place during a real-life impact. The shuttle table had a mass of 46.6 kg on its own, increasing to 56.1 kg with the standard NOCSAE headform in place. Furthermore, weight could be added to the shuttle table to simulate a higher body mass (see Figure 5).



*Figure 5: A schematic of the pneumatic horizontal impactor. Adapted from “The Use of a Pneumatic Horizontal Impact System for Helmet Testing”, L. Jeffries, C. Zerpa, E. Przysucha, P. Sanzo, and S. Carlson, 2017, *Journal of Safety Engineering*, 6(1), p. 8-13. Copyright 2017 by Journal of Safety Engineering.*

The reliability and validity of this pneumatic horizontal impactor were verified by Jeffries et al. (2017b). To test the reliability, 100 impacts were imparted on the headform with a helmet and compared even and odd trials for peak linear acceleration across the front, side, and rear impact locations. Trials were correlated using an intraclass correlation (ICC) in a split-half method. By location, ICC measured ranged between .79-.86, showing consistency across locations and consequently high reliability. To show evidence of validation, Jeffries et

al. (2017b) compared the impacts of the horizontal impactor to similar impacts of a standard NOCSAE drop rig. Trials were conducted with each system using the same impact velocity, helmet, and impact anvil materials. The ICC measures across impact locations ranged between .85-.95, which showed evidence of concurrent validity.

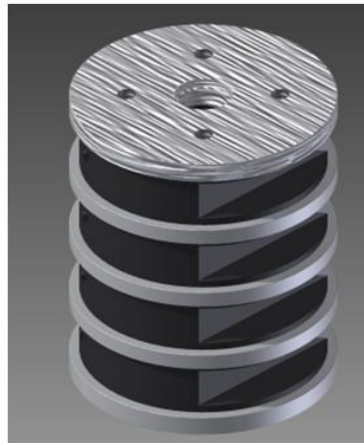
Headform. This study utilized a standard NOCSAE headform. The headform was a medium-sized model designed to represent the human head and simulate human mechanical responses to movement. The headform was 4.90 kg in mass and was equipped with appropriate facial features and bone structures designed to be representative of the 50th percentile adult head. As such, it was more anatomically representative of the human head than the Hybrid III model that has been used in many of the aforementioned studies (Zerpa et al., 2016). The headform was free to move in several directions including forward and backward, laterally, up and down, tilting forward and backward, and laterally rotating. The headform had accelerometers positioned inside of the head that allowed for linear acceleration to be measured in anterior-posterior, superior-inferior, and left-right directions. Figure 6 shows the NOCSAE headform that was subjected to impacts in this study.



Figure 6: Mechanical headform and neckform assembly.

Mechanical neckform. The neckform used for this study was designed to represent the 50th percentile of a human neck. The neckform was composed of four neoprene discs positioned between circular steel discs. The neckform contained component materials used to

prevent displacement of the discs. To further prevent displacement, the rubber discs of the model had a slight protrusion beyond the metal discs which allowed for a tight compression of the discs (Jeffries et al., 2017a). The components of the neckform were held together by a top plate and base bracket. The neckform, as shown in Figure 7, was designed with a hole through the centre of the discs and large cut outs in each rubber disc on the posterior aspect, which helped the neckform to simulate inertial effects of the human neck upon loading (Jeffries et al., 2017a, Zerpa et al., 2016). Neckform stiffness levels were manipulated by tightening the neck to correspond to different torque values, as determined by Carlson (2016).



*Figure 7: Mechanical neckform assembly. Adapted from “The Use of a Pneumatic Horizontal Impact System for Helmet Testing”, L. Jeffries, C. Zerpa, E. Przysucha, P. Sanzo, and S. Carlson, 2017, *Journal of Safety Engineering*, 6(1), p. 8-13. Copyright 2017 by Journal of Safety Engineering.*

Accelerometers, sensors, power supply, and software interfaces. The surrogate headform contained a piezoelectric sensor designed to measure the magnitude of impact (Jeffries et al., 2017a). A PCB© model 482A04 integrated circuit piezoelectric sensor (ICP) amplifier/power supply unit was used to convert analog output signals from the accelerometers to digital signals (Jeffries et al., 2017a). This conversion occurred via an analog to digital converter from AD Instruments® PowerLab26T (Jeffries et al., 2017a). The accelerometers measured acceleration in the superior-inferior, anterior-posterior, and left-

right directions, noted as Z, Y, and X, respectively (Jeffries et al., 2017a). Acceleration was measured at a sampling frequency of 20 kHz and converted to units of gravity (g) (Jeffries et al., 2017a). The conversion to g was obtained through the arithmetic function of PowerLab® Version 7.3.1 software as shown in Equation 4 (Jeffries et al., 2017a).

$$g_{(i)} = Ch_{(i)} / 0.01041 \quad (4)$$

where:

$g_{(i)}$ = acceleration value for each channel, in g.

$Ch_{(i)}$ = channel acquiring acceleration information from X, Y, or Z axis in measures of volts; and i represents the axis for each acceleration X, Y, and Z.

The X, Y, and Z channels were combined to create a resultant acceleration channel representing the total magnitude of impact. Furthermore, a 1000 Hz cut-off low-pass filter was applied to the resultant acceleration channel to eliminate the effect of high frequency noise generated during headform vibrations due to the impacts.

In addition, a Delsys Trigno™ wireless gyroscope sensor attached to the neckform was used to measure the angular displacements of the neck for each impact. The gyroscope measured the angular velocity of the head about the Z directions. A magnetometer integrated with the gyroscope sensor was used to measure the angular displacements about the X and Y directions. The sensors collected the data at a rate of 148 samples per second. All sensors were calibrated using an inclinometer placed on top of the surrogate headform.

To ensure the sensors did not slip when the head was impacted, they were reinforced with tape. The following image displays the Delsys Trigno™ wireless gyroscope sensor that was placed and taped on the top of the headform for dynamic impact tests. The headform with the Delsys Trigno™ wireless gyroscope sensor taped to the top is shown in Figure 8.



Figure 8: Delsy's Trigno™ Wireless Gyroscope Sensor.

Headguard models. The first headguard used in this study was a Century® Drive full face headguard. This headguard was composed of polyurethane and polyethylene foam outer shell, as well as polyvinyl gel and wool. The ear section of the Century® Drive headguard contained only a thin leather covering, with no additional foam padding. The Century® Drive model was mounted on the headform and neckform assembly is shown in Figure 9.



Figure 9: Century® Drive headguard model.

The second model used in this study was an Adidas Response Standard Semi-open Experienced Boxing Headguard®. It had an outer shell composed of polyurethane material, and an inner layer composed of a high-density foam and I-comfort+ quick dry and anti-slip

fabric. The Adidas® model was mounted on the headform and neckform assembly as shown in Figure 10 for the dynamic testing.



Figure 10: Adidas® headguard model.

Both commercial headguards were composed of an outer shell made from artificial leather, so they did not meet the AIBA (2019) requirement of high-grade leather. With this said, Adidas® and Century® Drive produced several models like these that are often used in training and competition settings.

Thermoplastic polyurethane. This study used 3D printed TPU inserts placed as a headguard on the headform. This study utilized two small TPU samples, and one large TPU sample, decided on the basis of fit within the headguard. The large sample was placed in the front location of the headguard, and the two small samples were placed on the front boss and side locations of the headguard. The 3D printed TPU inserts are shown in Figure 11.



Figure 11: TPU inserts. The three large (left) and small (middle, right) 3D-printed TPU inserts used in this study.

When placing the TPU inserts into the Century® Drive commercial headguard, cuts were made into the padding of the headguard via the inner felt layer. All interior foam padding in each location (front, front boss) was removed to be replaced with a TPU insert, with the outer leather shell being kept in place. Only the necessary amount of inner foam material was removed from the headgear to firmly fit the TPU insert (see Figure 12).



Figure 12: TPU inserts placed into Century® Drive headguard. Cut Century® Drive headguard with a large TPU insert at the front (right) and a small TPU insert at the front boss (left) impact locations.

After the TPU was in place, the inner felt leather was re-stitched. The purpose of this design was to create a section of the headguard where only TPU would be impacted, and the existing impact absorption materials would produce minimal to little effect. For side impacts, as the Century® Drive headguard had an open, thin ear covering, no material was cut out, and a TPU insert was placed within the opening of this section. Figure 13 displays an image of the side (ear) section of the TPU-Century® Drive headguard.



Figure 13: Side section of the TPU- Century® Drive headguard.

Procedure

Static testing. All three headguards underwent a static compression test, where the Chatillon® force tester compressed the headguard to analyze changes in the material properties (VanLandingham et al., 2005). Trials were conducted at both the front and side locations (Figure 17 and Figure 19, respectively). The Chatillon® force tester was modified to add a wooden mounting block formation that compressed the material at a 30° angle to produce a both a compression and shearing effect. Analyzing both compression and shear energy loading better replicates the complex loading situations that a material is subjected to in real life cases, with the two more often occurring in combination than individually (Ling et al., 2008).

Furthermore, the top block is equipped with a force sensor that recorded the loaded and unloaded forces of the material. The bottom block was connected to an aluminum bracket to prevent sliding of the material during testing. Each headguard was fitted between the wooden mounting blocks of the machine, shown in Figure 14.



Figure 14: Chatillon® TCD1100 Force Tester with modified block formation.

The Chatillon® TCD1100 Force Tester took data of force and displacement (F_v and total displacement as shown in Figure 15 below) of the material over the duration of static testing. The computation from force and displacement data to energy absorption was performed using a number of processes via the MATLAB® software. The following free-body diagram displays the breakdown of forces (shear force T , compressive force N , horizontal force F_H , vertical force F_v) and components of displacement (compression and shear displacement) when the material is compressed or uncompressed. These diagrams are shown in Figure 16.

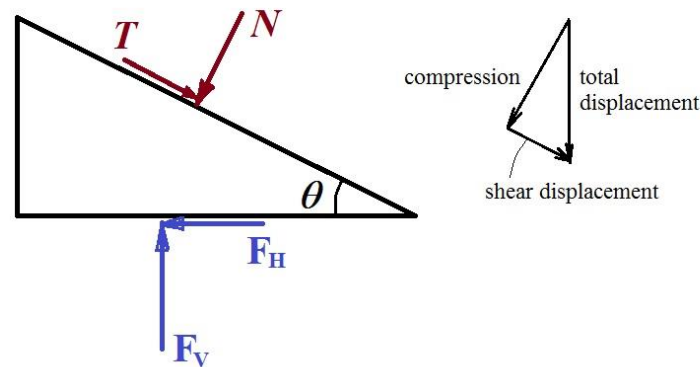


Figure 15: Free-body diagram (left) and components of displacement (right).

The force capacity of the Chatillon® TCD1100 Force Tester was set to 3000 N to prevent damaging of the machine. The testing speed was set to 25 mm per minute to ensure a slow enough speed for the testing to be considered static. A total of 15 cycles were conducted for each location of each headguard (Adidas®, Century® Drive, TPU-Century® Drive) respectively. The placement of the Adidas® headguard at the front location is shown in Figure 16.



Figure 16: Front static compression test of the Adidas® headguard.

Force and displacement data were extracted across all cycles by the Chatillon® system. At the same time three force signals, F_X , F_Y and F_Z , were obtained from the American Mechanical Technology Incorporated (AMTI®) force plate in the X, Y, and Z directions. The X and Y force vectors were added together to compute the horizontal resultant force vector (F_H). The vertical force vector (F_V) was simply the force measured in the Z direction. Horizontal force resultant vector (F_H) is shown in Equation 5.

$$F_H = \sqrt{F_X^2 + F_Y^2} \quad (5)$$

where:

F_X = force in the x direction

F_Y = force in the y direction

These data were then analyzed using a MATLAB® script that calculated the shear and compression forces in terms of the horizontal and vertical forces. Shear force (T) and compression force (N) were calculated using Equation 6 and Equation 7, respectively. In these equations, $\theta = 30^\circ$ is the wedge angle of the wooden mounting block formation.

$$N = F_V \cos\theta - F_H \sin\theta \quad (6)$$

$$T = F_H \cos\theta + F_V \sin\theta \quad (7)$$

To evaluate energy absorption, the same MATLAB® script were used to generate plots of force vs. displacement, and to calculate the total, compression, and shear energy absorptions. Equation 8, Equation 9, and Equation 10 show how energy absorptions were determined for the total, compression, and shear, respectively.

$$\text{Total Energy Absorption} = \frac{\text{enclosed area of } F_z \text{ versus total displacement plot}}{\text{area under loading plot of } F_z \text{ versus total displacement}} \quad (8)$$

$$\text{Compression Energy Absorption} = \frac{\text{enclosed area of N versus compression plot}}{\text{area under loading plot of N versus compression}} \quad (9)$$

$$\text{Shear Energy Absorption} = \frac{\text{enclosed area of T versus shear displacement plot}}{\text{area under loading plot of T versus shear displacement}} \quad (10)$$

The force vs. displacement data were used to determine the energy loaded and unloaded on the headguard material during the static testing. The percent of energy absorption was obtained by dividing the energy unloaded over the energy loaded.

Dynamic testing. All headguard dynamic tests were performed according to NOCSAE standards (NOCSAE, 2018). Headguards used in this study were positioned on a headform mounted to a mechanical neckform (NOCSAE, 2018). Neck strength was kept constant for all impacts. This neck strength was adjusted as shown in Figure 20 with a calibrated torque wrench between impact locations to maintain the 12-in-lbs strength designed to represent the 50th percentile male neck. (NOCSAE, 2018). Impact locations complied with NOCSAE (2018) standards for the front, side, and rear impacts on a medium sized headform.

Impact locations. Impacts were conducted for each of the 18 velocities for the front, front boss, and side locations. Impact locations were according to NOCSAE (2018) standards for a medium sized headform. Table 1 presents the specific measurements for a medium sized headform (NOCSAE, 2018).

Table 1

Impact location specifications for a medium-sized headform.

Impact Location	α	B	Z axis relative to basic plane	Y axis
Front	15 °	0 °	+78 mm	On the midsagittal plane
Front Boss	15 °	-60 °	+73 mm	56 mm anterior to coronal plane
Side	7 °	-90 °	+60 mm	On the coronal plane

Note. Adapted from “The Effect of Facial Protection, Impact Location, and Neckform Stiffness on Peak Linear Acceleration, Risk of Injury, and Energy Loading Measures of Horizontal Impacts on a Hockey Helmet”, Jeffries, 2017, p. 78, Master’s thesis, Lakehead University. Copyright 2017 by Leigh Jeffries.

For the different locations, the head and neck were rotated on the linear bearing table.

Figure 17, Figure 18, and Figure 19 display each individual impact location (front, front boss, and side), respectively as represented by NOCSAE (2018).

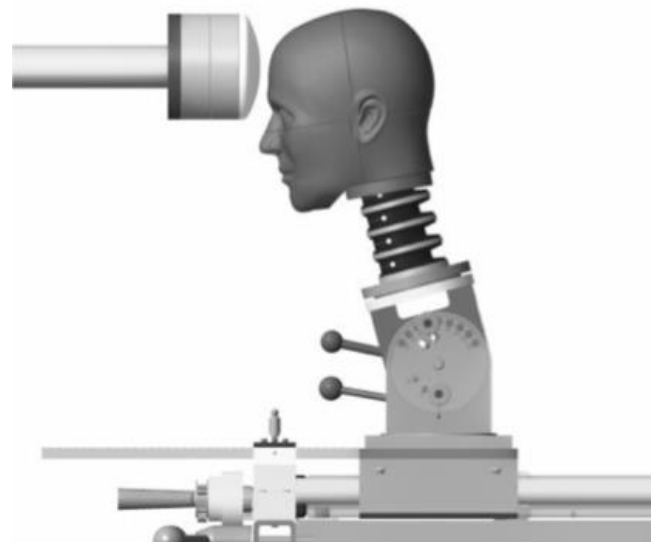


Figure 17: Front Impact Location (NOCSAE, 2018). Adapted from “Standard pneumatic ram test method and equipment used in evaluating the performance characteristics of protective headgear and face guards”, NOCSAE, 2018, p. 3. Copyright 2018 by NOCSAE.

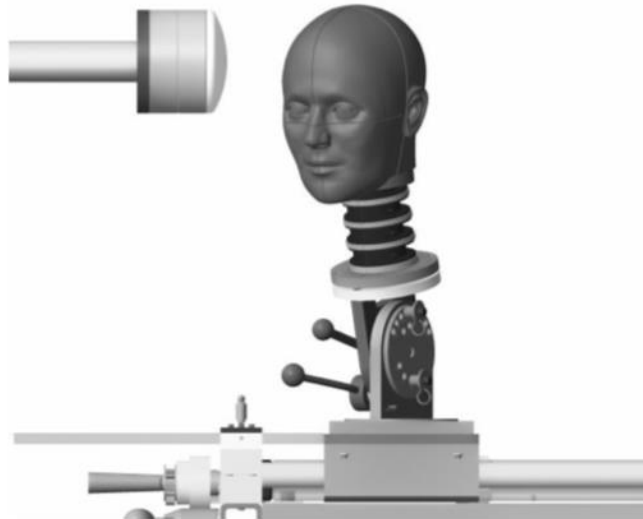


Figure 18: Front Boss Impact Location (NOCSAE, 2018). Adapted from “Standard pneumatic ram test method and equipment used in evaluating the performance characteristics of protective headgear and face guards”, NOCSAE, 2018, p. 8. Copyright 2018 by NOCSAE.

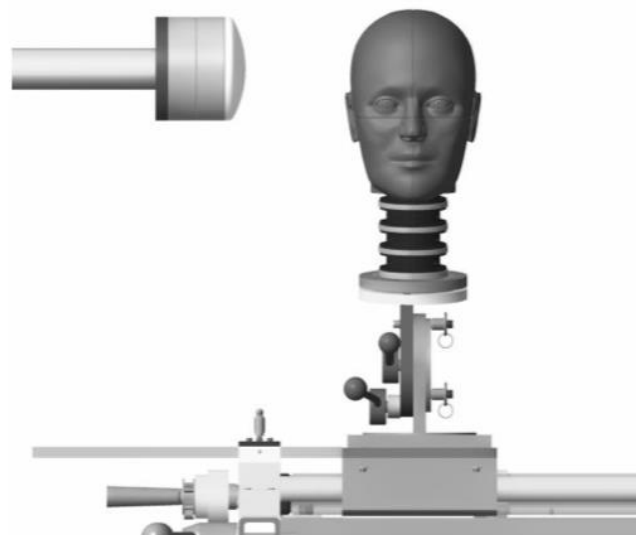


Figure 19: Side Impact Location (NOCSAE, 2018). Adapted from “Standard pneumatic ram test method and equipment used in evaluating the performance characteristics of protective headgear and face guards ”, NOCSAE, 2018, p. 7. Copyright 2018 by NOCSAE.

For the trials conducted with the TPU material, impacts were directed at the portion of the TPU-Century® Drive headguard where the TPU was inserted. These locations remained consistent to where the impacts occurred on the commercial headguards. Trials were

conducted for 3 headguard types, 3 impact locations, and 18 impact velocities. This design resulted in a total of N=162 impacts.

Impact velocity. Impacts were conducted at 18 different impact velocities at three different impact locations (front, front boss, side). These impact velocities were accomplished by adjusting the compressed air pressure to be released from the air tank. The pressure-velocity formula is shown in Equation 11 (Jeffries et al., 2017a):

$$v = 0.00005p^3 - 0.0063p^2 + 0.3307p - 2.9423 \quad (11)$$

where:

p = air pressure, in psi

v = velocity, in m/s.

Air pressure augmented in increments of 2 psi, with corresponding impact velocities beginning at 2.01 m/s and increasing at an average of 0.2 m/s to the highest velocity, 5.13 m/s. Each air pressure and its corresponding impact velocity are shown in Table 2.

Table 2

Compressed air tank pressure of the horizontal impactor and corresponding impact velocity.

Pressure (psi)	Impact Velocity (m/s)
24	2.01
26	2.14
28	2.42
30	2.62
32	2.83
34	3.12
36	3.25
38	3.47
40	3.61
42	3.64

44	3.86
46	3.94
48	4.11
50	4.26
52	4.48
54	4.56
56	4.65
58	5.13

Note. Adapted from “The Effect of Facial Protection, Impact Location, and Neckform Stiffness on Peak Linear Acceleration, Risk of Injury, and Energy Loading Measures of Horizontal Impacts on a Hockey Helmet”, Jeffries, 2017, p. 75, Master’s thesis, Lakehead University. Copyright 2017 by Leigh Jeffries.

Neck strength. The neck was torqued to ensure 12 in-lbs of stiffness prior to each subset of impacts (18 impacts at each location) for each headguard. This procedure ensured that the neck has not been weakened by the prior impacts. In cases where an impact caused the headguard to shift or loosen, it was readjusted within the subset of impacts. Figure 20 displays the method used for adjusting the strength of the neckform, using the torque wrench and a load cell.



Figure 20: Neck strength adjustment setup.

Linear acceleration. Linear accelerations in each of the directions (X, Y, and Z) were analyzed and displayed in LabChart® using the data obtained from PowerLab® via the accelerometers positioned in the headform. The resultant linear acceleration (RLA) was calculated within Labchart® using Equation 12.

$$RLA = \sqrt{a_x^2 + a_y^2 + a_z^2} \quad (12)$$

where:

a_x = linear acceleration in the x direction

a_y = linear acceleration in the y direction

a_z = linear acceleration in the z direction

Additionally, the peak resultant linear acceleration (PRLA) was recorded by the Labchart® software.

Angular acceleration. To obtain angular acceleration, a set of steps was taken, as the measured signals were angular velocity about the Z direction (from the gyroscope) and angular displacements about the X and Y directions (from the magnetometer).

Step 1: The signals obtained from the gyroscope sensor in units of volts and the magnetometer in units of microteslas were calibrated and converted to units of degrees.

Step 2: The angular velocity about Z was numerically integrated to obtain the angular displacement about Z. Resultant angular displacement was then calculated using Equation 13.

$$\theta = \sqrt{\theta_x^2 + \theta_y^2 + \theta_z^2} \quad (13)$$

where:

θ_x = angular displacement about the X direction

θ_y = angular displacement about the Y direction

θ_z = angular displacement about the Z direction

Step 3: Using a MATLAB® script, smoothed splines were used to model the individual and resultant angular displacements, and angular velocities were then calculated using the derivatives of splines.

Step 4: The smoothed splines and derivatives of splines were repeated on the angular velocities to obtain individual as well as resultant angular accelerations. Resultant angular acceleration was calculated as a vectorial sum of angular accelerations about the X, Y, and Z directions, as shown in Equation 14.

$$\alpha = \sqrt{\alpha_x^2 + \alpha_y^2 + \alpha_z^2} \quad (14)$$

where:

α_x = angular acceleration about the X direction

α_y = angular acceleration about the Y direction

α_z = angular acceleration about the Z direction

Risk of injury. GSI was calculated using the RLA measures via a MATLAB® script.

This calculation was done using Equation 2. The equation is restated below.

$$GSI = \int_0^T [a(t)]^{2.5} dt$$

where:

$a(t)$ = instantaneous resultant linear acceleration of the headform

T = impulse duration

To account for the instantaneous angular acceleration experienced by the headform, Angular Gadd Severity Index (AGSI) was used as a variable. The AGSI is similar to GSI,

where the resultant linear acceleration $a(t)$ is replaced with resultant angular acceleration $\alpha(t)$, expressed in radians/s². In GSI, the linear acceleration $a(t)$ is dimensionless, so for angular acceleration $\alpha(t)$ to become dimensionless, it needs to be normalized. The value used for normalization in this study was 88 radians/s². The adjustment was made by taking into consideration what the angular acceleration about the centre of mass of the head would be if 9.81 m/s² was applied to the top of skull. The adjustment was implemented by dividing the linear acceleration on the top of the head (9.81 m/s²) by the average distance of 11.15 cm measured from the centre of mass of the head to the top of the head (Clauser et al., 1969). Equation 15 presents the angular GSI adjustment.

$$9.81 \text{ m/s}^2 \div 0.1115 \text{ m} \approx 88 \text{ radian/s}^2 \quad (14)$$

With this adjustment made, pilot data analysis showed AGSI to be highly correlated with GSI and GAMBIT. With this established, it was used as a variable in this study. The formula for AGSI is shown in Equation 16.

$$\text{AGSI} = \int_0^T \left[\frac{\alpha(t)}{88} \right]^{2.5} dt \quad (15)$$

where:

$\alpha(t)$ = instantaneous resultant angular acceleration of the headform

T = impulse duration

To analyze the combined effects of linear and angular forces on the head, GAMBIT was also tested. The GAMBIT measures were also calculated with the use of a MATLAB® script. The current equation for GAMBIT is shown in Equation 17.

$$G_{max}(t) = \left[\left(\frac{a_{res}(t)}{250} \right)^2 + \left(\frac{a_{res}(t)}{25000} \right)^2 \right] \quad (16)$$

where:

$a_{res}(t)$ = instantaneous value of the resultant translational acceleration

$\alpha_{res}(t)$ = instantaneous value of the resultant rotational acceleration

This combination of variables was chosen as they provide a full examination of linear and angular impact forces both individually and in combination. Additionally, GSI is a variable that is recognized by NOCSAE (2017) for helmet testing. NOCSAE (2017) sets a threshold of 1200 as a pass/fail criterion.

Independent and dependent variables. The independent variables used in the analysis of this study were headguard type (Adidas®, Century® Drive, and TPU-Century® Drive) and impact location (front, front boss, side). The dependent variables measured and analyzed were PRLA (g), peak resultant angular acceleration (radians/s²), Gadd Severity Index (GSI), Angular Gadd Severity Index (AGSI), GAMBIT, and energy absorption (%).

Analysis. A number of different statistical analysis methods were performed to address each research purpose, with both inferential and descriptive statistics being tested. The first research purpose sought to analyze the material properties of TPU and boxing headguards statically to test the energy absorption capacity of the material across different boxing headgear locations. To address this question, the numerical integration obtained from the Chatillon® force tester was analyzed to evaluate the percentage of compression energy, shear energy, and total energy absorbed by each headguard condition. The changes in energy absorption (compression, shear, total) across all cycles were compared for each headguard condition and each impact location. Additionally, the means of these values were compared to show which headguards performed best overall in absorbing energy in static testing.

The second research purpose sought to examine the effect of headguard type and impact location on measures of PRLA and peak resultant angular acceleration during simulated dynamic impacts respectively. To address the research questions for the second purpose of this study, 3 impact locations (front, side front boss) x 3 headguard types

(Adidas®, Century® Drive, and TPU-Century® Drive) two-way independent measures ANOVA tests were performed for each dependent variable (PRLA, peak resultant angular acceleration) respectively. If an interaction effect was found, the interaction was explained using simple main effects via one-way ANOVAs. If no significant interactions were found for a respective dependent variable, the main effects for each independent variable were analyzed separately. Posthoc analyses and descriptive statistics were implemented using Tukey's test for mean pair comparison regarding the interactions and main effects.

The third research purpose sought to examine the effect of headguard type and impact location on head injury risk measures during simulated dynamic impacts. To address the research questions for the third purpose of the study 3 impact locations (front, side, front boss) x 3 headguard types (Adidas®, Century® Drive, and TPU-Century® Drive) two-way independent measures ANOVA tests were performed for each dependent variable (GSI, AGSI, GAMBIT) respectively. If an interaction effect was found, the interaction was explained using simple main effects via one-way ANOVAs. If no significant interactions were found for a respective dependent variable, the main effects for each independent variable were analyzed separately. Posthoc analyses and descriptive statistics were implemented using Tukey's test for mean pair comparison regarding the interactions and main effects.

Results

The results of this study addressed each research question separately when comparing the boxing headgears across impact locations during the static and dynamic testing. The static analysis included measures of total, compression and shear energies. The dynamic analysis included measures of linear and rotational accelerations. The dynamic analysis also included measures of risk of head injury based on measures of linear as well as rotational impacts, and their combination.

Static Testing

Research Question 1. Which boxing headguard (Century® Drive, Adidas®, and TPU-Century® Drive) absorbed the most energy when loaded with a compressive and shear force across locations (front and side) during static testing?

Front static tests. Prior to conducting the static results, the researcher noted inconsistent and markedly high energy absorption shown for the 1st cycle across headguard conditions. For this reason, the first cycle of each condition was removed and only 14 cycles were included in the statistical analysis. The results for the static tests conducted at the front headguard location indicated that the TPU-Century® Drive absorbed the highest mean percentage of total energy of the three headguards (M=42.38%), followed by the Century® Drive (M=31.98%), and then the Adidas® headguard, which absorbed the lowest percentage of energy (M=25.71%). Figure 21 shows a representation of the percent of total energy absorption when comparing the three headguards at the front location across 14 loading cycles.

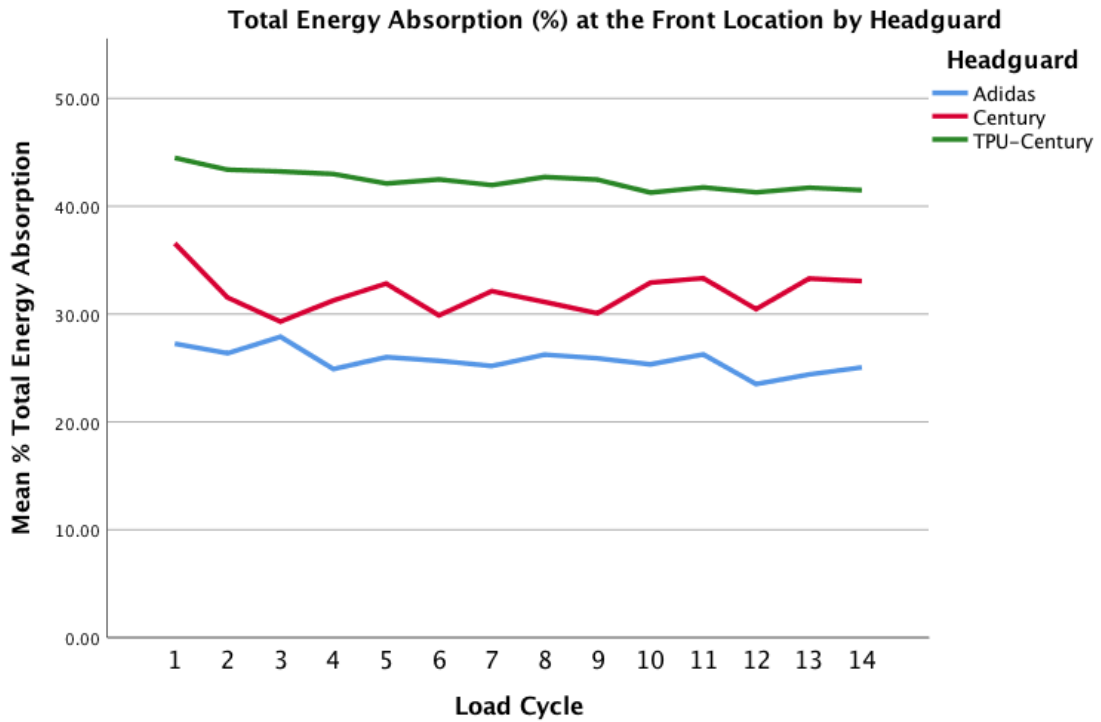


Figure 21: Total percent of energy absorption for the Adidas®, Century® Drive, and TPU-Century® Drive headguards at the front location during static testing.

When the amount of energy absorbed was broken into compression and shear energies, similar results were found in terms of headgear performance. The TPU-Century® Drive absorbed the highest mean percentage of compressive energy (M=46.25%), followed by the Century® Drive (M=36.39%), and then the Adidas® headguard, which absorbed the lowest percentage of compression energy (M=30.13%). A representation of the percent compressive energy absorption at the front location when comparing the three headguards across 14 loading cycles is shown in Figure 22.

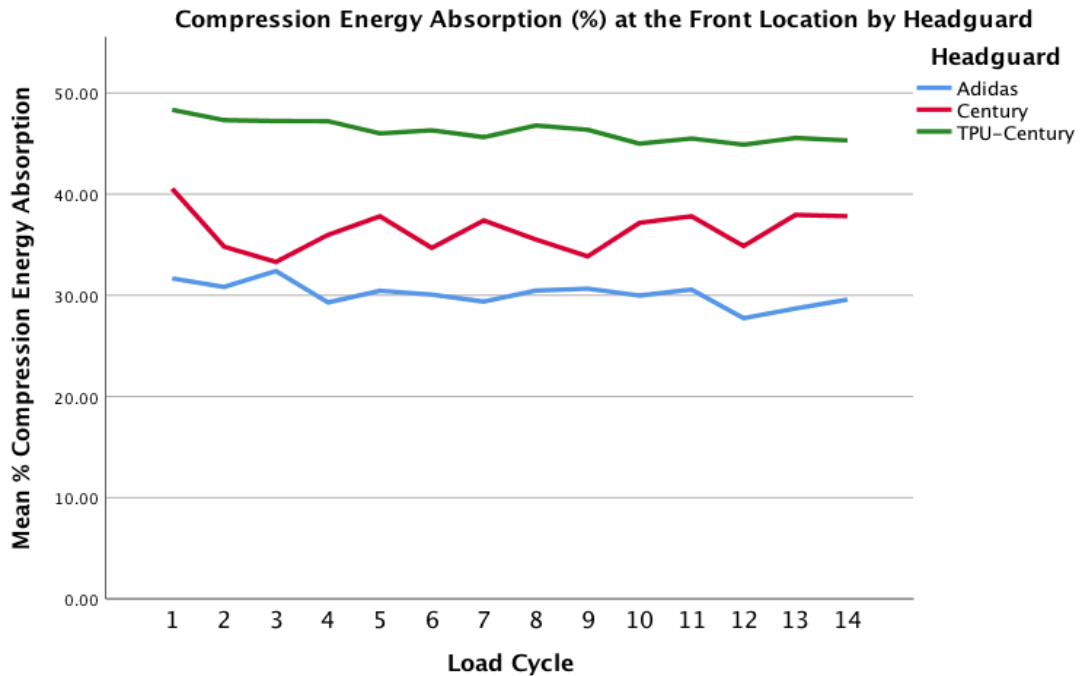


Figure 22: Percent compression energy absorption of the Adidas®, Century® Drive, and TPU-Century® Drive headguards at the front location during static testing.

In terms of shear energy, the TPU-Century® Drive again absorbed the highest percentage of shear energy (35.08%) when compared to the Century® Drive (M=22.85%), and Adidas® headguard (M=17.63%). A representation of the percent shear energy absorption at the front location when comparing the three headguards across 14 loading cycles is shown in Figure 23. It is important to note, however, that the percentage of shear energy absorbed was lower across all three headguards when comparing it to the percentage of compressive energy absorbed.

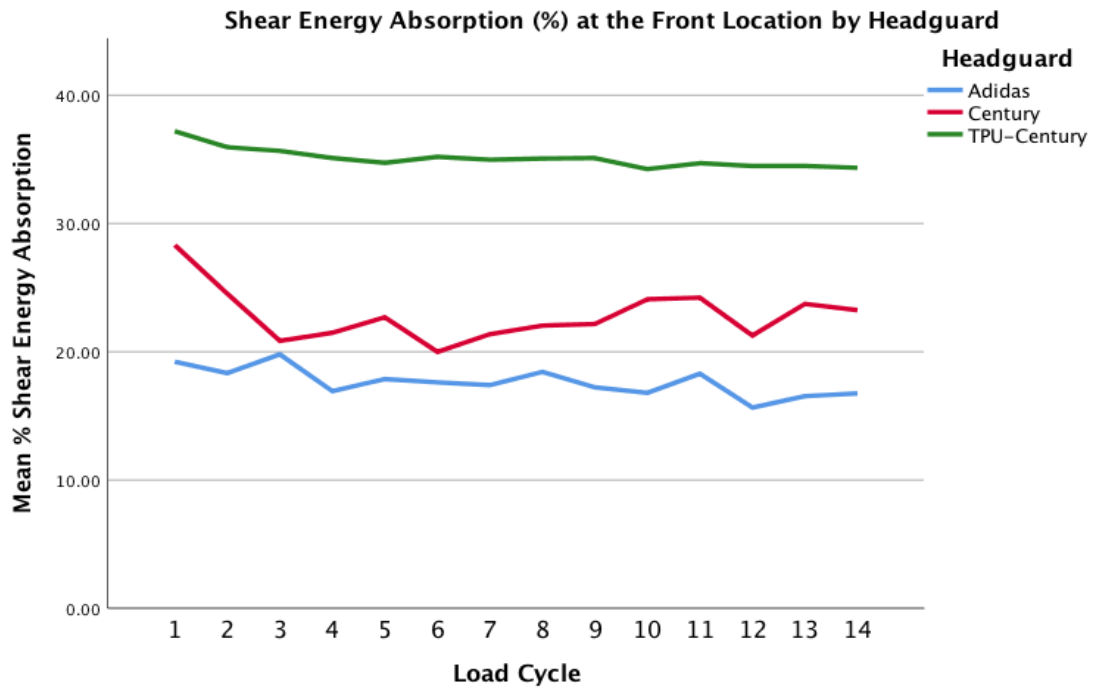


Figure 23: Percent shear energy absorption of the Adidas®, Century® Drive, and TPU-Century® Drive headguards at the front location during static testing.

Side static tests. The results of the static tests conducted at the side headguard location indicated that the TPU-Century® Drive absorbed the highest mean percentage of total energy (41.52%) when compared to the Adidas® headguard (M=34.42%), and Century® Drive (M=24.01%) headgears. A representation of the percent total energy absorption at the side location when comparing the three headguards across 14 loading cycles is shown in Figure 24.

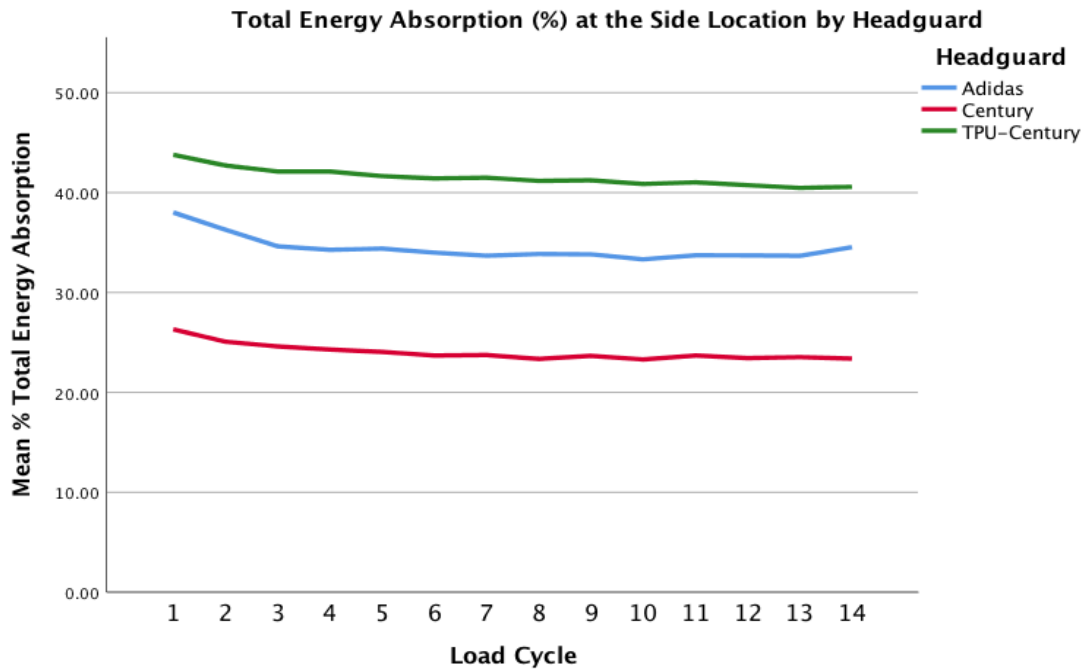


Figure 24: Total percent energy absorption of the Adidas®, Century® Drive, and TPU-Century® Drive headguards at the side location during static testing.

When the energy absorbed was broken into compression and shear energies, the TPU-Century® Drive absorbed the highest mean percentage of compressive energy (M=48.48%), when compared to the Adidas® (M=40.10%), and Century® Drive (M=28.66%) headgear. A representation of percent of compressive energy absorption at the side location when comparing the three headguards across 14 loading cycles is shown in Figure 25.

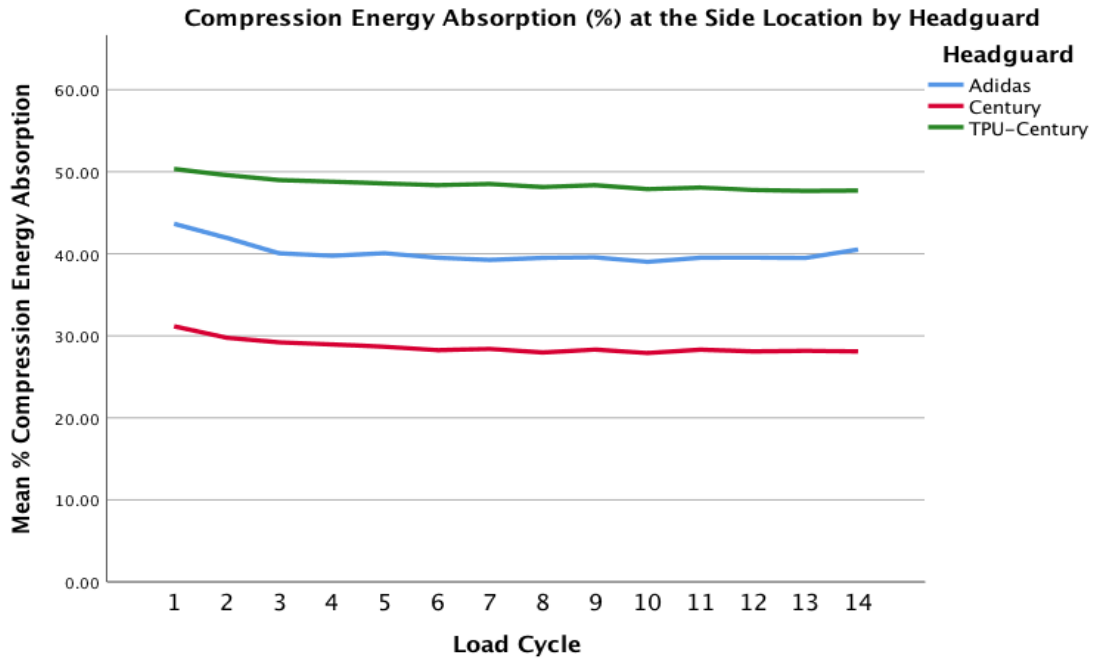


Figure 25: Percent compression energy absorption of the Adidas®, Century® Drive, and TPU-Century® Drive headguards at the side location during static testing.

Similarly, for the shear energy, the TPU-Century® Drive absorbed the highest percentage of energy (29.15%), when compared to the Adidas® headguard (M=22.48%), and Century® Drive (M=13.51) headgears. A representation of the percent shear energy absorption at the side location when comparing the three headguards across 14 loading cycles is shown in Figure 26.

It is noted that the percentage of shear energy absorbed was lower across all three headguards when comparing it to the percentage of compressive energy absorbed. This was similar to the results for the front location. However, at the side location, the Adidas® headguard absorbed more energies (total, compression, and shear) than the Century® Drive.

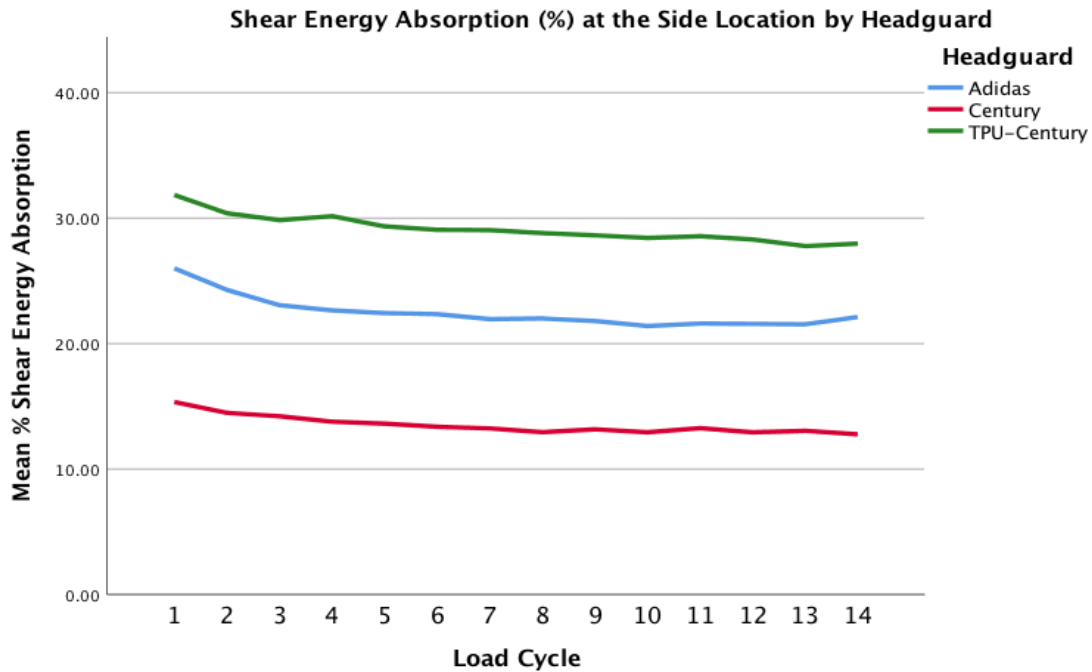


Figure 26: Percent shear energy absorption of the Adidas®, Century® Drive, and TPU-Century® Drive headguards at the side location during static testing.

Dynamic Testing

Research Question 2. Which boxing headguard (Century® Drive, Adidas®, and TPU-Century® Drive) would perform better in decreasing linear impact acceleration across different impact locations (front, front boss, and side) during dynamic testing?

Linear impact acceleration. Research question 2 sought to explore which boxing headguard (Adidas®, Century® Drive, TPU-Century® Drive) performed better in decreasing linear impact acceleration across different impact locations (front, front boss, and side). The researcher addressed this research question by conducting a 3-headguard (Adidas®, Century® Drive, TPU-Century® Drive) X 3-location (front, front boss, and side) independent measures ANOVA to examine the interaction effect between headguard and location on the measure of PRLA.

Before conducting the analysis of variance, the researcher explored SPSS functions in combination with the outlier labelling rule (Senthamarai Kannan et al., 2015) to identify extreme outliers possibly affecting the homogeneity of variance. The researcher decided to remove extreme values beyond two standard deviations from the mean and conducted the ANOVA with and without outliers. The analysis revealed that the extreme values did not have a significant effect on the PRLA variance for each group. Consequently, the researcher did not remove any extreme values from the data.

The results of a two-way independent measures ANOVA showed that there was not a significant interaction, $F(4,153)=1.087, p=.365$, between headguard condition (Adidas®, Century® Drive, TPU-Century® Drive) and impact location (front, front boss, side) on the measure of PRLA.

When examining the main effects, however, the results showed that there were statistically significant differences, $F(2,153)=17.066, p<.05, \eta^2=.182$ between headguard types (Adidas®, Century® Drive, TPU- Century® Drive) on the measure of PRLA. The Tukey's post-hoc analysis showed statistically significant differences in PRLA measures among the different types of headguard at $p<.05$. The TPU-Century® Drive performed the best in mitigating PRLA ($M=104.61g, SD=48.39$), when compared to the Century® Drive ($M=182.93g, SD=99.58$) and Adidas® ($M=184.94g, SD=92.27$) at $p<.05$. The differences in performance between the Century® Drive and Adidas®, however, were not significant ($p>.05$). Figure 27 displays a representation of the estimated marginal means of PRLA, expressed in g's, across headguard types.

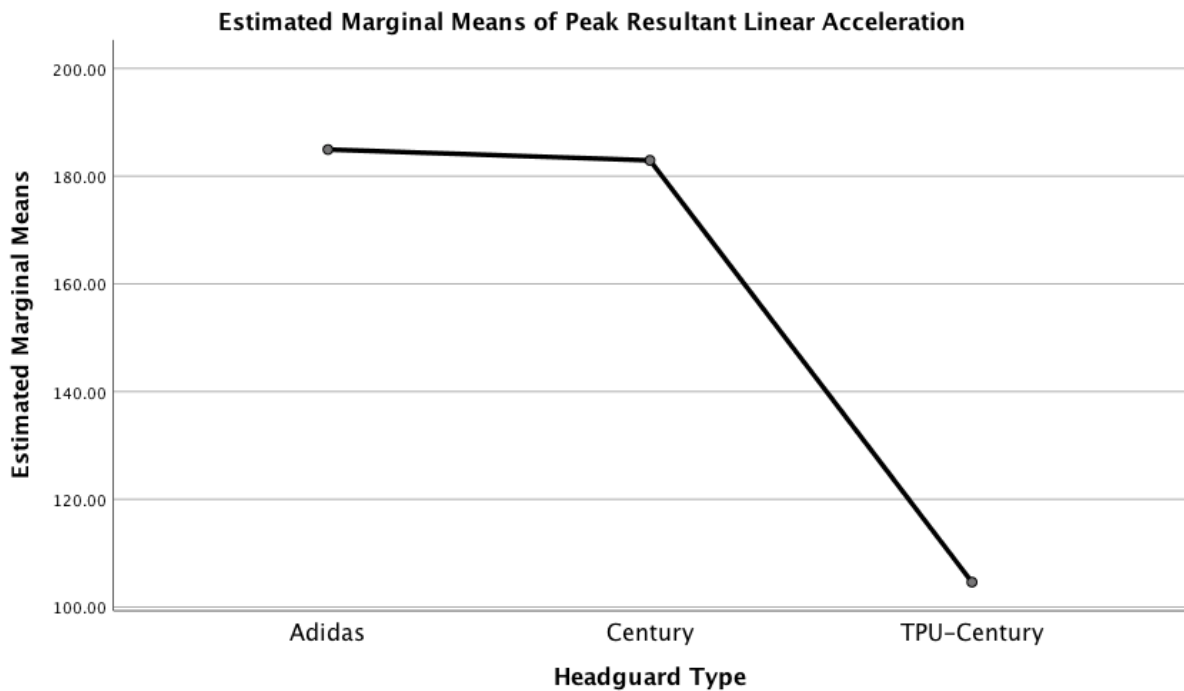


Figure 27: Estimated marginal means of PRLA across headguard types.

The main effect analysis also showed that there were statistically significant differences, $F(2,153)=4.237$, $p=.016$, $\eta^2=.052$, between impact locations (front, front boss, side) on the measure of PRLA. The Tukey's post-hoc analysis showed statistically significant differences between the impact locations at $p<.05$. The PRLA experienced by the headform was significantly lower for front boss impacts ($M=138.30g$, $SD=75.43$) when compared to side impacts ($M=182.73g$, $SD=108.91$) at $p<.05$. The differences in PRLA for front impacts ($M=151.45g$, $SD=80.21$) compared to front boss and side impacts were determined to be statistically insignificant ($p>.05$). Figure 28 displays a representation of the estimated marginal means of PRLA, expressed in g's, across impact locations.

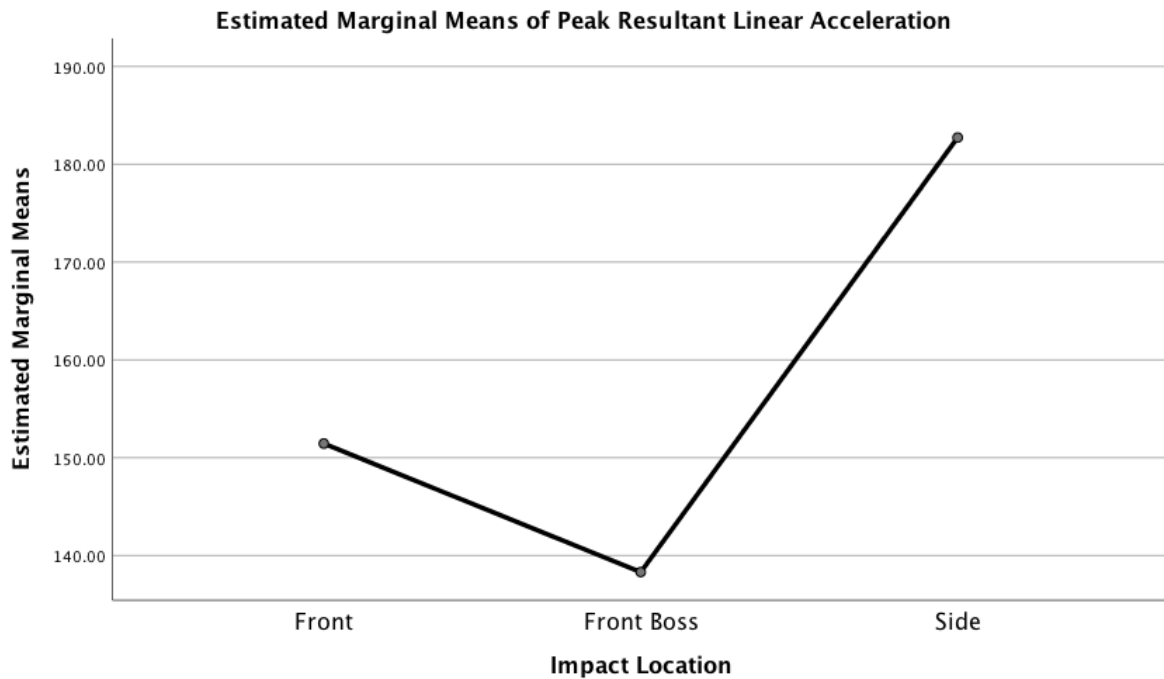


Figure 28: Estimated marginal means of PRLA across impact locations.

Research Question 3. Which boxing headguard (Century® Drive, Adidas®, and TPU-Century® Drive) would be more effective in mitigating angular acceleration at each impact location (front, front boss, side) during dynamic testing?

Angular acceleration. Research question 3 sought to explore which boxing headguard (Adidas®, Century® Drive, TPU-Century® Drive) performed better in mitigating angular impact acceleration across different impact locations (front, front boss, side). The researcher addressed this research question by conducting a 3-headguard (Adidas®, Century® Drive, TPU- Century® Drive) X 3-location (front, front boss, and side) independent measures ANOVA to examine the interaction effect between headguard and location on the measure of peak resultant angular acceleration.

The results of the two-way independent measures ANOVA showed a significant interaction, $F(4,153)=4.103$, $p=.003$, $\eta^2=.097$, between headguard condition (Adidas®, Century® Drive, TPU-Century® Drive) and impact location (front, front boss, side) on the

measure of peak resultant angular acceleration. Figure 29 displays a representation of this interaction.

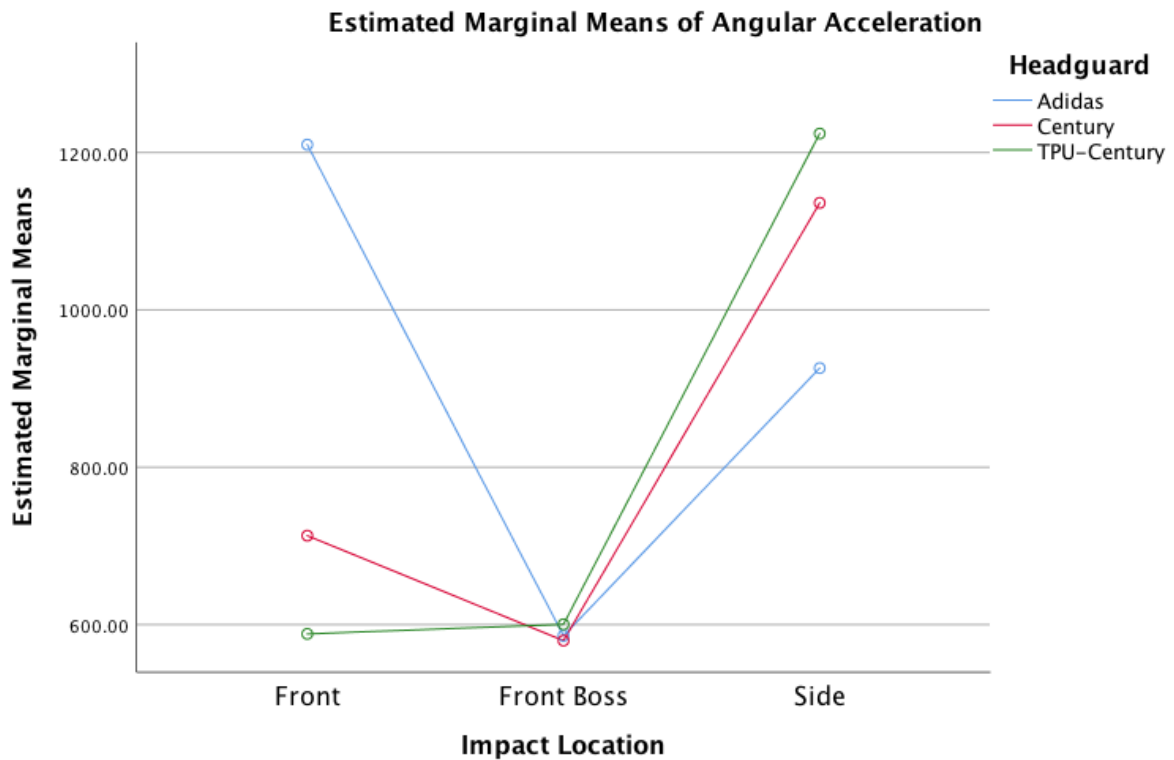


Figure 29: Interaction effect of headguard type and impact location on the estimated marginal means of angular acceleration.

The researcher conducted simple main effect analyses to further explain this interaction. The researcher began by conducting a set of one-way ANOVA tests to compare the three headguard types for each impact location respectively on the measure of peak resultant angular acceleration. Similarly, the researcher conducted another set of one-way ANOVA tests to compare the three impact locations for each headguard separately.

Comparing headguard types for each impact location. The results of the one-way ANOVA showed that at the front location, there were significant differences in peak resultant angular acceleration, $F(2, 51)=6.456, p=.003, \eta^2=.202$ among the three headguard types.

A Tukey's post-hoc analysis showed that for the front impacts, measures of peak resultant angular acceleration were the highest for the Adidas® headguard ($M=1209.99$

rad/s², SD=840.99) when compared to the Century® Drive headguard (M=713.06 rad/s², SD=431.40) and the TPU-Century® Drive headguard (M=588.15 rad/s², SD=108.47), at $p<.05$. The differences in performance between the two better performing headguards, the TPU-Century® Drive and the Century® Drive, were not statistically significant ($p>.05$) at the front location. Figure 30 displays a representation of the difference in the mean peak resultant angular acceleration measure, expressed in rad/s², across headguard conditions for front impacts.

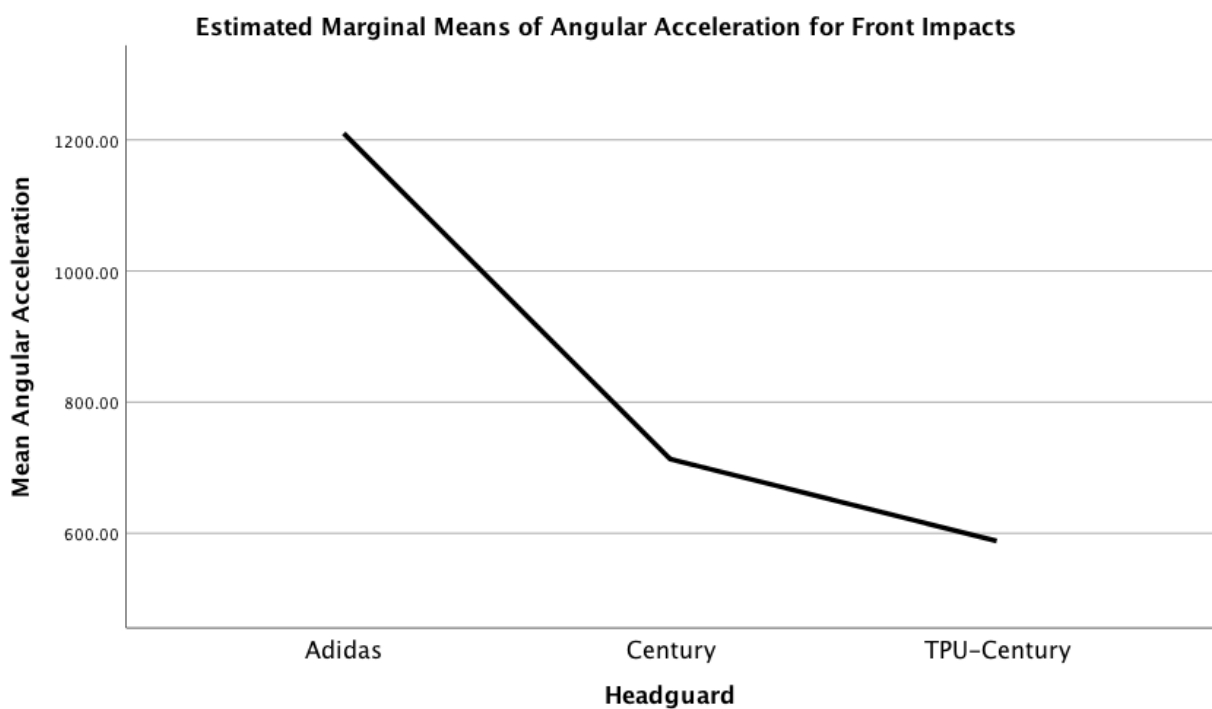


Figure 30: Estimated marginal means of angular acceleration across headguard types for front impacts.

At the front boss location, there were not statistically significant differences $F(2, 51)=.153, p=.858$, in peak resultant angular acceleration measure between the Century® Drive (M=579.57 rad/s², SD=144.01), Adidas® (M=585.75 rad/s², SD=89.57), and TPU-Century® Drive (M=600.30 rad/s², SD=105.65) headguards.

At the side location, there were not statistically significant differences, $F(2, 51)=.869, p=.425$, in peak resultant angular acceleration measure between the Adidas® (M=925.98

rad/s², SD=481.02), Century® Drive (M=1135.95 rad/s², SD=730.42), and TPU-Century® Drive (M=1224.07 rad/s², SD=831.75) headguards.

Comparing the impact locations for each headguard. For the ANOVAs conducted by headguard types, there were significant differences found in peak resultant angular acceleration measure across impact locations for the Adidas® headguard $F(2, 51)=5.572$, $p=.006$, $\eta^2=.179$.

The Tukey's post-hoc analysis showed that for Adidas® headguard, peak resultant angular acceleration was lowest for front boss impacts (M=585.74 rad/s², SD=89.57), when compared to front impacts (M=1209.99 rad/s², SD=840.99), at $p<.05$. The differences in the mean peak resultant angular acceleration measure for side impacts (M=925.98 rad/s², SD=481.02), when compared to front and front boss impacts, were not statistically significant ($p>.05$ for both). Figure 31 displays a representation of the difference in mean peak resultant angular acceleration measure, expressed in rad/s², across impact locations for the Adidas® headguard.

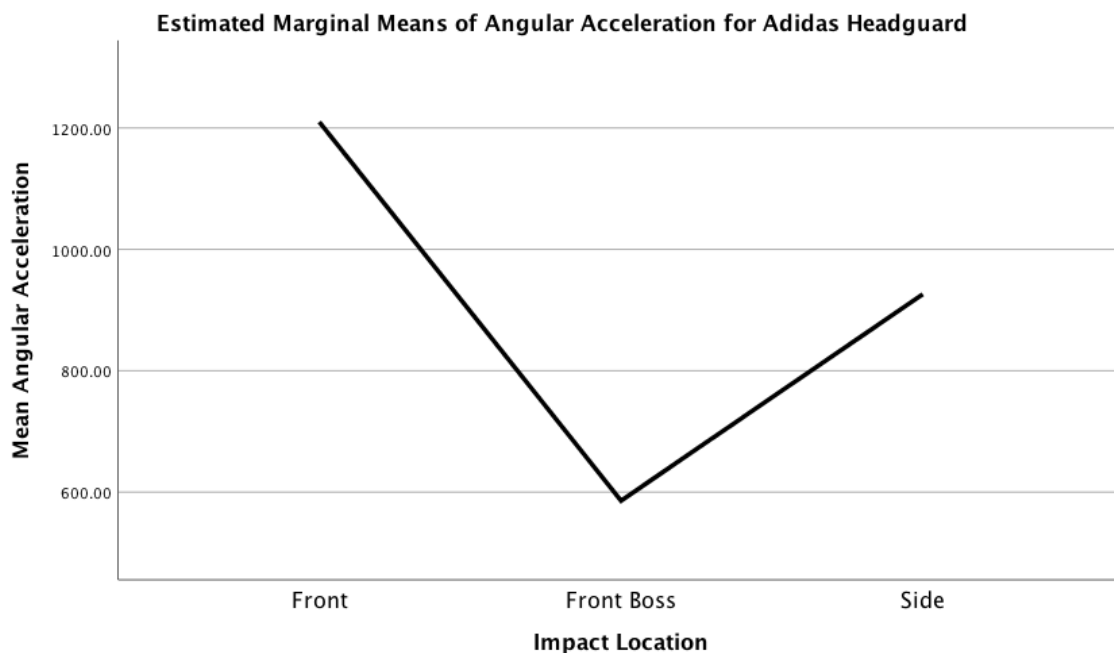


Figure 31: Estimated marginal means of angular acceleration across impact locations for Adidas® headguard impacts.

Significant differences were also seen in the peak resultant angular acceleration measure across impact locations for Century® Drive headguard impacts, $F(2, 51)=6.154$, $p=.004$, $\eta^2=.194$. The Tukey's post-hoc analysis showed that the mean peak resultant angular acceleration was significantly higher ($p<.05$ for both) for impacts at the side ($M=1135.95$ rad/s², $SD=730.42$) compared to impacts at the front ($M=713.06$ rad/s², $SD=431.40$) and front boss ($M=579.57$ rad/s², $SD=144.01$). The differences in front vs. front boss impacts were not statistically significant for the Century® Drive headguard ($p>.05$). Figure 32 displays a representation of the difference in mean peak resultant angular acceleration measure, expressed in rad/s², across impact locations for the Century® Drive headguard.

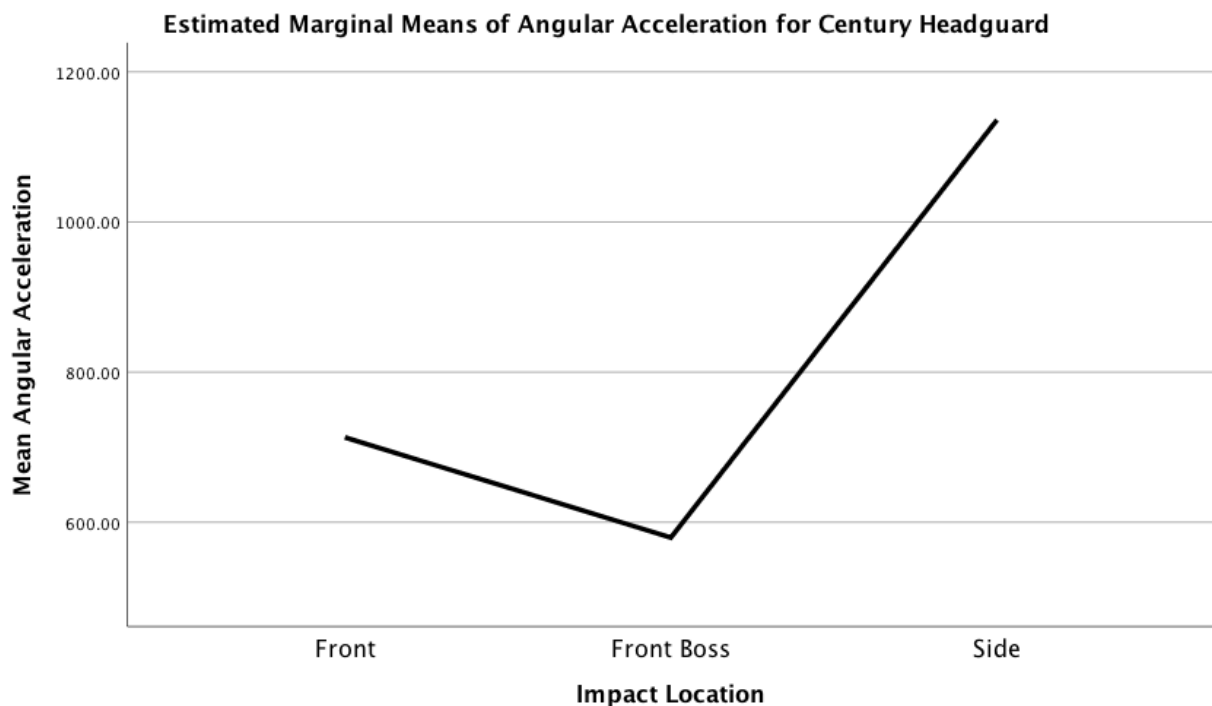


Figure 32: Estimated marginal means of angular acceleration across impact locations for Century® Drive headguard impacts.

For the TPU-Century® Drive headguard impacts, significant differences were also seen in the peak resultant angular acceleration measure across impact locations, $F(2, 51)=9.993$, $p<.05$, $\eta^2=.282$. The Tukey's post-hoc analysis showed that the mean peak resultant angular acceleration measure was significantly higher ($p<.05$ for both) for impacts

at the side ($M=1224.07 \text{ rad/s}^2$, $SD=831.74$) compared to front boss ($M=600.30 \text{ rad/s}^2$, $SD=105.65$) and front impacts ($M=588.15 \text{ rad/s}^2$, $SD=108.47$). The differences between the mean peak resultant angular acceleration measure for front and front boss impacts were not statistically significant ($p>.05$) for the TPU-Century® Drive headguard. Figure 33 displays a representation of the difference in mean peak resultant angular acceleration measure, expressed in rad/s^2 , across impact locations for the TPU-Century® Drive headguard.

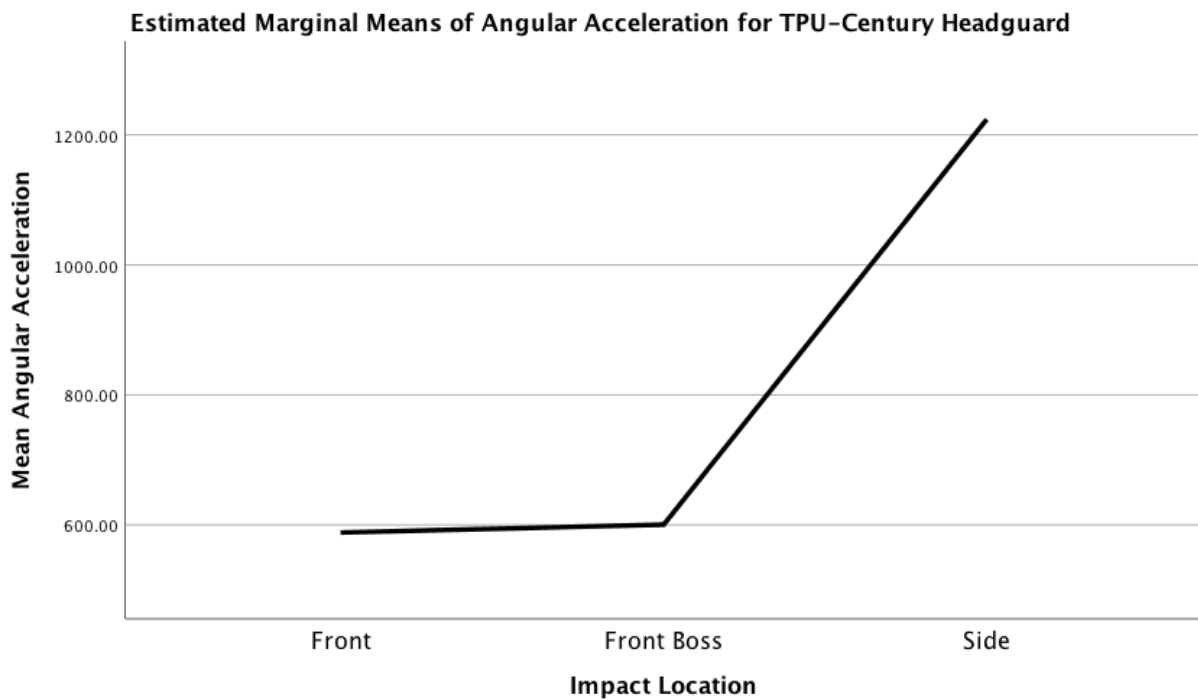


Figure 33: Estimated marginal means of angular acceleration across impact locations for TPU-Century® Drive headguard impacts.

Head Injury Risk

Research Question 4. Which boxing headguard (Century® Drive, Adidas®, and TPU-Century® Drive) would perform better at decreasing the risk of head injury due to the effect of linear impact acceleration across different headguard locations (front, front boss, and side) during dynamic testing?

Gadd severity index (GSI). Research question 4 sought to determine which boxing headguard (Adidas®, Century® Drive, TPU-Century® Drive) performed better in decreasing the risk of head injury due to the effect of linear impact accelerations across different impact locations (front, front boss, and side). The researcher addressed this research question by conducting a 3-headguard (Adidas®, Century® Drive, TPU- Century® Drive) X 3-location (front, front boss, and side) independent measures ANOVA to examine the interaction effect between headguard and location on the measure of GSI.

The results of the two-way independent measures ANOVA did not reveal a significant interaction $F(4,153)=.716, p=.582$, between headguard condition (Adidas®, Century® Drive, TPU-Century® Drive) and impact location (front, front boss, side) on the measure of GSI.

The analysis of the main effects, however, showed that there were significant differences $F(2,153)=12.280, p<.05, \eta^2=.138$, between headguard types (Adidas®, Century® Drive, TPU-Century® Drive) on the measure of GSI.

The Tukey's post-hoc analysis showed statistically significant differences among the different types of headguards at $p<.05$. The TPU-Century® Drive headguard performed the best in mitigating GSI ($M=348.72, SD=271.50$) when compared to the Century® Drive ($M=853.41, SD=770.14$) and Adidas® ($M=863.28, SD=701.27$), at $p<.05$. The differences in performance between the Century® Drive and Adidas®, were not statistically significant ($p>.05$). Figure 34 displays a representation of the estimated marginal means of GSI across headguard conditions.

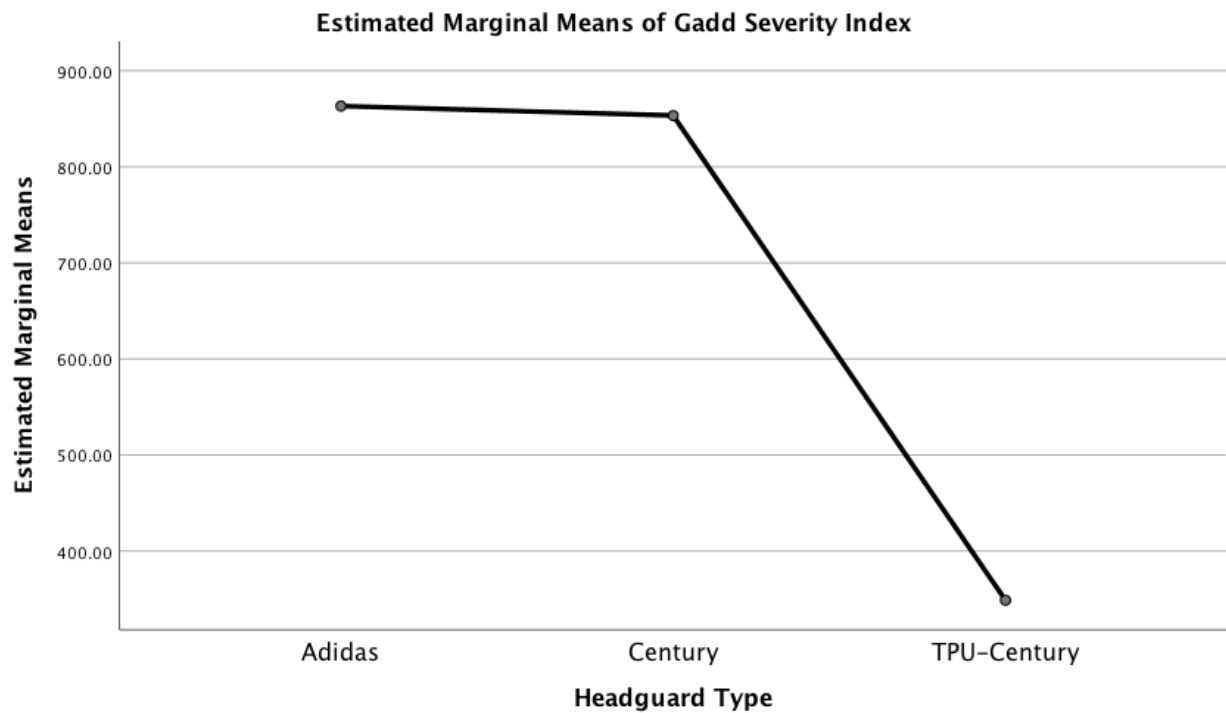


Figure 34: Estimated marginal means of Gadd Severity Index across headguard conditions.

The main effects test did not show significant differences, $F(2,153)=2.695$, $p=.071$ in GSI scores across the impact locations, front ($M=669.56$, $SD=607.49$), front boss ($M=561.04$, $SD=518.24$), and side ($M=834.81$, $SD=811.62$). Figure 35 displays a representation of the estimated marginal means of GSI across impact locations.

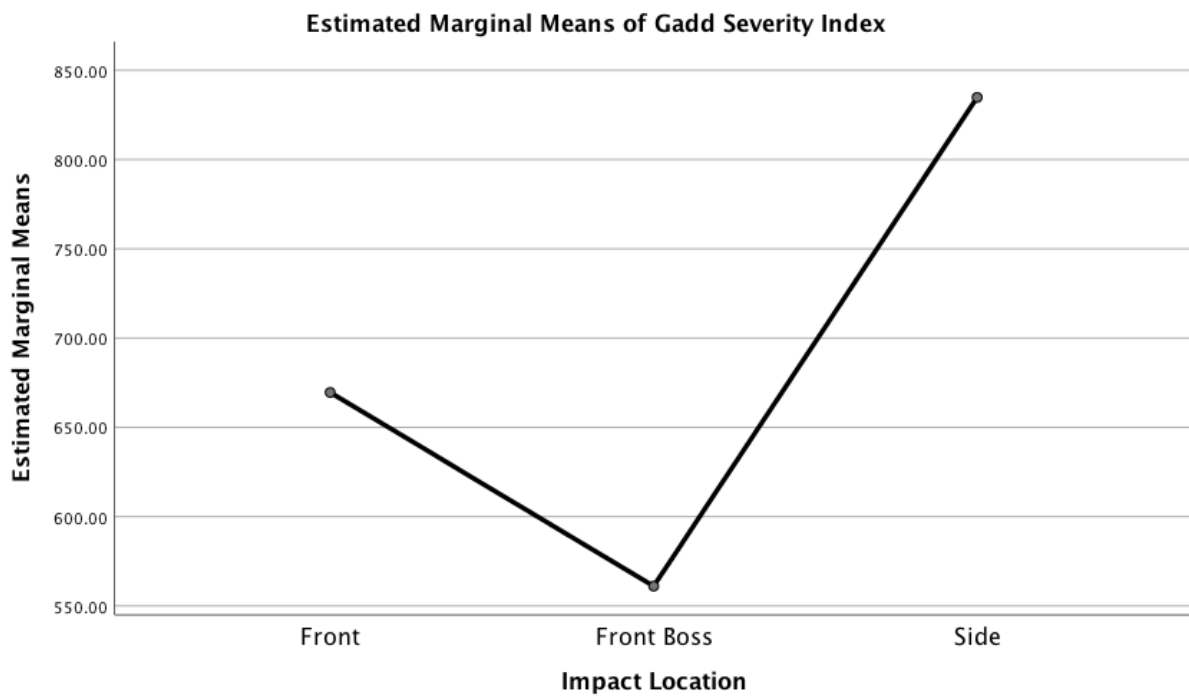


Figure 35: Estimated marginal means of Gadd Severity Index across impact locations.

Research Question 5. Which boxing headguard (Century® Drive, Adidas®, and TPU-Century® Drive) would perform better at decreasing the risk of head injury due to the effect of angular impact acceleration across different locations (front, front boss, and side) during dynamic testing?

Angular Gadd Severity Index (AGSI). Research question 5 sought to determine which boxing headguard (Adidas®, Century® Drive, TPU-Century® Drive) performed better in decreasing the risk of head injury due to the effect of angular impact accelerations across different impact locations (front, front boss, and side). The researchers addressed this research question by conducting a 3-headguard (Adidas®, Century® Drive, TPU-Century® Drive) X 3-location (front, front boss, and side) independent measures ANOVA to examine the interaction effect between headguard and location on the measure of AGSI.

The results of the two-way independent measures ANOVA showed a significant interaction effect, $F(4,153)=6.082, p<.05, \eta^2=.137$, between headguard condition (Adidas®, Century® Drive, TPU-Century® Drive) and impact location (front, front boss, side) on the measure of AGSI. Figure 36 shows a representation of this interaction.

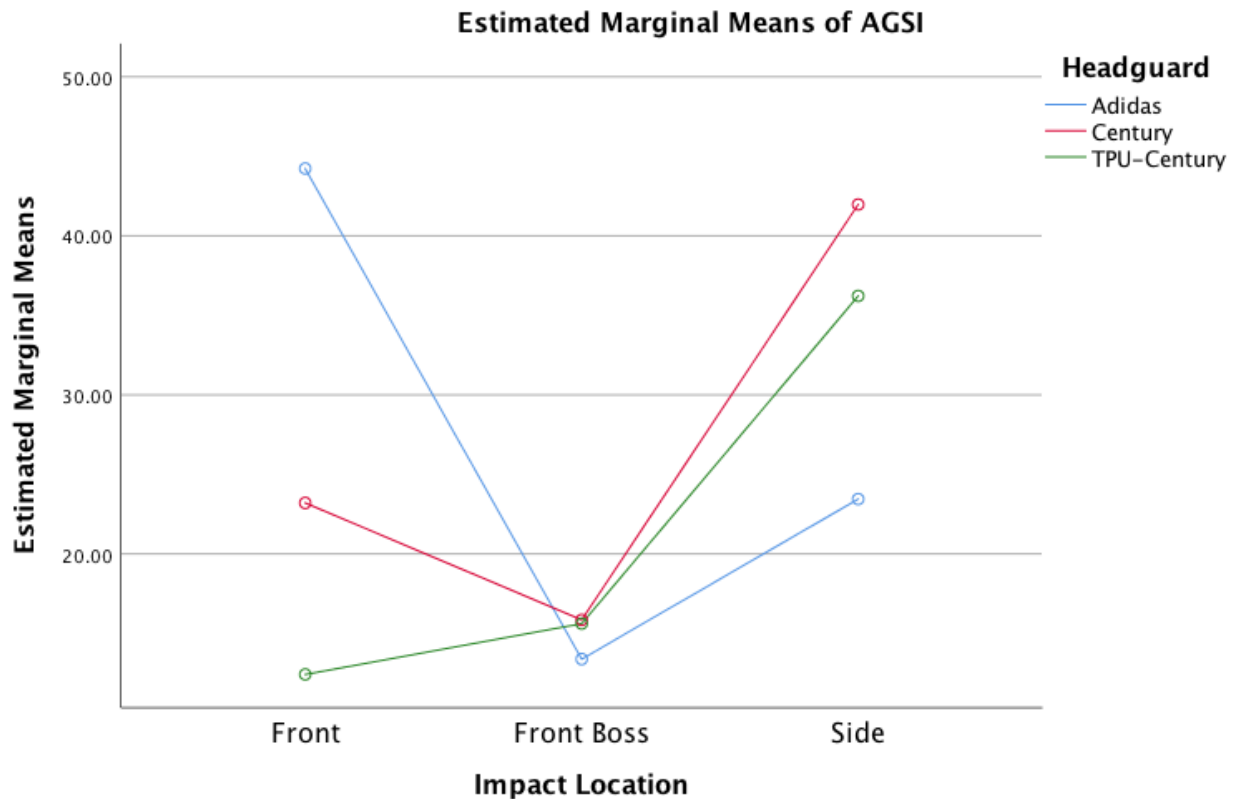


Figure 36: Interaction effect of headguard type and impact location on the estimated marginal means of Gadd Severity Index

The researcher conducted simple main effect analyses to further explain this interaction. The researcher began by conducting a set of one-way ANOVA tests to compare the three headguard types for each impact location respectively on the measure of AGSI. Similarly, the researcher conducted another set of one-way ANOVA tests to compare the three impact locations for each headguard separately.

Comparing headguard types for each impact location. The results of the one-way ANOVA showed that at the front location, there were significant differences in AGSI, $F(2,$

51)=11.795, $p<.05$, $\eta^2=.316$ across headguard conditions. A Tukey's post-hoc analysis showed that the Adidas® headguard performed significantly worse ($M=44.23$, $SD=30.07$) than the TPU-Century® Drive ($M=12.42$, $SD=6.02$) and the Century® Drive ($M=23.21$, $SD=16.04$) headguards ($p<.05$ for both) at the front location. There was not a significant difference between the two better performing headguards, the TPU-Century® Drive, and the Century® Drive. Figure 37 displays a representation of the difference in mean AGSI scores across headguard conditions for front impacts.

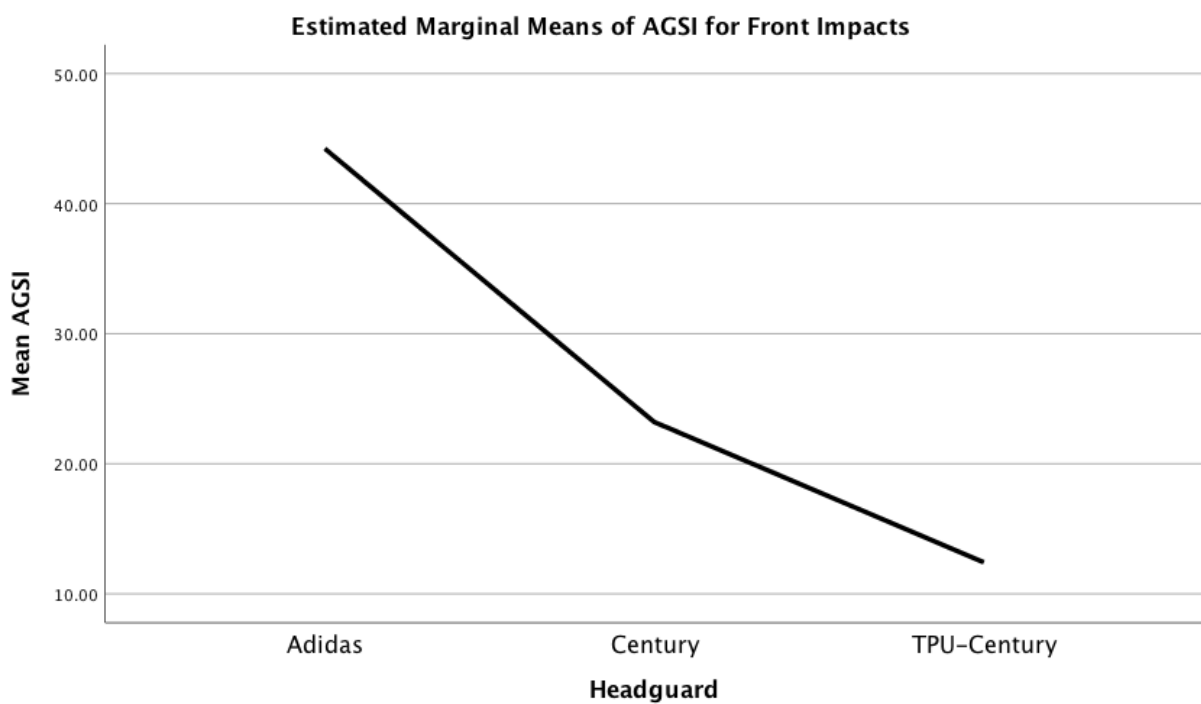


Figure 37: Estimated marginal means of AGSI across headguard types for front impacts.

At the front boss location, there were not statistically significant differences in AGSI measures, $F(2, 51)=.217$, $p=.805$, between the Adidas® headguard ($M=13.850$, $SD=9.33$), the TPU-Century® Drive ($M=15.61$, $SD=9.28$), and the Century® Drive headguard ($M=15.85$, $SD=16.94$). Similarly, at the side location, there were not statistically significant differences in AGSI measures, $F(2, 51)=1.844$, $p=.169$, between the Adidas® headguard ($M=23.45$,

SD=16.77), TPU-Century® Drive headguard (M=36.22, SD=27.10), and Century® Drive headguard (M=41.97, SD=40.19).

Comparing the impact locations for each headguard. Results of a one-way ANOVA showed that for Adidas® headguard impacts, there were significant differences between impact locations, $F(2, 51)=10.497$, $p<.05$, $\eta^2=.292$, on AGSI scores. For this headguard, a Tukey's post-hoc test showed that AGSI scores were lowest at the front boss (M=13.39, SD=9.33), followed by side impacts (M=23.45, SD=16.77), however, these differences were not statistically significant ($p>.05$). Impacts to the front produced significantly higher AGSI (M=44.23, SD=30.07) compared to other locations for this headguard ($p<.05$ for both). Figure 38 displays a representation of the estimated marginal means of AGSI for the Adidas® headguard across impact locations.

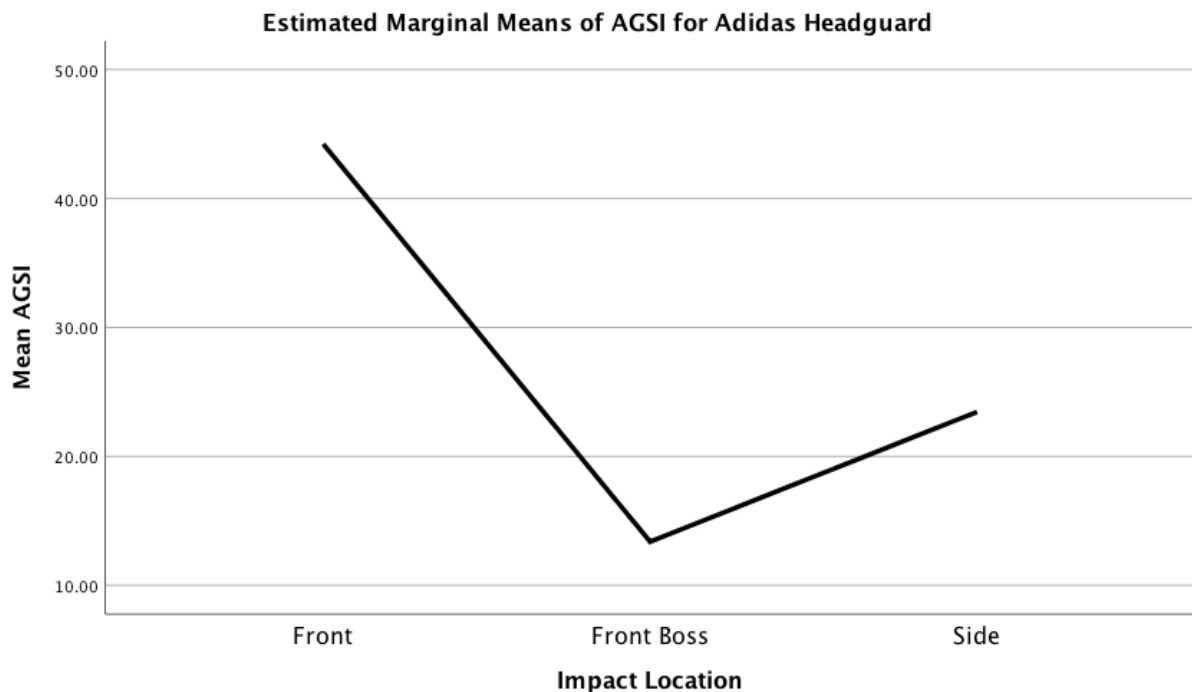


Figure 38: Estimated marginal means of AGSI for Adidas® headguard across impact locations.

For Century® Drive impacts there were also significant differences between impact locations, $F(2, 51)=4.534$ $p=.015$, $\eta^2=.151$, on AGSI scores. The Tukey's post-hoc test

showed that for this headguard, AGSI was significantly higher ($p < .05$) for side impacts ($M = 41.97$, $SD = 40.19$) compared to front boss impacts ($M = 15.85$, $SD = 16.94$). Differences in front impacts ($M = 23.21$, $SD = 16.04$) compared to front boss and side impacts were not statistically significant ($p > .05$ for both). Figure 39 displays a representation of the estimated marginal means of AGSI for the Century® Drive headguard across impact locations.

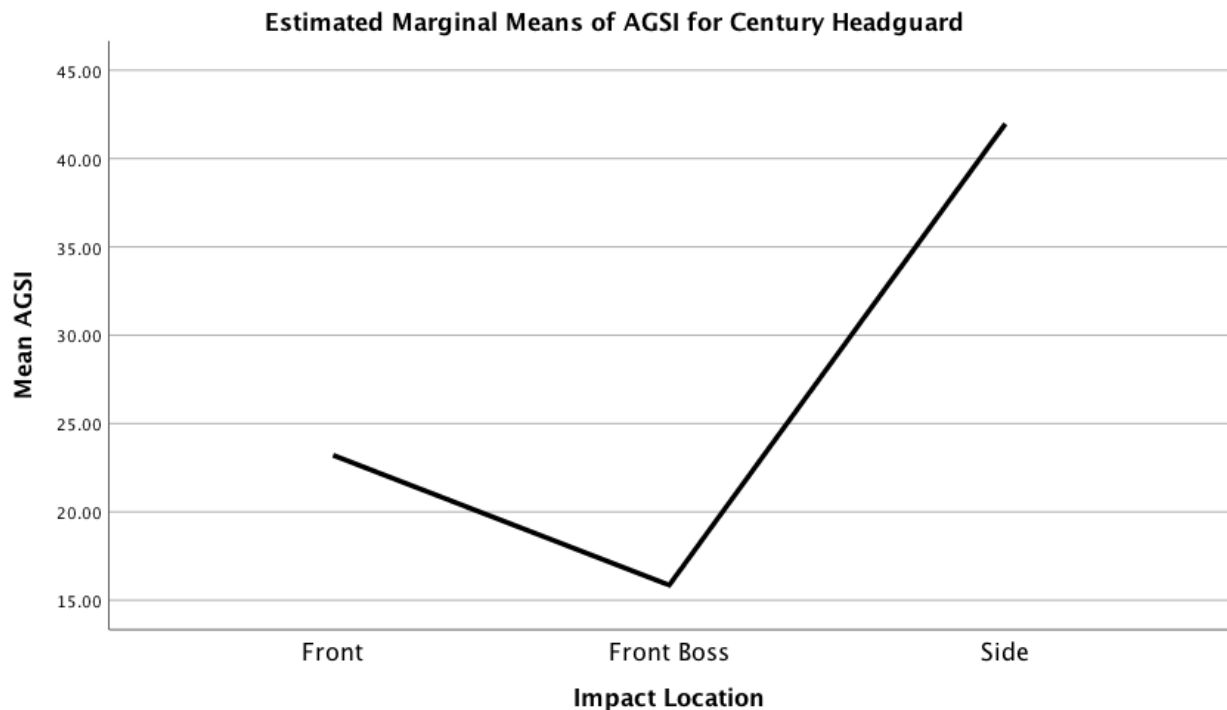


Figure 39: Estimated marginal means of AGSI for Century® Drive headguard across impact locations.

For TPU-Century® Drive impacts there were significant differences between impact locations, $F(2, 51) = 10.520$, $p < .05$, $\eta^2 = .292$ on AGSI scores. For this headguard, AGSI scores seemed to be the lowest at the front location ($M = 12.42$, $SD = 6.02$), followed by the front boss location ($M = 15.61$, $SD = 9.28$), however, the Tukey's post-hoc test did not find statistical significance in the differences between these locations ($p > .05$). For this headguard, AGSI was significantly higher for side impacts ($M = 36.22$, $SD = 27.10$) when compared to impacts at the front and front boss ($p < .05$ for both). Figure 40 displays a representation of the estimated marginal means of AGSI for the TPU-Century® Drive headguard across impact locations.

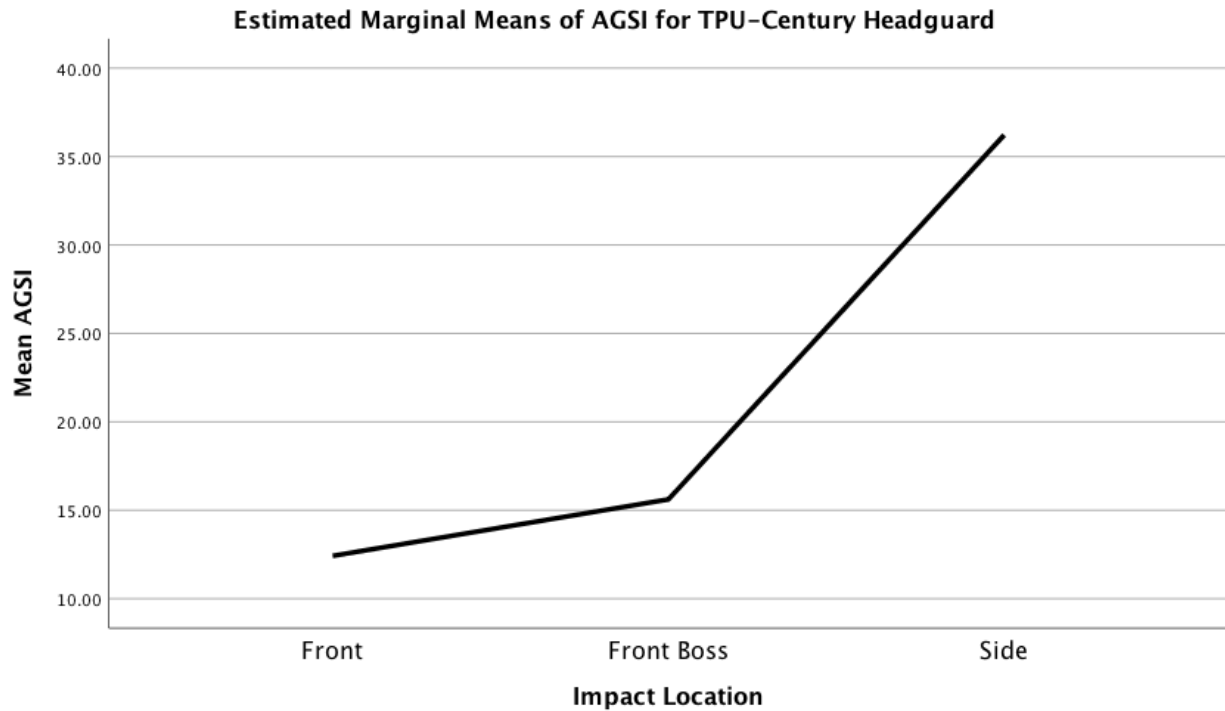


Figure 40: Estimated marginal means of AGSI for TPU-Century® Drive headguard across impact locations.

Research Question 6. Which boxing headguard (Century® Drive, Adidas®, and TPU-Century® Drive) would perform better at decreasing the risk of head injury due to the shared effect of linear and angular impact accelerations across different headguard locations (front, front boss, and side) during dynamic testing?

GAMBIT. Research question 6 sought to determine which boxing headguard (Adidas®, Century® Drive, TPU-Century® Drive) performed better in decreasing the risk of head injury due to the shared effect of linear and angular impact accelerations across different impact locations (front, front boss, and side). The researcher addressed this research question by conducting a 3-headguard (Adidas®, Century® Drive, TPU-Century® Drive) X 3-location (front, front boss, and side) independent measures ANOVA to examine the interaction effect between headguard and location on the measure of GAMBIT.

The results of the two-way independent measures ANOVA showed a significant interaction effect, $F(4,153)=3.510$, $p=.009$, $\eta^2=.084$, between headguard condition (Adidas®, Century® Drive, TPU-Century® Drive) and impact location (front, front boss, side) on the measure of GAMBIT. Figure 41 shows a representation of this interaction.

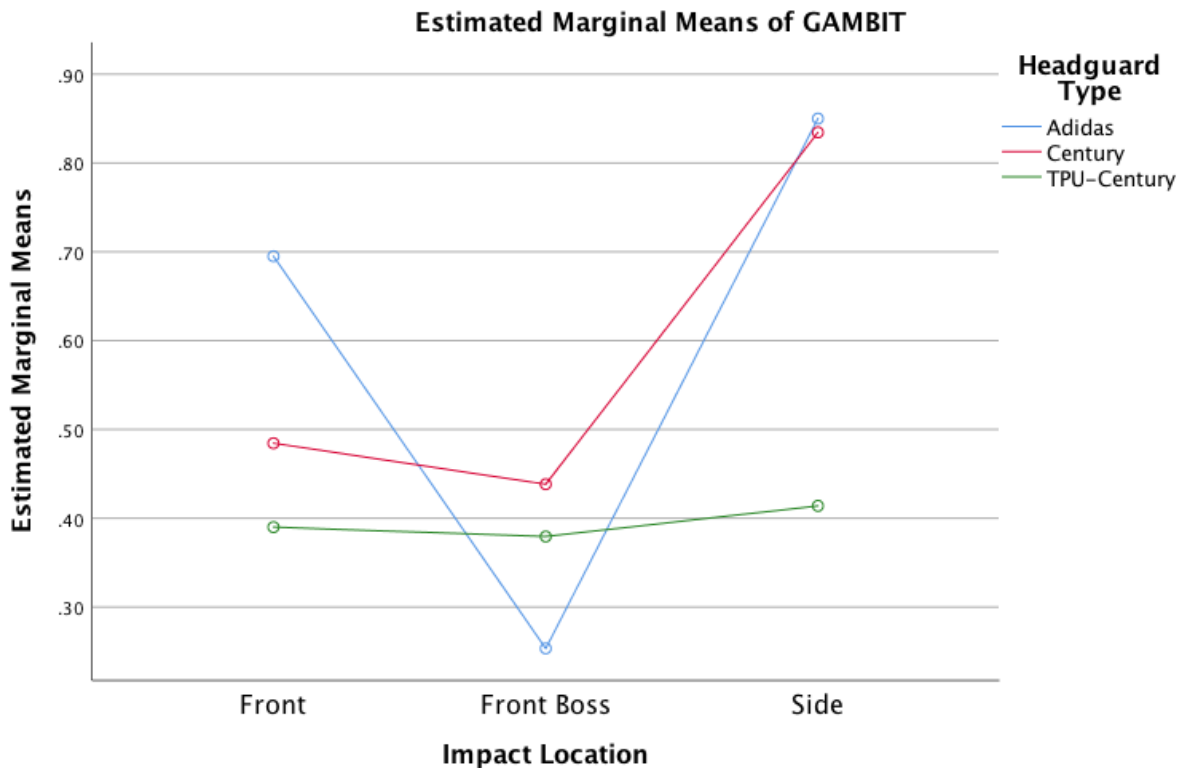


Figure 41: Interaction effect of headguard type and impact location on the estimated marginal means of GAMBIT.

The researcher conducted simple main effect analyses to further explain this interaction. The researcher began by conducting a set of one-way ANOVA tests to compare the three headguard types for each impact location respectively on the measure of GAMBIT. Similarly, the researcher conducted another set of one-way ANOVA tests to compare the three impact locations for each headguard separately.

Comparing headguard types for each impact location. The results of the one-way ANOVA showed that at the front location, there were significant differences in GAMBIT, $F(2, 51)=3.513$, $p=.037$, $\eta^2=.121$ across headguard conditions. A Tukey's post-hoc analysis

showed that the Adidas® headguard (M=.70, SD=.40) performed significantly worse ($p<.05$) in mitigating GAMBIT when compared to the TPU-Century® Drive headguard (M=.39, SD=.23). Differences in Century® Drive headguard results at this location (M=.48, SD=.40) compared to Adidas® and TPU-Century® Drive headguard results were not statistically significant ($p<.05$ for both). Figure 42 displays a representation of the difference in mean GAMBIT scores across headguard conditions for front impacts.

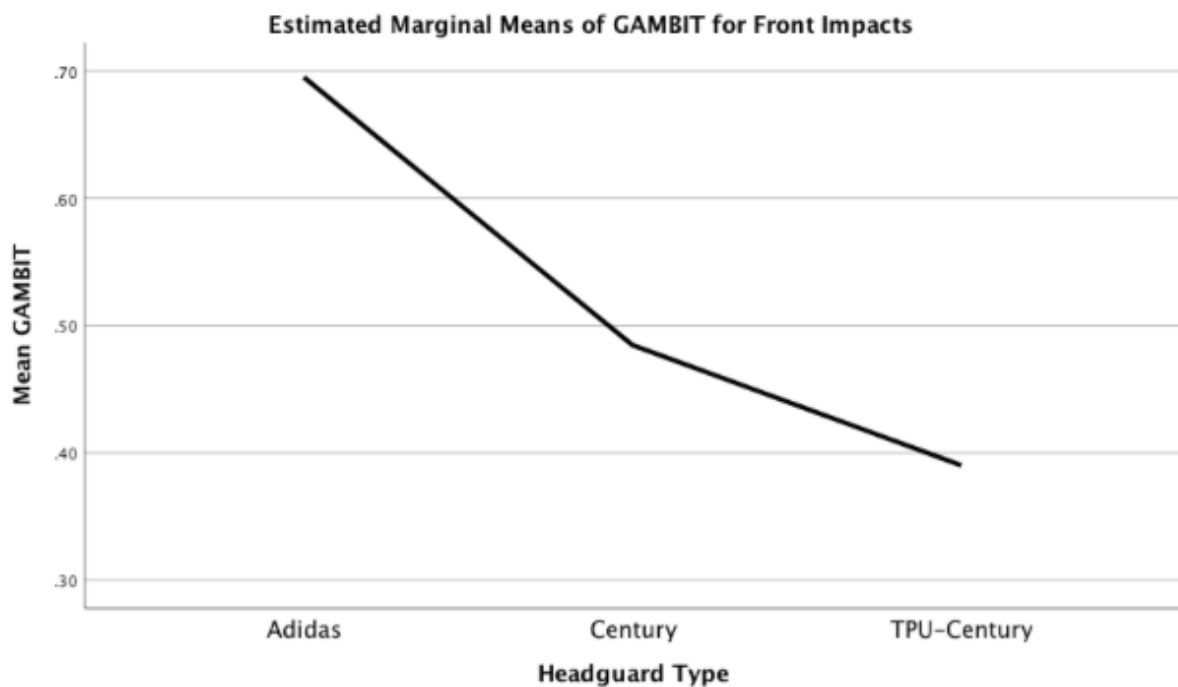


Figure 42: Estimated marginal means of GAMBIT across headguard types for front impacts.

At the front boss location, there were not significant differences, $F(2, 51)=1.423$, $p=.250$, in GAMBIT measures between the Adidas® (M=.25, SD=.36), TPU-Century® Drive (M=.38, SD=.19), and Century® Drive (M=.44, SD=.42) headguards. At the side location, significant differences in GAMBIT scores were found across headguard conditions, $F(2, 51)=5.919$, $p=.005$, $\eta^2=.188$. The Tukey's post-hoc analysis showed that at the side location, the TPU-Century® Drive performed significantly better (M=.41, SD=.23) than the Century® Drive (M=.83, SD=.58), and Adidas (M=.85, SD=.42) headguards ($p<.05$ for both). The differences between the Century® Drive and Adidas® headguards were not statistically

significant ($p>.05$). Figure 43 displays a representation of the difference in mean GAMBIT scores across headguard conditions for side impacts.

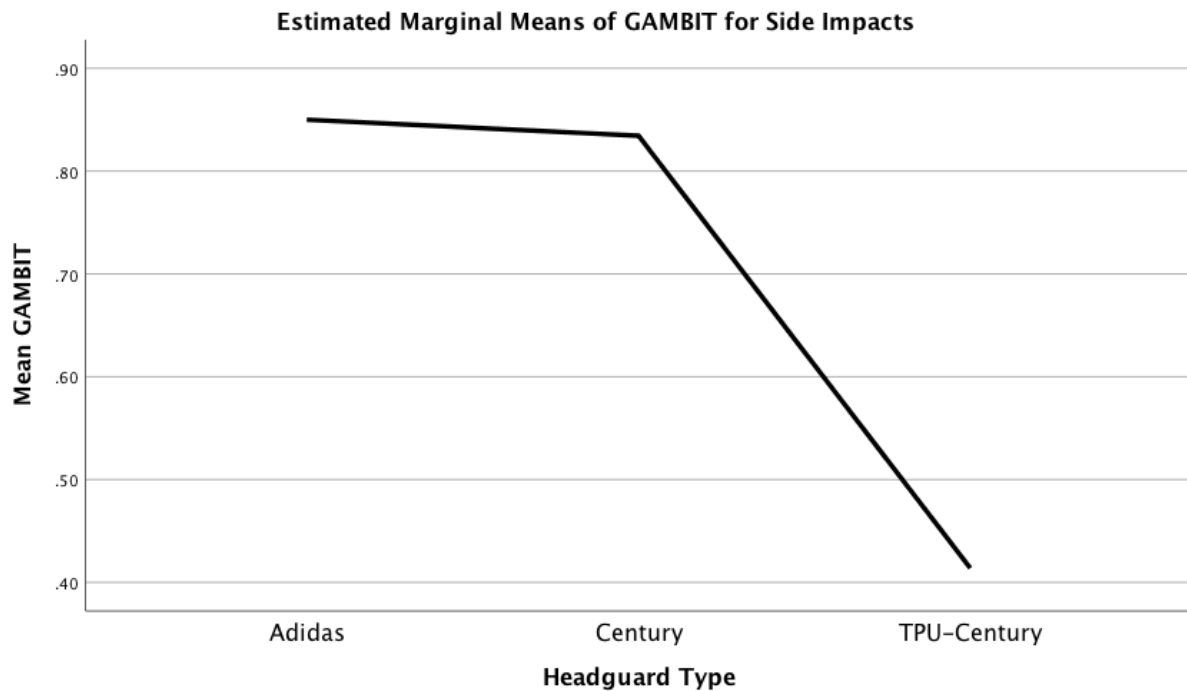


Figure 43: Estimated marginal means of GAMBIT across headguard types for side impacts.

Comparing the impact locations for each headguard. Results of a one-way ANOVA showed that for Adidas® headguard impacts, there were significant differences between impact locations, $F(2, 51)=11.194$, $p<.05$, $\eta^2=.305$, on GAMBIT scores. The Tukey's post-hoc analysis showed that for Adidas® headguard impacts, GAMBIT scores were significantly lower at the front boss location ($M=.25$, $SD=.36$) compared to the front location ($M=.70$, $SD=.40$), and the side location ($M=.85$, $SD=.42$), ($p<.05$ for both). The differences between GAMBIT scores for the front and side impacts were not statistically significant ($p>.05$). Figure 44 displays a representation of the difference in mean GAMBIT scores across impact locations for Adidas® headguard impacts.

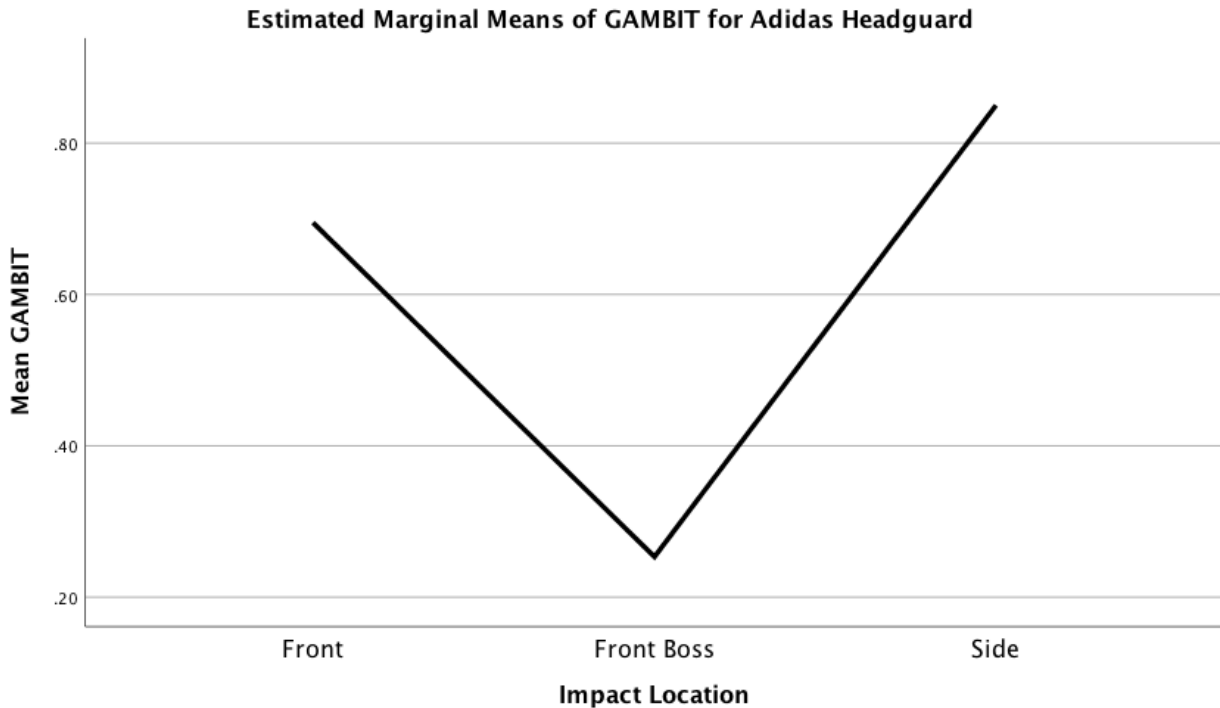


Figure 44: Estimated marginal means of GAMBIT for Adidas® headguard across impact locations.

For Century® Drive impacts, there were significant differences between impact locations, $F(2, 51)=3.787, p=.029$, on GAMBIT scores. Century Drive® headguard impacts, GAMBIT scores seemed to be the lowest at the front boss location ($M=.44, SD=.42$), followed by the front location ($M=.48, SD=.40$). GAMBIT scores seemed to be the highest at the side location ($M=.83, SD=.58$). The Tukey's post-hoc analysis showed that for this headguard, differences in GAMBIT scores were statistically significant between front boss impacts vs. side impacts ($p<.05$), but not between other locations ($p>.05$ for both). Figure 45 displays a representation of the difference in mean GAMBIT scores across impact locations for Century® Drive impacts.

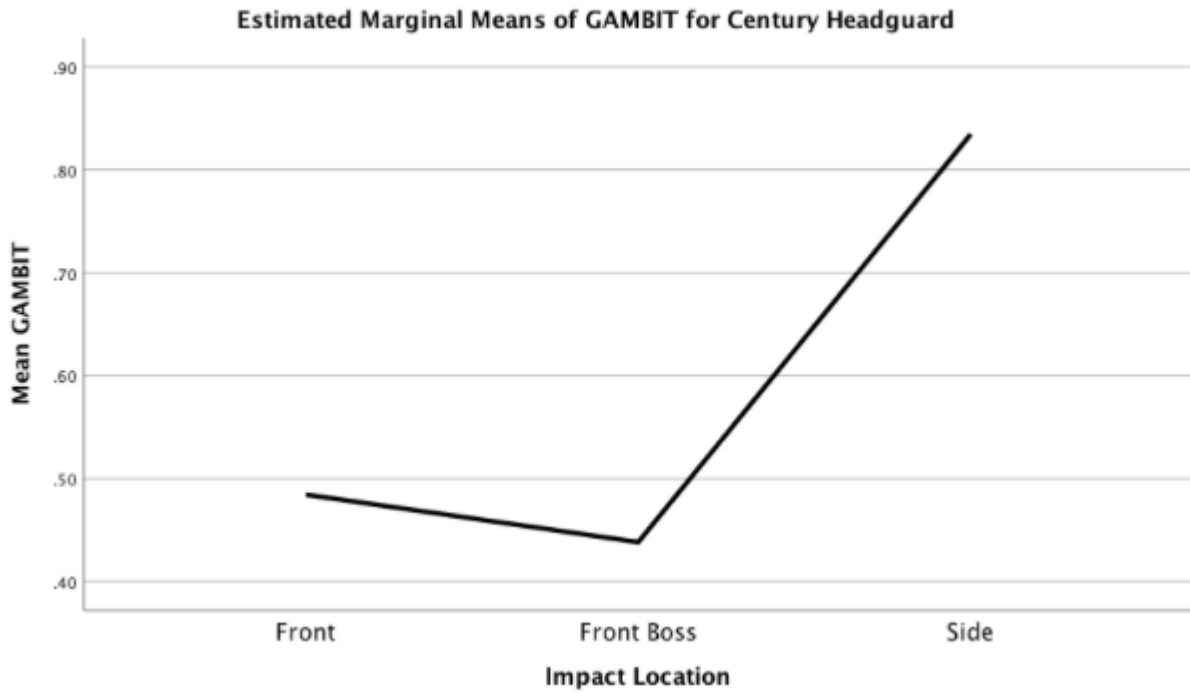


Figure 45: Estimated marginal means of GAMBIT for Century® Drive across impact locations.

For TPU-Century® Drive impacts, there were not significant differences $F(2, 51)=.119, p=.888$, in GAMBIT scores between front boss ($M=.38, SD=.19$), front ($M=.39, SD=.23$), and side ($M=.41, SD=.23$) impact locations.

Discussion

The sport of boxing has historically been considered a dangerous sport, particularly due to its concussion risk (Bledsoe et al., 2005), but little equipment interventions are enforced to lessen these risks. At this point in time, the primary equipment types for concussion prevention are headguards and mouthguards, but little evidence supports the use of these to prevent concussions outside of specific sports such as cycling, skiing and snowboarding (Daneshvar et al., 2011). No evidence currently exists to explore the use of TPU material for concussion mitigation in the sport of boxing.

Current commercial boxing headguards are composed of a range of different materials and vary in structure, and little standards exist to establish guidelines for their production. The AIBA (2019), only requires headguards to contain a high-quality leather outer shell and does not state any specific material requirements for inner materials. Consequently, variations in inner materials are seen between models. For example, the two commercial headguards used in this study, the Adidas® and Century® Drive use materials such as polyurethane, polyethylene, and high-density foam.

The current study created a modified boxing headguard by inserting 3D printed TPU liners into a Century® Drive boxing headguard to explore its capability to mitigate concussion risk when compared to two commercial headguards. This TPU material was chosen as it has displayed effectiveness for reducing accelerations (Barker et al., 2018). The TPU material has also been shown to be useful for energy absorption due to its tailorable and flexible structure (Bates et al., 2019).

Alternatively, little evidence has been shown to support the use of TPU in sport-specific impact testing, and it has been rarely used in protective headwear despite its established benefits. There are a number of ways that headguards and TPU material can be

tested. Two common testing methods that were performed in this study are in the form of static testing and dynamic testing.

Static compression testing can be performed with the method of testing stiffness of a material. Stiffness is the amount of force needed to achieve a certain deformation of a structure (Baumgart, 2000). Stiffness is further described by Baumgart (2000) as being quantified by “load” divided by “deformation”. The function of a stiff outer shell of a material is to distribute the impact energy over a large area in order to avoid a concentrated load (Di Landro et al., 2002). Using energy analysis in place of typical linear acceleration measure provides an advantage in that the dynamic response of helmets material properties can be analyzed across impact locations (Zerpa et al., 2016). More specifically, this analysis accounts for the force generated during an impact as well as the deflection of the helmet materials to resist damage caused by the force at each location (Zerpa et al., 2016).

Dynamic testing is a testing that accounts for a head’s dynamic (or impact) responses such as linear and angular accelerations. Taylor et al. (2016) note that finite element modelling (FEM) of the brain and data from kinematic response curves of linear and rotational accelerations can be key measures of concussion risk. More specifically, these measures allow for interpretation of the heads dynamic responses and how this can influence strain to brain tissues resulting in injury (Taylor et al., 2016). Dynamic impact testing in this context allows for real life impacts that would be seen in a boxing match to be replicated, encompassing a wide range of possible conditions. Full analysis of protective headwear using dynamic response and brain deformation over the entire helmeted surface is crucial for improving helmet technology to reduce concussive injury incidences (Taylor et al., 2016). In spite of research showing injury can occur at almost any location on the head, helmet testing has often been limited to a single or minimal number of impact areas (Taylor et al., 2016). To

address these concerns, the current study utilized multiple impact locations and velocities to explore a range of dynamic head responses.

Static Testing

As noted by Di Landro et al. (2002), a stiff outer shell of a helmet allows for distribution of impact energy over a large area in order to avoid a concentrated load. As such, testing material's responses to compression through the use of static compression testing can provide information on how a boxing headguard is able to absorb energy, as a result reducing the stress experienced by the head by a concentrated load. To examine the material's capacity to absorb impacts, Research Question 1 sought to explore which boxing headguard absorbed the most energy when loaded with a compressive and shear forces across locations (front and side). Static testing results showed that the TPU-Century® Drive headguard was most effective in absorbing shear energy, compression energy, and total energy at both locations (front, side).

Front energy absorption. Across 14 static energy loading and unloading cycles at the front location, mean energy absorption by the TPU-Century® Drive in terms of total, compression, and shear energies was 42.38%, 46.25%, and 35.08% respectively. The Century® Drive headguard was the second most effective headguard for total, compression, and shear energy absorptions, absorbing an average of 31.98%, 36.39%, and 22.85%, respectively across the 14 cycles. The Adidas® headguard was the least effective in energy absorption across cycles for these measures, absorbing an average of 25.71%, 30.13%, and 17.63%, respectively. These findings indicate that the addition of a single TPU insert to the front location of the Century® Drive headguard resulted in close to a 10% increase in capability of the headgear to absorb total, compression, and shear energies.

Side energy absorption. At the side location, the average of 14 energy loading and unloading cycles showed that the TPU-Century® Drive was the most effective in absorbing

total, compression, and shear energies, absorbing 41.52% , 48.48%, and 29.15%, respectively. The Adidas® headguard was the second most effective headguard for at this location for total, compression, and shear energy absorptions, absorbing an average of 34.42%, 40.10%, and 22.48%, respectively across the 14 cycles. The Century® Drive headguard was the least effective across cycles for these measures, absorbing an average of 24.01%, 28.66%, and 13.51%, respectively. Compared to the Adidas headguard®, the TPU-Century® Drive absorbed an average of over 7% more energy for the side location. The addition of a single TPU insert to the Century® Drive headguard's side location yielded more than twice as much shear energy (29.15% versus 13.51%), and more than 15% more total and compression energies absorbed.

As noted by Zerpa et al. (2016), this type of analysis can provide more information on protective headwear's properties across locations during impacts. Information from these types of tests can help equipment manufacturers improve weaker helmet areas to dissipate energy, decrease rebound velocity, and minimize brain tissue damage risk when the head is impacted (Zerpa et al., 2016). Results from these tests may infer that the Adidas® headguard is less effective in absorbing energy at the front, while the Century® Drive is weaker at the side. This may highlight that these headguards require improvement at these locations to make them safer in reducing loads placed on the head (Di Landro et al., 2002). The implications of these results also support the inclusion of TPU material in boxing headguards for absorbing impact energy. The TPU material is a relatively light material that did not increase or decrease the size or shape or weight of the Century® Drive headguard upon being added. As shown by the static testing results, TPU inclusion in the Century® Drive headguard resulted in marked improvements in shear and compression energy absorptions across both locations (front, side). These findings parallel the research presented by Bates et

al. (2019) and Rizzo et al. (2020), which showed TPU material to be useful for energy absorption.

Dynamic Testing

Analysis of kinematic response such as linear and rotational accelerations provide an interpretation of the head's dynamic responses and how these influence brain tissue injury risk (Taylor et al., 2016). The current study utilized a number of dynamic impact conditions to measure head injury risk through the use of linear and angular (rotational) accelerations as well as several specific injury risk measures.

Linear acceleration. To explore linear impact effects, Research Question 2 sought to determine which boxing headguard (Century® Drive, Adidas®, and TPU- Century® Drive) would perform better in decreasing linear impact acceleration across different impact locations (front, front boss, and side) during dynamic testing. There was not a significant interaction between headguard type and impact location on the measure of PRLA ($p > .05$). These results suggest that the headguards do not perform differently based on impact location for minimizing PRLA of the head. Additionally, there was not a significant main effect when exploring the differences between impact locations on the measure of PRLA. These findings suggest that impact locations, specifically front, front boss, and side, do not significantly influence linear motion of the head when impacted.

Significant main effects were seen across headguards on the measure of PRLA ($p < .05$). The TPU-Century® Drive headguard performed significantly better than the Century® Drive headguard and the Adidas® headguard when observed across impact locations collectively ($p < .05$). When compared to the Century® Drive and Adidas® headguards, which produced very similar average PRLA results (182.93g vs. 184.94g, respectively), the TPU-Century® Drive headguard reduced PRLA by more than 40%. This finding suggests that the use of TPU material in boxing headguards can produce meaningful

reductions in concussion risk due to linear accelerations. McIntosh and Patton (2015b) previously showed Adidas® headguards to perform poorly in reducing acceleration in drop tests. Alternatively, O’Sullivan and Fife (2016) found Adidas® headguards to be stronger in linear acceleration mitigation compared to other headguards. O’Sullivan and Fife’s (2016) study, however; noted that all headguards tested failed the American Society for Testing and Materials (ASTM) RLA threshold of 150g. In the current study, the Adidas® and Century® Drive headguards failed this threshold as well, while the TPU-Century® Drive performed better and passed the threshold value below what is recommended by ASTM ($M=104.61g$, $SD=48.39$). These findings also build on the work of Barker et al. (2018), who found TPU to be effective at reducing lower accelerations at low velocities. The current study showed TPU to be effective across a wide range of impact velocities. These findings seem novel in the area of boxing headguard testing, highlighting the effectiveness of TPU in reducing concussion risk caused by linear accelerations. Further analysis of the TPU-Century® Drive headguard showed that PRLA was mitigated below the ASTM threshold across all locations. This further outcome proves the effectiveness of TPU, showing that its PRLA mitigation benefits are not location-dependent, but rather that it is effective at all locations.

Although rotational accelerations, or a combination of rotational and linear accelerations, are more significant indicators of concussion risk, linear acceleration alone is still a good predictor of peak pressure occurring within the brain (Meaney & Smith, 2011). As noted with static testing, dissipation of energy over a materials surface results in less concentrated loads placed on the head (Di Landro et al., 2002). Subsequently, it can be suggested that the increased absorption capability of the TPU-Century® Drive headguard may have influenced the reductions in PRLA of the head when impacted.

GSI. This measure integrates acceleration over time, providing an accurate head injury risk assessment that can be replicated under different impact conditions (NOCSAE,

2017). As GSI is the measure of instantaneous resultant linear acceleration of the head (see Equation 2), analysis of GSI measures produced similar results to PRLA. To analyze this risk measure, Research Question 4 sought to determine which boxing headguard (Century® Drive, Adidas®, and TPU-Century® Drive) would perform better at decreasing the risk of head injury due to the effect of linear impact acceleration across different headguard locations (front, front boss, and side). There was not a significant interaction effect between headguard type and impact location on the measure of GSI, nor a significant main effect between impact location on the measure of GSI ($p > .05$ for both). As shown with linear acceleration, this finding suggests that head injury risk from linear forces is not location dependent. More specifically, it suggests that when the head is impacted at the front, front boss, or side, there is not significant changes in concussion risk from a linear motion alone. With this said, this contrasts previous research indicating that direction of strain has a strong effect on damage to brain structures (Gennarelli et al., 1982; Meaney & Smith, 2011). This suggests that the lack of differences across locations is more driven by similarities in performance across locations for each headguard than through the dynamics of the headform itself.

Significant differences in GSI measures were shown between headguard conditions when exploring headguard performance across all impact locations collectively. As was seen with PRLA, the TPU-Century® Drive headguard performed significantly better than the Adidas and Century® Drive headguards ($p < .05$), with the latter two not performing significantly differently ($p > .05$). The TPU-Century® Drive headguard exhibited nearly a 60% reduction in average GSI when compared to the other two headguards. To create a more simplified expression of linear testing results, Table 3 displays the significant main effect test results for linear impact measures (PRLA, GSI).

Table 3

Results for significant main effect tests for linear impact measure testing.

Dependent measure	Independent measure	Significance	Most effective headguard	Relevant figure
PRLA	Headguard Type	Significant	TPU-Century® Drive	Figure 27
GSI	Headguard Type	Significant	TPU-Century® Drive	Figure 34

When comparing GSI measures to the threshold of 1200 GSI stated by NOCSAE (2017), the Adidas® headguard had n=18 impacts that surpassed this threshold, including cases at all 3 impact locations. The Century® Drive headguard surpassed this threshold in a total of n=17 impacts, with cases of this also occurring at all 3 locations. There were no impacts beyond this threshold with TPU-Century® Drive headguard trials, with the highest GSI measure recorded being GSI=949.06 when this headguard was used. This finding suggests a strong and consistent influence of TPU material on reducing concussion risk occurring from linear forces. This outcome may imply that several incidences of possible concussive impacts would be mitigated if TPU material was used in the headguard. As such, TPU material may have a significant effect in reducing strain posed by linear impacts onto the brain. The reductions in GSI found with use of TPU parallels the findings of Zerpa et al. (2020), who found TPU to provide significant GSI reductions when used in cycling helmets. With this, it can be suggested that TPU material should be incorporated into headguard design at the front, front boss, and side to reduce the risk of concussion risk caused by linear forces.

Angular acceleration. Results of analysis of angular forces imparted on the headform revealed more varying results across headguard types and impact locations. Angular acceleration of the head causes a “jarring” effect of the head, producing more deformation in

the brain than this type of force would in other tissues of the body (Meaney & Smith, 2011). Again, rotational accelerations are stronger predictors of concussion than linear accelerations (Meaney & Smith, 2011). To explore this, Research Question 3 sought to determine which boxing headguard (Century® Drive, Adidas®, and TPU-Century® Drive) would be more effective in mitigating angular acceleration at each impact location (front, front boss, side).

The results of this study revealed a significant interaction between headguard type and location on the measure of peak resultant angular acceleration. When evaluating this interaction by individual location, significant differences were seen between headguards for front impacts. For front impacts, the Adidas® headguard performed significantly worse than the Century® Drive and TPU-Century® Drive. Front boss and side impacts did not produce significant differences between headguards.

When comparing impact locations for each individual headguard, all 3 headguards yielded significant differences between locations. For the Adidas® headguard, impacts to the front produced significantly higher mean peak resultant angular acceleration measures compared to impacts to the front boss. The combination of the last two findings suggests poor frontal impact protection ability of the Adidas® headguard. The researcher noticed weakening and deterioration of the Adidas® headguard's front material across the higher end of impact velocities. Additionally, a marked increase was seen between two consecutive impacts at velocities of 3.86 m/s and 3.94 m/s, where peak resultant angular acceleration doubled from 647.55 rad/s² to 1712.11 rad/s² respectively. This increase in peak resultant angular acceleration for Adidas® front impacts was maintained as impact velocities continued to increase. This outcome may highlight a lack of durability of the front protection materials of the Adidas® headguard and may indicate that it is unable to withstand impacts at higher velocities.

For both the Century® Drive and TPU-Century® Drive headguards, side impacts produced significantly higher mean peak resultant angular acceleration values than front and front boss impacts. For both of these headguards, front boss and front impacts were not significantly different. Although side impact performance for these headguards were not significantly different from the Adidas® headguard, this finding suggests that the advantages provided by these headguards for front impacts is not shared for side impacts. When comparing these results to the threshold of 4500 rad/s² of angular acceleration noted by Ommaya et al. (2002), the current study found no impacts resulted in angular acceleration that came even close to meeting this threshold. These findings build on the research of McIntosh and Patton (2015a), as well as Dau et al. (2006), who both found significant reductions in angular acceleration on headguard impacts compared to bare head impacts. Dau et al. (2006) tested angular acceleration when a headform was impacted with a hook punch. Consequently, their study found much higher peak angular acceleration measures than the current study, with Dau et al. (2006), finding the measure to surpass the 4500 rad/s² threshold even with the use of a headguard. This outcome may infer that more rotational forces are placed on the head with a “hook” impact as opposed to a straight impact, with the latter being used in the current study. Nonetheless, the current study further builds on previous research by showing significant benefits in mitigating angular acceleration through the use of the Century® Drive and TPU-Century® Drive headguards. It is also important to note that although McIntosh and Patton (2015a) and Dau et al. (2006) used higher upper end impact velocities (8.43 m/s and 9.57 m/s, respectively) than the current study (5.13 m/s), the current study used a much heavier impact instrument. McIntosh and Patton (2015a) used a 4 kg semi rigid fist model, while Dau et al. (2006) used human punches, with the average adult arm being 5.335 kg (Plagenhoef et al., 1983). With this study using a 13.1 kg impacting rod, the peak momentum (the product of mass times velocity) placed on the head is actually higher

for this study than the two aforementioned studies, despite having lower peak impact velocities. As such, these findings further suggest that the headguards, particularly the Century® Drive and TPU-Century® Drive, maintain their effectiveness in mitigating angular acceleration of the head at higher impact momenta.

AGSI. This measure integrates angular acceleration over time to provide an injury risk assessment, resulting from head rotation. As such, Research Question 5 sought to determine which boxing headguard (Century® Drive, Adidas®, and TPU-Century® Drive) would perform better at decreasing the risk of head injury due to the effect of angular impact acceleration across different locations (front, front boss, and side). The results of this analysis revealed a significant interaction between headguard and impact location on the measure of AGSI. This implies that differences in headguard performance are seen at different impact locations for mitigating AGSI.

When evaluating this interaction by individual location, significant differences were seen between headguards for front impacts. For front impacts, the Adidas® headguard performed significantly worse than the TPU-Century® Drive and Century® Drive headguards, with the latter two headguards not performing significantly differently. Significant differences were not seen in AGSI measures between headguards at the front boss or side location.

When comparing impact locations for each individual headguard, all 3 headguards yielded significant differences between locations. When isolating results for the Adidas® headguard alone, impacts to the front produced significantly higher AGSI measures when compared to front boss or side impacts, which were not significantly different. The combination of these two findings, as with the peak resultant angular acceleration, suggest that the Adidas® headguard performs poorly for front impacts when compared to the Century® Drive and TPU-Century® Drive. This outcome may highlight a weakness in the

protective capability of the front material and design of the Adidas® headguard. Similar to the linear impact results, a marked increase was seen in Adidas® AGSI measures for front impacts towards the upper end of impact velocities. This outcome may again infer issues with durability and high velocity impact performance with the Adidas® headguard.

When isolating AGSI results for the Century® Drive headguard, side impacts produced significantly higher mean peak resultant angular acceleration measures when compared to front boss impacts. Front impacts were not significantly different from front boss or side impacts. AGSI measures were significantly higher than front and front boss impacts for the TPU-Century® Drive, with the latter two not being significantly different. These findings again display poor performance in the sides of the Century® Drive and TPU-Century® Drive headguards when compared to other areas of the headguards. Impacts to the side of the head represent an impact in the coronal plane, which has shown to produce the most damage to the internal structures of the brain (Gennarelli et al. 1982). These types of side impact, in addition to all other impact locations used in the current study, are deemed legal strike locations by the AIBA (2019). With this considered, the TPU design structure may need to be adapted to provide better protection to the side of the head. For example, having the TPU material cover a larger area of the side of the head may be able to better reduce the rotational forces placed on the head by side impacts.

These results do not determine a headguard that is consistently better or worse in mitigating angular impact effects across all locations. However, a theme emerges that the Adidas headguard is worse in mitigating angular effects for front impacts, particularly at higher velocities. Another emerging theme is that the TPU-Century® Drive headguard and the Century® Drive construction are less effective for reducing angular impact effects at the side when compared to the front and, in most cases, the front boss. Furthermore, the lack of significant difference between the Century® Drive and TPU-Century® Drive performance in

peak resultant angular acceleration and AGSI suggest that the TPU material may not be as effective for mitigating angular impact forces as it is for linear forces. As previous literature has been more focused on the linear impact mechanics of TPU, and has not examined extensively the angular impact mechanics, this represents relatively novel information. Future research should look to further explore the angular dynamics of TPU when impacted. Nonetheless, when looking at the differences in the angular acceleration measure in the headguards alone, O'Sullivan and Fife (2016) also noted significant differences in headguard performance across impact locations. This outcome may be due to the differences in structure and design of the headguards at different locations, with both headguards in this study providing more protection at the front and front boss as opposed to the side (see Figures 9, 10, and 13).

GAMBIT. When assessing concussion risk, evaluating linear and rotational acceleration impact effects individually is useful; however, concussions more commonly occur from these two accelerations in combination (Meaney et al., 1995). The measure of GAMBIT provides an injury risk index that incorporates both linear and angular accelerations (see Equation 3). With this considered, Research Question 6 sought to determine which boxing headguard (Century® Drive, Adidas®, and TPU-Century® Drive) would perform better at decreasing the risk of head injury due to the shared effect of linear and angular impact accelerations across different headguard locations (front, front boss, and side). A significant interaction effect was seen between headguard type and impact location on the measure of GAMBIT.

When evaluating this interaction by individual location, significant differences were seen between headguards for front and side impacts, but not for front boss impacts. For front impacts, the TPU-Century® Drive headguard performed significantly better than the Adidas® headguard. These findings further display poor performance for front impacts by the

Adidas® headguard. For side impacts, the TPU-Century® Drive headguard performed significantly better than both the Century® Drive and Adidas® headguards, which were not significantly different from one another. These findings indicate that the addition of TPU into a headguard is advantageous for mitigating the combination of angular and linear acceleration at the side. While the Century® Drive and TPU-Century® Drive headguards were not significantly different for front impacts, these headguards did both provide a significant advantage at the front in mitigating this combination when compared to the Adidas®. The advantages offered by the TPU material for side impacts were seen in the PRLA results, but not as much in the peak resultant angular acceleration results. As such, the reduction in GAMBIT offered by TPU material is likely driven by its linear impact effect performance.

When comparing impact locations for each individual headguard, the Adidas® and Century® Drive headguards yielded significant differences between locations, while the TPU-Century® Drive headguard did not. For Adidas impacts, front boss impacts produced significantly lower mean GAMBIT values than front and side impacts, which were not significantly different. This outcome is relatively similar to the simple main effect results of peak resultant angular acceleration and AGSI, where each measure showed front boss impacts to be significantly lower than front impacts. On the Adidas® headguard, slight ridges on the padding can be observed near each side of the front boss location, where there is a very small increase in the thickness of the padding covering each temple area. Although this detail of the padding is very small, it might be a factor that contributed to the significant reductions seen in GAMBIT measures for the front boss.

For the Century® Drive headguard, front boss impacts produced significantly lower GAMBIT values when compared to side impacts. This finding is relatively similar to the Century® Drive results for peak resultant angular acceleration, where the headguard produced significantly higher GAMBIT at the side when compared to front and front boss. It

is also similar to the AGSI results, where side impacts again produced significantly higher results at the side when compared to front boss. The combination of these results consistently shows weaker side impact performance for the Century® Drive headguard. Significant differences in both linear and angular acceleration between impact locations were also seen in the study by O'Sullivan and Fife (2016). This may highlight an issue in the lack of standardization of boxing headguards, showing the need for impact absorption to be relatively consistent across the headguard. Similarly, Zerpa et al. (2020) noted differences in linear concussion risk mitigation across locations with the use of TPU in cycling helmets. Zerpa et al. (2020) also found lesser results of TPU at the side location compared to other locations. Similarly, Zerpa et al. (2020) noted that this may be due to geometrical differences in the helmets. It is important to note that, although the Century® Drive headguard consistently performed worse at the side, its side performance is not significantly worse than that of the Adidas® headguard. That is, the decreases in performance seen for side impacts do not suggest it is an inferior headguard for side impact protection, but rather that it is not as effective at the side in comparison to its other locations. The decrease in effectiveness at the side however is still a cause for concern due to the aforementioned increased strain placed on the brain by coronal plane impacts (Meaney et al., 1995). This outcome may highlight the need for further development of headguard padding to more closely resemble the padding offered at the front and front boss locations. As the side padding of both headguards used in this study is thinner and more open than the front and front boss padding, this may be where the issue stems from. Table 4 displays a simplified expression of the interaction tests for headguard type and impact location on measures of peak resultant angular acceleration, AGSI, and GAMBIT. Results are shown for all differences between headguards and noted where these differences were deemed significant.

Table 4

Interaction tests for headguard type and location on measures of angular acceleration, AGSI, and GAMBIT.

Dependent measures	Interaction significance (headguard *location)	Most effective headguard by location				Relevant figure
		Front	Front boss	Side		
Angular Acceleration	Significant	TPU-Century® Drive	Century® Drive	Adidas®		Figure 29
AGSI	Significant	TPU-Century® Drive	Adidas®	Adidas®		Figure 36
GAMBIT	Significant	TPU-Century® Drive	Adidas®	TPU-Century® Drive		Figure 41

Note: Bolded TPU headguard denotes which location the TPU performed better than the others.

As can be seen in this table, the only cases that showed significant differences between headguards were those where the TPU-Century® Drive was the top performing headguard. This highlights several examples of locations and variables where the TPU-Century Drive headguard offered a significant advantage over at least one of the other headguards. This result builds on previous research that has shown TPU material to have positive effects in mitigating linear acceleration and linear injury risk measures (Zerpa et al., 2020; Barker et al., 2018). In addition to providing these benefits, the addition of TPU into the boxing headguard also provides a benefit when the linear and angular forces are both considered. This demonstrates its effectiveness in a novel and more complex concussion risk context. The importance of this finding is supported by the idea that concussions occur primarily from combined angular and linear forces as opposed to linear or angular force individually (Meaney et al., 1995).

The thresholds for GAMBIT noted by Newman et al. (1999) suggest that a GAMBIT score of $g=1$ corresponds to a 50% chance of AIS=3 (serious head injury), while a score of $g=0.4$ corresponds to a 50% chance of AIS=1 (minor head injury). Mean GAMBIT results showed that the Adidas® headguard surpassed the 0.4 threshold for front ($M=.70$, $SD=.40$) and side impacts, falling well under it for front boss impacts ($M=.25$, $SD=.36$). Again, this highlights the advantages of the front boss protection of the Adidas® headguard in comparison to its other locations. The Century® Drive headguard surpassed the 0.4 threshold at the front ($M=.48$, $SD=.40$), front boss ($M=.44$, $SD=.42$), and side ($M=.83$, $SD=.58$). The TPU-Century® Drive headguard was below the threshold for front ($M=.39$, $SD=.23$) and front boss ($M=.38$, $SD=.19$). The TPU-Century® Drive headguard was just above the threshold for side impacts ($M=.41$, $SD=.23$). With this said, as previously stated, this was still significantly lower than the mean GAMBIT values produced at the side in Century® Drive and Adidas® Drive impacts. In addition to this, when looking at individual impacts, several cases went above the $g=1$ threshold (corresponding to a 50% chance of serious head injury) for the Adidas® headguard ($n=14$) and Century® Drive headguard ($n=13$). Alternatively, no cases of TPU-Century® Drive went beyond this threshold. This finding infers a strong and consistent ability of the TPU material to mitigate concussion risk. Despite the TPU having better ability in mitigating linear forces compared to angular ones, its GAMBIT measures show that it is capable of reducing concussion risk as a whole when the two forces are collectively considered by one measure. The benefits of TPU material shown in this study resemble the research presented by Zerpa et al. (2020), Barker et al. (2018), and Rizzo et al. (2020), which showed benefits of TPU in impact protection. As such, the findings of this study provide positive evidence in support of the use of TPU in boxing headguards, showing it to be an effective concussion risk mitigation tool in many different aspects. This highlights a possible avenue for further concussion research and suggests that TPU should be

incorporated into commercial boxing headguard designs at the front, front boss, and side locations.

Conclusion

With previous research displaying a lack of conclusive evidence regarding the benefits of boxing headguards, a lack of enforcement of headguard use has been seen in boxing competition (Dickinson & Rempel, 2016). With this considered, this study attempted to explore how different boxing headguards performed at different impact locations in mitigating a number of injury risk measures. This study also attempted to explore the effect of thermoplastic polyurethane (TPU) material in mitigating these measures when introduced into a commercial headguard. These variables were tested through static and dynamic measures, with dynamic testing utilizing a headform and neckform assembly designed to accurately simulate the human response to impact. Using a number of impact velocities and impact locations, the testing was designed to replicate the types of striking situations to which a boxer may be subjected in a real bout. Three boxing headguards were compared across locations (front, front boss, side), these being an Adidas® headguard, a Century® Drive headguard, and a TPU-Century® Drive headguard.

The results of this study showed the addition of TPU to the headguard to be effective in lowering linear concussion risk indexes, these being PRLA and GSI. The TPU was also the most effective in absorbing energy, suggesting its material properties are beneficial for reducing concentrated loads to the head (Di Landro et al., 2002). The TPU also produced significant reductions in measures of GAMBIT, a concussion risk index that accounts for both linear and angular accelerations. Results for peak resultant angular acceleration, AGSI, and GAMBIT were dependent on impact location, suggesting angular forces are more dependent on where the headguards are struck. Differences in GAMBIT were also location dependent, with the addition of TPU to the commercial headguard offering significant reductions at the front and side locations. The TPU-headguard combination produced no incidences where it surpassed the NOCSAE (2017) threshold for GSI, nor ever surpassing the

serious concussion risk threshold for GAMBIT established by Newman et al. (1999).

Alternatively, several incidences where these thresholds were surpassed were seen in the two commercial headguards. This outcome suggests several possible concussion incidences that may have been mitigated by the use of TPU. These findings show significant benefits of the TPU material when used in a boxing headguard, primarily for limiting linear forces placed on the head (Newman, 1986).

This study expands on the work of several previous researchers as it sought to provide a more extensive examination on concussion risk mitigation of boxing headguards. For example, it expands on the work of McIntosh and Patton (2015a), as well as Dau et al. (2006), who explored the effectiveness of boxing headguards in mitigating angular and linear impact measures. The current study built on this literature by incorporating the use of TPU material, as well as a wider range of impact velocities and a more complex injury risk measure, this being GAMBIT. Furthermore, this study expands on the work of Zerpa et al. (2020), as well as Barker et al., (2018), who provided evidence of the effectiveness of TPU material in mitigating linear acceleration. The current study builds on this by exploring the effectiveness of TPU in mitigating angular forces and injury risk measures that represent a combination of linear and angular forces. This outcome provides an avenue for future research in regard to TPU use in boxing headguards and may suggest for equipment manufacturers to start to incorporate TPU into headguard design.

Strengths

The introduction of TPU material into the boxing headguard is the primary strength of this study. Despite its established benefits, concussion research using TPU has been relatively limited, and no research has integrated it into boxing headguard testing. Static and dynamic testing showed a number of advantages provided by the TPU material, primarily with linear forces.

Another strength of this study was the range of impact conditions and concussion risk measures included. Inclusion of multiple impact locations and a wide range of impact velocities created a closer replication of impacts that occur in a real boxing match. Use of both accelerometers and gyroscope sensors allowed for both translational and rotational movements of the head to be analyzed, also more closely resembling the combination of head motions that a boxer would sustain when struck. Analysis of the GAMBIT variable allowed for these measures to be analyzed in a combined injury risk index that has not been commonly used in previous headguard research.

Limitations

This study also faced a number of limitations that future research should look to explore. Physical constraints of the pneumatic impactor prevented the usage of impact angle as a variable. As such, the range of head movement in boxing that results in the head being struck at different angles could not be accounted for. Additionally, the physical shape of the impactor rod did not permit the use of a boxing glove in impacts. Although this study did not require the inclusion of a boxing glove as the aim was to compare different headgear, for future research the impacting rod may need to be modified to attach a boxing glove to replicate different mechanisms of injury in the sport of boxing. Alternatively, not including a boxing glove when comparing different headguards is better for reliability tests and would ensure more consistent impacts across conditions.

Another limitation of the study was the stiffness of the neckform. The neckform was adjusted to represent the 50th percentile male neck. As such, the findings of this study more closely replicate results for males and may differ for female subjects.

Furthermore, the method of insertion of the TPU inserts into the boxing headguard may represent a reliability concern. The researcher had to cut out the padding of the Century® Drive headguard to fit the inserts into the front and front boss, and simply fit the

insert into the gap of the ear padding. With this lack of design standardization, it is difficult to determine if results would have changed if the inserts were placed differently within the headguard. With this said, the researcher attempted to have the TPU inserts as the primary point of contact when this headguard was being impacted.

The final limitation of the study was the possible movement of the wireless gyroscope sensors. Due to the physical construction of the sensors, they had to be held onto the head with a tape, and as such, it cannot be guaranteed that they were not loosened or dislodged across impacts. To address this concern as well as possible, the researcher examined the measures across replications to ensure consistency and checked the sensors between impacts to confirm that they did not shift or loosen from the head.

Future Directions

Future research should look to incorporate TPU and other impact absorption materials into currently produced headguards. As headguard research has shown inconclusive results to support or caution the use of headguards, introduction of new materials and headguard modifications should be proposed and tested. Comparison of other helmet materials, similar to the methods of Razaghi et al. (2018) may be useful for further displaying the effectiveness of thermoplastic polyurethane in static and dynamic testing. Analyzing the energy absorption capability of TPU in comparison to commercial liners such as EPP, EPS, and PVA and other rubbers, foams, and sponges, may propose more effective headguard modifications (Razaghi et al., 2018).

Future research should also seek to explore the performance of these headguards and materials under more complex conditions, such as a wider range of impact angles and neck strengths. Dynamic testing should be performed with the headform positioned at multiple oblique angles to explore the effect of headguards when impacted at different angles. This

may better replicate the range of positions that a headguard may be impacted at in a real boxing match.

The interaction effects between headguard type and impact location on measures of peak resultant angular acceleration, AGSI, and GAMBIT should be more closely explored. The results of this study showed that the Century® Drive and TPU-Century® Drive performed significantly better for front impacts, while the Adidas® headguard was more effective at the front boss impacts in comparison to its other locations. Exploration of more headguards may be useful in further exploring these interactions to determine why these differences occur, possibly highlighting advantages of different impact materials.

Finally, future research should look to explore impact conditions like those used in this study, also incorporating bare head impacts across locations. This approach would allow for headguard performance to be explored using the bare head as a reference point. From this, the true effectiveness of headguard use can be more accurately examined, showing if there is a true advantage of using a headguard to reduce concussion risk.

References

- Adams, J. H., Graham, D. I., Murray, L. S., & Scott, G. (1982). Diffuse axonal injury due to nonmissile head injury in humans: An analysis of 45 cases. *Annals of Neurology*, *12*(6), 557-563. doi:10.1002/ana.410120610
- Adkitte, R., Bardgujar, S., Yeole, U., Gawali, P., & Gharote, G. (2016). Prevalence of injuries in competitive boxers: A retrospective study. *Saudi Journal of Sports Medicine*, *16*(2), 106. doi:10.4103/1319-6308.180154
- Advanced Mechanical Technology Inc. (n.d) Choosing a force plate. (n.d.). Retrieved from <https://www.anti.biz/fps-guide.aspx>
- AIBA (2019). Technical and Competition Rules. Retrieved from <https://d152tffy3gbaeg.cloudfront.net/2019/03/AIBA-Technical-Competition-Rules-.pdf>.
- American Medical Association. (2007). Boxing. Retrieved from https://ama.com.au/sites/default/files/documents/AMA_Position_Statement_on_Boxing_1997._Reaffirmed_2007.pdf.
- Ametek Inc. (2008). Chatillon® TCD Series Console, For Use with TCD110, TCD225 and TCD1100 Series Digital Force Testers, User's Guide. Retrieved from <https://manualzz.com/doc/6614116/tcd-series-console-user-manual>
- Barker, J., Corrales, M., Gierczycka, D., Bruneau, D., Bustamante, M., & Cronin, D. (2018). Contribution of energy-absorbing structures to head kinematics in football helmet impacts. In *IRCOBI conference 2018*.
- Barth, J. T., Freeman, J. R., Broshek, D. K., & Varney, R. N. (2001). Acceleration-Deceleration Sport-Related Concussion: The Gravity of It All. *Journal of athletic training*, *36*(3), 253–256.
- Bartsch, A. J., Benzel, E. C., Miele, V. J., Morr, D. R., & Prakash, V. (2012). Boxing and mixed martial arts: preliminary traumatic neuromechanical injury risk analyses from

- laboratory impact dosage data. *Journal of Neurosurgery*, 116(5), 1070–1080.
doi:10.3171/2011.12.jns111478
- Bates, S. R., Farrow, I. R., & Trask, R. S. (2019). Compressive behaviour of 3D printed thermoplastic polyurethane honeycombs with graded densities. *Materials & Design*, 162, 130-142. doi:10.1016/j.matdes.2018.11.019
- Baumgart, F. (2000). Stiffness – an unknown world of mechanical science? *International Journal of the Care of the Injuries*, 31(2), S-14-S-B2.
- Bledsoe, G. H., Li, G., & Levy, F. (2005). Injury Risk in Professional Boxing. *Southern Medical Journal*, 98(10), 994-998. doi:10.1097/01.smj.0000182498.19288.e2
- Boxing Canada (2017). Articles and Rules. Retrieved from <http://boxingcanada.org/wp-content/uploads/2017/10/Rules-and-Articles-October-2017.pdf>.
- Browne, K. D., Chen, X., Meaney, D. F., & Smith, D. H. (2011). Mild Traumatic Brain Injury and Diffuse Axonal Injury in Swine. *Journal of Neurotrauma*, 28(9), 1747-1755.
doi:10.1089/neu.2011.1913
- Carroll, C. P., Cochran, J. A., Price, J. P., Guse, C. E., & Wang, M. C. (2010). The AIS-2005 Revision in Severe Traumatic Brain Injury: Mission Accomplished or Problems for Future Research?. *Association for the Advancement of Automotive Medicine. Annual Scientific Conference*, 54, 233–238. Retrieved from <https://www.ncbi.nlm.nih.gov/pmc/articles/PMC3242550/>
- Canadian Medical Association. (2001). Boxing. Retrieved from <https://cma-policies.andornot.com/documents/PolicyPDF/PD01-13.pdf>.
- Carlson, S. (2016). The influence of neck stiffness, impact location, and angle on peak linear acceleration, shear force, and energy loading measures of hockey helmet impacts. (Master's thesis). Lakehead University, Thunder Bay, Canada.

- Clauser, C., McConville, J., & Young, J. (1969). Weight, volume, and center of mass of segments of the human body. Retrieved November, from https://www.ece.uvic.ca/~bctill/papers/mocap/Clauser_etal_1969.pdf
- Cournoyer, J., & Hoshizaki, T. B. (2019). Head dynamic response and brain tissue deformation for boxing punches with and without loss of consciousness. *Clinical Biomechanics*, *67*, 96–101. doi:10.1016/j.clinbiomech.2019.05.003
- Cournoyer, J., Post, A., Rousseau, P., & Hoshizaki, B. (2016). The Ability of American Football Helmets to Manage Linear Acceleration With Repeated High-Energy Impacts. *Journal of Athletic Training*, *51*(3), 258-263. doi:10.4085/1062-6050-51.4.08
- Daneshvar, D. H., Baugh, C. M., Nowinski, C. J., Mckee, A. C., Stern, R. A., & Cantu, R. C. (2011). Helmets and Mouth Guards: The Role of Personal Equipment in Preventing Sport-Related Concussions. *Clinics in Sports Medicine*, *30*(1), 145-163. doi:10.1016/j.csm.2010.09.006
- Dau, N., Chien, H. C., Sherman, D., & Bir, C. (2006). Effectiveness of Boxing Headgear for Limiting Injury. Retrieved November, from https://www.researchgate.net/publication/267790987_Effectiveness_of_Boxing_Headgear_for_Limiting_Injury
- Dickinson, P., & Rempel, P. (2016). Prohibiting headgear for safety in amateur boxing? Opinion of the Canadian boxing community: An online poll. *Sports Medicine - Open*, *2*(1). doi:10.1186/s40798-016-0043-2
- Di Landro, L., Sala, G., & Olivieri, D. (2002). Deformation mechanisms and energy absorption of polystyrene foams for protective helmets. Retrieved from <https://www.sciencedirect.com/science/article/pii/S0142941801000733>
- Donegan, M. (2012). Resultant Vector. What Is It? How Do I Calculate It? Retrieved from <http://blog.prosig.com/2012/01/12/calculate-resultant-vector/>

- Estwanik, J. J., Boitano, M., & Ari, N. (1984). Amateur Boxing Injuries at the 1981 and 1982 USA/ABF National Championships. *The Physician and Sportsmedicine*, *12*(10), 123-128. doi:10.1080/00913847.1984.11701972
- Galgano, M., Toshkezi, G., Qiu, X., Russell, T., Chin, L., & Zhao, L. R. (2017). Traumatic Brain Injury: Current Treatment Strategies and Future Endeavors. *Cell transplantation*, *26*(7), 1118–1130. doi:10.1177/0963689717714102
- Gennarelli, T. A., Thibault, L. E., Adams, J. H., Graham, D. I., Thompson, C. J., & Marcincin, R. P. (1982). Diffuse axonal injury and traumatic coma in the primate. *Annals of Neurology*, *12*(6), 564–574. doi:10.1002/ana.410120611
- Gennarelli, T. A., Thibault, L. E., Tomei, G., Wisner, R., Graham, D., & Adams, J. (1987). Directional dependence of axonal brain injury due to centroidal and non-centroidal acceleration. *SAE Technical Paper Series*. doi:10.4271/872197
- Giza, C. C., & Hovda, D. A. (2001). The Neurometabolic Cascade of Concussion. *Journal of Athletic Training*, *36*(3), 228–235. Retrieved from <https://www.ncbi.nlm.nih.gov/pmc/articles/PMC155411/>
- Giza, C. C., Kutcher, J. S., Ashwal, S., Barth, J., Getchius, T. S. D., Gioia, G. A., Gronseth, G. S., Guskiewicz, K., Mandel, S., Manley, G., McKeag, D. B., Thurman, D. J., & Zafonte, R. (2013). Summary of evidence-based guideline update: Evaluation and management of concussion in sports: Report of the Guideline Development Subcommittee of the American Academy of Neurology. *Neurology*, *80*(24), 2250–2257. doi:10.1212/wnl.0b013e31828d57dd
- Greenwald, R. M., Gwin, J. T., Chu, J. J., & Crisco, J. J. (2008). Head Impact Severity Measures For Evaluating Mild Traumatic Brain Injury Risk Exposure. *Neurosurgery*, *62*(4), 789–798. doi:10.1227/01.neu.0000318162.67472.ad

- Hsu, S., Wu, S., Rau, C., Hsieh, T., Liu, H., Huang, C., . . . Hsieh, C. (2019). Impact of Adapting the Abbreviated Injury Scale (AIS)-2005 from AIS-1998 on Injury Severity Scores and Clinical Outcome. *International Journal of Environmental Research and Public Health*, *16*(24), 5033. doi:10.3390/ijerph16245033
- Hutchinson, J., Kaiser, M. J., & Lankarani, H. M. (1998). The Head Injury Criterion (HIC) functional. *Applied Mathematics and Computation*, *96*(1), 1–16. doi:10.1016/s0096-3003(97)10106-0
- Jeffries, L. (2017). The effect of facial protection, impact location, and neckform stiffness on peak linear acceleration, risk of injury, and energy loading measures of horizontal impacts on a hockey helmet impacts. (Master's thesis). Lakehead University, Thunder Bay, Canada.
- Jeffries, L., Zerpa, C., Przysucha, E., Sanzo, P., & Carlson, S. (2017a). The Use of a Pneumatic Horizontal Impact System for Helmet Testing. *Journal of Safety Engineering*, *6*(1), 8-13. doi:10.5923/j.safety.20170601.02
- Jeffries, L., Carlson, S., Zerpa, C., Przysucha, E., & Sanzo, P. (2017b). Establishing Evidence of Reliability and Validity for the Use of a Pneumatic Helmet Impact System. Retrieved from <https://commons.nmu.edu/cgi/viewcontent.cgi?referer=https://www.google.ca/&httpsredir=1&article=1240&context=isbs>.
- Jordan, B. D., & Campbell, E. A. (1988). Acute Injuries Among Professional Boxers in New York State: A Two-Year Survey. *The Physician and Sportsmedicine*, *16*(1), 87–91. doi:10.1080/00913847.1988.11709407
- Jordan, B. D., Voy, R. O., & Stone, J. (1990). Amateur Boxing Injuries at the US Olympic Training Center. *The Physician and Sportsmedicine*, *18*(2), 80–90. doi:10.1080/00913847.1990.11709974

Keenan, A., & Mahaffey, B. (2017). Concussion Care: Moving Beyond the Standard.

Missouri Medicine, 114(5), 340–343. Retrieved from

<https://www.ncbi.nlm.nih.gov/pmc/articles/PMC6140182/>

Kerr, Z. Y., Collins, C. L., Mihalik, J. P., Marshall, S. W., Guskiewicz, K. M., & Comstock,

R. D. (2014). Impact Locations and Concussion Outcomes in High School Football

Player-to-Player Collisions. *Pediatrics*, 134(3), 489-496. doi:10.1542/peds.2014-0770

Kimpara, H., & Iwamoto, M. (2011). Mild Traumatic Brain Injury Predictors Based on

Angular Accelerations During Impacts. *Annals of Biomedical Engineering*, 40(1), 114-

126. doi:10.1007/s10439-011-0414-2

Larsson, L. E., Melin, K. A., Nordstrom-Ohrberg, G., Silfverskiold, B. P., & Ohrberg, K.

(1954). Acute head injuries in boxers; clinical and electroencephalographic studies. *Acta*

Psychiatrica Et Neurologica Scandinavica Supplementum, 95, 2-42. Retrieved from

<https://pubmed.ncbi.nlm.nih.gov/13258327/>

Liao, S., Lynall, R. C., & Mihalik, J. P. (2016). The Effect of Head Impact Location on Day

of Diagnosed Concussion in College Football. *Medicine & Science in Sports &*

Exercise, 48(7), 1239-1243. doi:10.1249/mss.0000000000000896

Lin, T., Lou, C., & Lin, J. (2017). The Effects of Thermoplastic Polyurethane on the

Structure and Mechanical Properties of Modified Polypropylene Blends. *Applied*

Sciences, 7(12), 1254. doi:10.3390/app7121254

Ling, C., Ivens, J., Cardiff, P., & Gilchrist, M. D. (2018). Deformation of EPS Foam Under

Combined Compression-Shear Loading: Experimental and Computational Analysis. *EPJ*

Web of Conferences, 183, 01009. doi:10.1051/epjconf/201818301009

Ling, H., Hardy, J., & Zetterberg, H. (2015). Neurological consequences of traumatic brain

injuries in sports. *Molecular and Cellular Neuroscience*, 66, 114–122.

doi:10.1016/j.mcn.2015.03.012

- Matser, E. J. T., Kessels, A. G. H., Lezak, M. D., Troost, J., & Jordan, B. D. (2000). Acute Traumatic Brain Injury in Amateur Boxing. *The Physician and Sportsmedicine*, 28(1), 87–92. doi:10.3810/psm.2000.01.645
- McCown, I. A. (1959). Boxing injuries. *The American Journal of Surgery*, 98(3), 509-516. doi:10.1016/0002-9610(59)90545-8
- Mcintosh, A. S., & Patton, D. A. (2015a). Boxing headguard performance in punch machine tests. *British Journal of Sports Medicine*, 49(17), 1108-1112. doi:10.1136/bjsports-2015-095094
- Mcintosh, A. S., & Patton, D. A. (2015b). The impact performance of headguards for combat sports. *British Journal of Sports Medicine*, 49(17), 1113–1117. <https://doi.org/10.1136/bjsports-2015-095093>
- Mckee, A. C., & Daneshvar, D. H. (2015). The neuropathology of traumatic brain injury. *Handbook of Clinical Neurology Traumatic Brain Injury, Part I*, 45-66. doi:10.1016/b978-0-444-52892-6.00004-0
- McLean, A., Fildes, B., Kloeden, C., Digges, K., Anderson, R., Moore, V., Simpson, D. (1997). Prevention of Head Injuries to Car Occupants: An Investigation of Interior Padding Options. University of Adelaide. Retrieved from https://www.monash.edu/__data/assets/pdf_file/0011/216767/atsb160.pdf
- Meaney, D. F., & Smith, D. H. (2011). Biomechanics of Concussion. *Clinics in Sports Medicine*, 30(1), 19-31. doi:10.1016/j.csm.2010.08.009
- Meaney, D. F., Smith, D. H., Shreiber, D. I., Bain, A. C., Miller, R. T., Ross, D. T., & Gennarelli, T. A. (1995). Biomechanical Analysis of Experimental Diffuse Axonal Injury. *Journal of Neurotrauma*, 12(4), 689-694. doi:10.1089/neu.1995.12.689
- Mullally, W. J. (2017). Concussion. *The American Journal of Medicine*, 130(8), 885-892. doi:10.1016/j.amjmed.2017.04.016

- NOCSAE. (2016). Standard performance specification for newly manufactured ice hockey helmets. (ND 030-11m16). Overland Park, USA: National Operating Committee on Standards for Athletic Equipment. Retrieved from <https://nocsae.org/wp-content/uploads/2018/05/ND030-11m16MfrdIceHockeyHelmetsStandardPerformance.pdf>
- NOCSAE. (2017). Standard Test Method and Equipment Used in Evaluating the Performance Characteristics of Headgear/Equipment. Retrieved from <https://nocsae.org/wp-content/uploads/2018/05/1514996961ND00117m17bDropTestMethod.pdf>.
- NOCSAE. (2018). Standard Pneumatic Ram Test Method and Equipment Used in Evaluating the Performance Characteristics of Protective Headgear and Face Guards. Retrieved from <https://nocsae.org/wp-content/uploads/2018/05/ND081-18am19-005.pdf>.
- Newman, J. A. (1986). A generalized acceleration model for brain injury threshold (GAMBIT). 121-131. Retrieved from http://www.ircobi.org/wordpress/downloads/irc1986/pdf_files/1986_9.pdf
- Newman, J. A., Barr, C., Beusenbergh, M., Fournier, E., Shewchenko, N., Welbourne, E., & Withnall, C. (1999). A new biomechanical assessment of mild traumatic brain injury. Part 2: Results and conclusions. Retrieved from https://www.researchgate.net/publication/255576050_A_new_biomechanical_assessment_of_mild_traumatic_brain_injury_Part_2_results_and_conclusions
- Ommaya, A. K., Goldsmith, W., & Thibault, L. (2002). Biomechanics and neuropathology of adult and paediatric head injury. *British Journal of Neurosurgery*, 16(3), 220-242. doi:10.1080/02688690220148824
- O'Sullivan, D. M., & Fife, G. P. (2016). Impact attenuation of protective boxing and taekwondo headgear. *European Journal of Sport Science*, 16(8), 1219-1225. doi:10.1080/17461391.2016.1161073

- Ouckama, R. (2013). Time series measurement of force distribution in ice hockey helmets during varying impact conditions. (Doctoral dissertation). McGill University, Montreal, Canada.
- Peerless, S. J., & Rewcastle, N. B. (1967). Shear injuries of the brain. *Canadian Medical Association Journal*, *96*(10), 577–582. Retrieved from <https://www.ncbi.nlm.nih.gov/pmc/articles/PMC1936040/>
- Pellman, E. J., Viano, D. C., Tucker, A. M., Casson, I. R., & Waeckerle, J. F. (2003). Concussion in Professional Football: Reconstruction of Game Impacts and Injuries. *Neurosurgery*, *53*(4), 799-814. doi:10.1093/neurosurgery/53.3.799
- Plagenhoef, S., Evans, F. G., & Abdelnour, T. (1983). Anatomical Data for Analyzing Human Motion. *Research Quarterly for Exercise and Sport*, *54*(2), 169-178. doi:10.1080/02701367.1983.10605290
- Porter, M., & O'Brien, M. (1996). Incidence and Severity of Injuries Resulting From Amateur Boxing in Ireland. *Clinical Journal of Sport Medicine*, *6*(2), 97-101. doi:10.1097/00042752-199604000-00006
- Purcell, L. K., & Leblanc, C. M. (2011). Boxing participation by children and adolescents. *Paediatrics & Child Health*, *17*(1), 39–39. doi:10.1093/pch/17.1.39
- Razaghi, R., Biglari, H., & Karimi, A. (2018). A comparative study on the mechanical performance of the protective headgear materials to minimize the injury to the boxers head. *International Journal of Industrial Ergonomics*, *66*, 169–176. doi:10.1016/j.ergon.2018.03.004
- Rizzo, F., Dagostino, T., Cuomo, S., Pinto, F., & Meo, M. (2020). High-velocity impact investigation on thermoplastic polyurethane/CFRP T-stiffened panel. *Materials Today: Proceedings*. doi: 10.1016/j.matpr.2020.02.163

- Rowson, S., Bland, M. L., Campoletano, E. T., Press, J. N., Rowson, B., Smith, J. A., Sproule, D. W., Tyson, A. M., & Duma, S. M. (2016). Biomechanical Perspectives on Concussion in Sport. *Sports Medicine and Arthroscopy Review*, *24*(3), 100–107. doi:10.1097/jsa.0000000000000121
- Rowson, S., & Duma, S. M. (2013). Brain Injury Prediction: Assessing the Combined Probability of Concussion Using Linear and Rotational Head Acceleration. *Annals of Biomedical Engineering*, *41*(5), 873–882. doi:10.1007/s10439-012-0731-0
- Rush, B. (2011). Shearing Injury, Shear Strain. *Encyclopedia of Clinical Neuropsychology*, 2285-2286. doi:10.1007/978-0-387-79948-3_277
- Sahler, C. S., & Greenwald, B. D. (2012). Traumatic Brain Injury in Sports: A Review. *Rehabilitation Research and Practice*, 1-10. doi:10.1155/2012/659652
- Senthamarai Kannan, K., Manoj, K., & Arumugam, S. (2015). Labeling Methods for Identifying Outliers. *International Journal of Statistics and Systems*, *10*(2), 231-238. Retrieved from https://www.researchgate.net/publication/283755180_Labeling_Methods_for_Identifying_Outliers#fullTextFileContent
- Sethi, N. K. (2016). Post-concussion return to boxing protocol. *South African Journal of Sports Medicine*, 61-62. doi:10.17159/2078-516x/2016/v28i2a464
- Signoretti, S., Lazzarino, G., Tavazzi, B., & Vagnozzi, R. (2011). The Pathophysiology of Concussion. *Pm&r*, *3*. doi:10.1016/j.pmrj.2011.07.018
- Taylor, K., Hoshizaki, T. B., Hoshizaki, T. B., & Gilchrist, M. D. (2016). Dynamic Head Response and Maximum Principal Tissue Strain for Helmeted (American Football) and Non-helmeted Impacts. Retrieved from <http://www.ircobi.org/wordpress/downloads/irc16/pdf-files/32.pdf>

- Tommasone, B., & McLeod, T. C. V. (2006). Contact Sport Concussion Incidence. *Journal of Athletic Training, 41*(4), 470-472. Retrieved from <https://www.ncbi.nlm.nih.gov/pmc/articles/PMC1748409/>.
- Toth, C., McNeil, S., & Feasby, T. (2005). Central Nervous System Injuries in Sport and Recreation. *Sports Medicine, 35*(8), 685–715. doi:10.2165/00007256-200535080-00003
- Unterharnscheidt, F., & Higgins, L.S. (1969). Traumatic lesions of brain and spinal cord due to nondeforming angular acceleration of the head. *Texas reports on biology and medicine, 27* 1, 127-66. Retrieved from <https://pubmed.ncbi.nlm.nih.gov/4976573/>
- USA Boxing (2017). National Rule Book. Retrieved from <https://www.teamusa.org/usa-boxing/usa-boxing-national-rule-book>.
- VanLandingham, M. R., Chang, N.-K., Drzal, P. L., White, C. C., & Chang, S.-H. (2005). Viscoelastic characterization of polymers using instrumented indentation. I. Quasi-static testing. *Journal of Polymer Science Part B: Polymer Physics, 43*(14), 1794–1811. doi:10.1002/polb.20454
- Vieira, R. D., Paiva, W. S., Oliveira, D. V., Teixeira, M. J., Andrade, A. F., & Sousa, R. M. (2016). Diffuse Axonal Injury: Epidemiology, Outcome and Associated Risk Factors. *Frontiers in Neurology, 7*. doi:10.3389/fneur.2016.00178
- Walilko, T. J., Viano, D. C., & Bir, C. A. (2005). Biomechanics of the head for Olympic boxer punches to the face. *British Journal of Sports Medicine, 39*(10), 710-719. doi:10.1136/bjism.2004.014126
- Welch, M. J., Sitler, M., & Kroeten, H. (1986). Boxing Injuries From an Instructional Program. *The Physician and Sportsmedicine, 14*(9), 81-89. doi:10.1080/00913847.1986.11709169
- World Medical Association. (2017). WMA Statement on Boxing. Retrieved from <https://www.wma.net/policies-post/wma-statement-on-boxing/>.

- Zazryn, T. R. (2003). A 16 year study of injuries to professional boxers in the state of Victoria, Australia. *British Journal of Sports Medicine*, 37(4), 321-324.
doi:10.1136/bjism.37.4.321
- Zazryn, T. R., Mccrory, P. R., & Cameron, P. A. (2009). Neurologic Injuries in Boxing and Other Combat Sports. *Physical Medicine and Rehabilitation Clinics of North America*, 20(1), 227-239. doi:10.1016/j.pmr.2008.10.004
- Zerpa, C., Carlson, S., Elyasi, S., Przysucha, E., & Hoshizaki, T. (2016). Energy dissipation measures on a hockey helmet across impact locations. *Journal of Safety Engineering*, 5(2), 27-35. doi:10.5923/j.safety.20160502.01
- Zerpa, C., Liu, M., & Parihar, S. (2020). An improved cycling helmet technology to mitigate head injuries. 38(1). doi:<https://commons.nmu.edu/isbs/vol38/iss1/22>